BNL 20550

PROCEEDINGS

of the

1975 ISABELLE SUMMER STUDY

July 14 - 25, 1975

Volume I

BROOKHAVEN NATIONAL LABORATORY
ASSOCIATED UNIVERSITIES, INC.
UPTON, NEW YORK 11973

BNL 20550

PROCEEDINGS

of the

1975 ISABELLE SUMMER STUDY

July 14 - 25, 1975

In Two Volumes

Volume I

Summary Reports of Working Groups

Brookhaven National Laboratory
Associated Universities, Inc.
Upton, New York 11973

NOTICE

This report was prepared as an account of work sponsored by the United States Government. Neither the United States nor the Energy Research and Development Administration, nor any of their employees, nor any of their contractors, subcontractors, or their employees, makes any warranty, express or implied, or assumes any legal liability or responsibility for the accuracy, completeness or usefulness of any information, apparatus, product or process disclosed, or represents that its use would not infringe privately owned rights.

PREFACE

The 1975 ISABELLE Summer Study, held at Brookhaven from July 14 to 25, was attended by over 100 representatives from many universities and nearly every high energy physics laboratory in the western hemisphere as well as many Brookhaven staff members. The aim was to improve, reinforce, or modify the concepts which have gone into the "Proposal for the Construction of a 200 GeV proton-proton Storage Accelerator Facility" (BNL Report 20161). The opening two days were used to review the present status of the project. For the remainder of the time, specific topics in the areas of experimental physics and machine design were studied by fifteen working groups. Their conclusions were presented by the Chairmen of the working groups at a review session on the last day of the Summer Study.

Summaries from the working groups as well as contributions from individual authors are collected in the present Proceedings. The original plan was to bring summaries and contributed papers in a single volume. Technical reasons force their separation into two volumes; we apologize for the inconvenience resulting from this division.

The task of editing the papers was shared by J.C. Herrera and A.M. Thorndike with the BNL Co-Chairmen of the working groups.

Finally, acknowledgment is due to the unfailing efforts of the conference secretary, Paula Hughes, to the secretaries typing the manuscripts, and to the cooperation of R.P. Brown of the Photography and Graphic Arts Division where these Proceedings were assembled and printed.

The 1975 ISABELLE Summer Study Organizing Committee

H. Hahn, G. Kalbfleisch, A. Pevsner, L. Sulak

WORKING GROUPS AND CHAIRMEN

- Initial and Low-Luminosity Experiments	M.L. Good K.J. Foley
- Weak Interactions and Other High-Luminosity Experiments	C. Rubbia M. Sakitt
- Large Equipment and Facilities	S.C.C. Ting S. Ozaki
- Experimental Insertions	J. Sandweiss T.F. Kycia
- Theory	F.E. Low T.L. Trueman
- New and Unthinkable Ideas	L.M. Lederman N.P. Samios
- Lattice	L. Smith M. Month
- Beam Transfer, Injection and Ejection	L.C. Teng A. van Steenbergen
- Stacking and Acceleration	W. Schnell E.C. Raka
- Performance Limitations	E. Keil E.D. Courant
- Magnets and Cryogenics	D.B. Thomas A.D. McInturff
- Radiation Effects	P.A. Sanger G.T. Danby
- Vacuum System	J.P. Hobson H.J. Halama
- Computer Control and Monitoring	K.B. Mallory D.G. Dimmler
- Options	M. Tigner R. Chasman
- Novel Acceleration Schemes	W.J. Willis R.B. Palmer

Visiting Participants

F. Arendt, Karlsruhe
M. Bardon, NSF
D.A. Baynham, RHEL
D. Berley, NSF
D. Blechschmidt, CERN
G. Bronca, Saclay
H. Bruck, Saclay
R.A. Burnstein, Ill.
W.C. Carithers, Rochester
C.Y. Chang, Maryland
A.W. Chao, SLAC
D.C. Cheng, Santa Cruz
C.Y. Chien, Johns Hopkins
Y. Cho, ANL
N. Cunliffe, RHEL
M. Duong-van, SLAC
R.M. Edelstein, Carnegie-Mellon
D.A. Edwards, FNAL
E. Engels, Pitts.
A. Faltens, LBL
G.R. Farrar, Caltech
V. Fitch, Princeton
W.B. Fowler, FNAL
A. Garren, LBL
J. Gareyte, CERN
M.L. Good, SUNY
K. Goulianos, Rockefeller
J.P. Gourber, CERN
P. Grannis, SUNY
D. Green, Carnegie-Mellon
O. Gröbner, CERN
F. Halzen, Wisc.
H.G. Hereward, CERN
W. Hermannsfeldt, ERDA
J.P. Hobson, National Res. Council
A. Hofmann, CERN
K. Hübner, CERN
R. Imlay, Wisc.
A. Kanofsky, Lehigh
E. Keil, CERN
J.E. Kiskis, MIT
B. Knapp, Nevis
M.A. Kramer, CCNY
M.N. Kreisler, Mass.
R.E. Lanou, Jr., Brown
L.M. Lederman, Columbia
F.E. Low, MIT
J. Maidment, RHEL
R.D. Majka, Yale
K.B. Mallory, SLAC
A. Mann, Penn.
J.N. Marx, Yale
B.T. Meadows, Cincinnati
E. Messerschmid, Freiburg
C.O. Mikaelian, Penn State
U. Nauenberg, Colorado
C.L. Olson, Sandia Lab.
A. Pais, Rockefeller
R.H. Pantell, Stanford
C. Pellegrini, Culham
J. Perot, Saclay
J.M. Peterson, LBL
A. Pevsner, Johns Hopkins
L.G. Pondrom, Wisc.
D.J. Ranft, Leipzig
R.H. Remsbottom, Wisc.

J.L. Rosen, Northwestern
L. Rosenson, MIT
C. Rubbia, Harvard
A.G. Ruggiero, FNAL
J. Russ, Carnegie-Mellon
J.J. Russell, Southeastern Mass. U.
J. Sandweiss, Yale
P.A. Sanger, FNAL
R.T. Schermer, LASL
P. Schlein, UCLA
W. Schnell, CERN
W. Selove, Penn.
R. Serber, Columbia
L. Smith, LBL
G.A. Snow, Maryland
P. Sokolsky, Nevis
K. Steffen, DESY
B.P. Strauss, FNAL
L. Sulak, Harvard
D. Sutter, FNAL
L.C. Teng, FNAL
D.B. Thomas, RHEL
M. Tigner, Cornell
S.C.C. Ting, MIT
S.B. Treiman, Princeton
W.A. Wallenmeyer, ERDA
S.T. Wang, ANL
H.H. Williams, Penn.
W.J. Willis, CERN
R.C. Wolgast, LBL
M.E. Zeller, Yale

TABLE OF CONTENTS

Volume I

Page

Initial and Low-Luminosity Experiments 1

M.L. GOOD

Design of a Lepton Detector for ISABELLE 9

R. BURNSTEIN, W.C. CARITHERS, M. DUONG-VAN, R. IMLAY, M. KREISLER, U. NAUENBERG, C. RUBBIA, G. SNOW, L. SULAK, H.H. WILLIAMS, E. PASCHOS, M. SAKITT, C.L. WANG, L.L. WANG

Large Equipment and Facilities 52

L. ROSENSON, S. TING, J. RUSSELL, W. SELOVE, S. LINDENBAUM, W. LOVE, R. LOUTTIT, S. OZAKI, F. PAIGE, E. PLATNER, S. PROTOPOPESCU

Experimental Insertions 70

J. SANDWEISS, T.F. KYCIA

New and Unthinkable Ideas 84

L.M. LEDERMAN

Lattice 111

L. SMITH

Beam Transfer, Injection and Ejection 117

L.C. TENG, A. VAN STEENBERGEN

Stacking and Acceleration 126

W. SCHNELL

Performance Limitations 133

E. KEIL

Magnets and Cryogenics 140

D.B. THOMAS

Radiation Effects 149

P.A. SANGER, G.T. DANBY

Vacuum System 151

J.P. HOBSON

Page

Computer Control and Monitoring..... 160
K.B. MALLORY

Options..... 163
M. TIGNER

Novel Acceleration Schemes..... 170
W.J. WILLIS

TABLE OF CONTENTS

Volume II

A 4π Detector Experiment for ISABELLE

SUH-URK CHUNG, PAUL GRANNIS, DANIEL GREEN

Measuring Coulomb-Nuclear Interference as a First Round ISA Experiment

J.N. MARX, R.D. MAJKA

Elastic Scattering and Diffraction Dissociation in the Angular Range 1 - 50 mrad

R.M. EDELSTEIN, M. ZELLER

Small Angle Single Arm Spectrometer for ISABELLE

C.Y. CHANG, E. ENGELS, M. KRAMER, R. LANOU, L. PONDROM

A Single Arm Spectrometer to Study High $P_\perp$ Processes Near 90° at ISA

C.Y. CHIEN, H. GORDON, A. KANOFSKY, M.A. KRAMER, J. RUSS

A Brief Comment on Large $P_\perp$ Muons Near 90°

JANOS KIRZ

Experiments Using a Single Arm Spectrometer in the Intermediate Angle Region at ISABELLE

A. KANOFSKY

High P_T π^o Detector at ISABELLE

P. GRANNIS, D. GREEN

Single Particle Spectra at High Transverse Momentum as a Function of X

M.L. GOOD

Search for Fractionally Charged Quarks at ISABELLE

K.J. FOLEY, B.T. MEADOWS

Monopole Searches at ISABELLE

G. GIACOMELLI, A.M. THORNDIKE

On the Possibility of Searches for Particles by Threshold Effects Using Precise Determination of the ISA Energy

A. KANOFSKY

A Versatile Central Spectrometer for ISABELLE

D. CHENG, K. GOULIANOS, B. KNAPP, J. ROSEN, P. SCHLEIN

Advantages of Asymmetric Operation of ISABELLE

R.F. PEIERLS

Jets in Large P_T Reactions at ISABELLE

FRANK E. PAIGE

$W^{\pm}$ Pairs and Neutral Currents at ISABELLE

K.O. MIKAELIAN

Downstream Calorimeters for ISABELLE

W. SELOVE

A Calorimeter Experiment for Jet Studies and Other Uses of Modular Calorimeters

A. KANOFSKY

ISABELLE with One Low-β Insertion

A. GARREN

Closed Orbit Adjustment

D. EDWARDS

Some Effects of Random Errors in ISA Magnets

A.W. CHAO

Control of Betatron Tune and Resonances

J. GAREYTE, J.P. GOURBER

Betatron Tune Change Due to Direct Space-Charge Forces in the ISA

A.W. CHAO, J.C. HERRERA, M. MONTH

Sources and Characteristics of ISA Beam Loss

A. van STEENBERGEN, L.C. TENG

ISA Beam Dump Absorber

A. van STEENBERGEN

Injection-Ejection Protection Logic

H. BROWN

ISA Beam Scraper System

J. PETERSON, A. van STEENBERGEN, L.C. TENG

Caloric Deposition Downstream of the ISA Beam Scrapers
L. BLUMBERG, J. RANFT, A. STEVENS, A. van STEENBERGEN
ISA Beam Scraper Criteria
A. van STEENBERGEN
Synchronization and Tolerances for Transfer of Beam from AGS to ISA
J. PETERSON, L.C. TENG

ISABELLE Kicker Magnets, Septa and Scrapers
A. FALTENS
An Estimate of Limits to the Longitudinal Coupling Impedance
A. FALTENS, L.J. LASLETT
Accelerating RF System
S. GIORDANO
Stacking RF System
S. GIORDANO
Shunt Impedance Criteria
J. CLAUS
Phase Displacement Acceleration for the ISABELLE Stack
E. MESSERSCHMID, M. MONTH

Transverse Stability of Coasting Beams in ISABELLE
E. KEIL, A. RUGGIERO
Dependence of the Longitudinal Bunched Beam Stability on the Choice of the RF Harmonic Number in ISABELLE
A. RUGGIERO
Transverse Stability of the Bunched Beam During Acceleration in ISABELLE
A RUGGIERO
Longitudinal Coupling Effects Due to Beam-Beam Interaction
C. PELLEGRINI
Coasting Beam Theory Applied to Bunches
H.G. HEREWARD

Magnet Protection

D.A. BAYNHAM

Conductor Considerations for ISABELLE Dipoles

A.D. Mc INTURFF, B.P. STRAUSS, R.H. REMSBOTTOM

ISABELLE Magnet Correction System

G. PARZEN

50 kG Dipole

P. DAHL, G. PARZEN

Some Remarks on Mechanical and Thermal Behavior of the Coil

J. PEROT

Some Three-Dimensional Magnetostatic Relaxation Programs

L.J. LASLETT

Shielding Criteria and Design Considerations

S.J. LINDENBAUM

Displacement Damage for 300 GeV Protons

PHILLIP SANGER

Radiation Heating: Experience and Projections

G.T. DANBY

Thermal Desorption of Gases from Aluminum Alloy Al 6061 Their Rates and Activation Energies

H.J. HALAMA , J.C. HERRERA

Alternative Interpretation of the Measurements of Specific Outgassing Rates of Materials

J.P. HOBSON

Beam Clearing and Space-Charge Tune Depression

J.C. HERRERA

Clearing Requirements in ISABELLE Based on the Electron Proton Instability

O. GRÖBNER

η Measurements in Glow Discharged Chambers at the ISA

D. BLECHSCHMIDT

Ion Desorption Cross Section of Carbon Containing Molecules on Aluminum and Stainless Steel

M.L. YU

Pressure Measurements at ISABELLE

D. BLECHSCHMIDT

Experimental Insertions

H.J. HALAMA

Demountable Ultrahigh Vacuum Sections for ISABELLE

J.P. HOBSON

Outline of a Cold Bore Design for ISABELLE

R.C. WOLGAST

Computer Control and Monitoring

D.G. DIMMLER

A Summary of the Discussions on Organization and Design of an ISABELLE Control System

R.J. NAWROCKY

Some Guidelines for Control System Design

K.K. LI

Computer System Requirements

D. LOWENSTEIN

A New Approach to Control System Interfaces

K.B. MALLORY

$\bar{p}$-p Option

F. HALZEN, E. PASCHOS, R. PEIERLS, D.P. SIDHU, T.L. TRUEMAN

Heating Effects of an Unseparated $\bar{p}$ Beam in the ISA Ring

V. FITCH

On the Contamination During Antiproton Injection into ISABELLE

K. HÜBNER

Single Ring $\bar{p}$-p Colliding Beams as an Interim ISABELLE

D. BERLEY, A. CARROLL, A. MANN

Status of the ISABELLE e-p Option at Time of Summer Study 1975

R. CHASMAN

Review of e-p Collision Geometries

K. STEFFEN, J. MAIDMENT AND Y. CHO

Comments on Injection into ISABELLE Electron Ring

J. MAIDMENT

Storing and Accelerating Electrons in One of the p-Rings of ISABELLE

M. TIGNER

Does the Proton Beam in an e-p Colliding Device Deteriorate by Individual e-p Coulomb Interactions ?

H. BRUCK

INITIAL AND LOW-LUMINOSITY EXPERIMENTS

Summary Report of Working Group*

M. L. Good

SUNY, Stony Brook

I. Introduction

The work of this group went somewhat beyond that implied by its title, in that we certainly considered experiments which, while useful and necessary, either were not particularly low-luminosity, or required special conditions on the machine, and hence should not be considered as truly initial experiments. A more descriptive title would be "hadron physics", but with massive, dedicated, multiparticle spectrometers and jet searches via calorimeters excluded. These latter topics are covered in the report of the section on Large Equipment and Facilities of Ozaki and Ting.

We proceeded as follows: an initial roster of some 25 physicists met to discuss working procedures, and the field was divided up according to areas of physics interest, rather than techniques. Working subgroups were formed, and were charged with producing experiments at the proposal level of detail, addressed to specific physical measurements. If after doing this, it was found that other physics could be done with the same apparatus, this was duly noted; but the thrust was toward definiteness on specific measurements rather than toward encompassing as much as possible with a particular experimental approach.

The verbal report given by the outside chairman at the end of the study described the achievements of the several working

* C. Y. Chang, D. Cheng, C. Y. Chien, S. U. Chung, R. Edelstein, E. Engels, K. Foley, M. L. Good, H. Gordon, K. Goulianos, P. Grannis, D. Green, A. Kanofsky, J. Kirz, B. Knapp, M. Kramer, R. Lanou, R. Majka, J. Marx, B. Meadows, R. Peierls, L. Pondrom, J. Rosen, J. Russ, P. Schlein, A. Thorndike, M. Zeller.

subgroups, available then in draft form. In this written version, the final reports are here to speak for themselves, and so we will attempt only to summarize the results, and to list insights that were gained during the study.

II. Summary of Results

A gratifying outcome of these studies is that all of the experiments examined were capable of being performed with the machine as proposed. Special vacuum pipes were required by some; a special quadrupole is needed by the small-angle particle spectrometer; a special tune for the Coulomb-nuclear interference; these points are discussed in the report on Experimental Insertions — but at no point did an experimenter come in waving a sheaf of papers and say "I can't do my experiment". The machine seems to be highly usable, as far as hadron physics is concerned.

What does this physics consist of? All of it is of fundamental interest, and much of it is exciting. A brief overview of the areas studied follows:

1) Total Cross Section. This may be determined from counting all reaction products,[1] and by small-angle elastic scattering[2,3] via the optical theorem. Both the question of the continued rise of total cross section and of the value of the real part, which reflects the even higher domain[2] are of prime theoretical interest.

2) Multiplicity Distributions and Short Range Correlation studies.[1] These can answer the questions of whether the particle

---

1. Suh-Urk Chung, Paul Grannis, Daniel Green, "A 4π Detector Experiment for ISABELLE", these Proc.

2. R. D. Majka and J. N. Marx, "Measuring Coulomb-Nuclear Interference as a First Round ISA Experiment", these Proc.

3. R. M. Edelstein and M. Zeller, "Elastic Scattering and Diffraction Dissociation in the Angular Range 1 - 50 mrad", these Proc.

clustering seen at ISR energies is an asymptotic phenomenon or a slowly energy-dependent one, and whether the diffractive component remains static or not. At ISABELLE energies separation of the diffractive component up to masses of 30 GeV for the diffractively excited system is possible.

The existence, or lack, of a central plateau in the rapidity distribution for charged particles should be much more clear at these energies — at the ISR the plateau has barely emerged[1] if at all.

3) Elastic Scattering. The differential cross section can be obtained over a range of t extending from the Coulomb-nuclear interference region[2] through the diffractive peak out to wherever the cross section drops to 10^{-34} $cm^2/(GeV)^2$ (Ref. 3). This will give a measurement of the ratio of real to imaginary parts to 5% and study the s dependence of the diffractive peak slope, and of any dip structures. The range of s covered, extends from the ISR value to a factor of 50 higher.

A modification of the basic elastic scattering apparatus seems ideally suited to studying low-mass diffractive dissociation by analysis of the decay products.[3]

4) Single Particle Spectra. A small angle spectrometer working through a slot in the first quadrupole can measure, with complete particle identification, hadron spectra at fixed $p_\perp$ and over a broad range of x.[4] Transverse momenta out to ~1 GeV/c and down to the agreeably small value of 0.2 GeV/c, are covered. These measurements, over a range of s from 2500 $(GeV)^2$ to $1.6 \times 10^5 (GeV)^2$, are of basic import for understanding hadronic collisions.

The proton spectrum near $x = 1$ and small $p_\perp$ can be used to study the high-mass dissociation of the other proton, the domain of

---

4. C. Y. Chang, E. Engels, M. Kramer, R. Lanou, L. Pondrom, "Small Angle Single Particle Spectrometer for ISABELLE", these Proc.

triple-Regge theory.[4] Here it is desirable to lower the effective beam energy spread, to improve the mass resolution of the recoiling system. This means either a special low-intensity beam fill, or the design of a dispersive crossing region, as discussed in Ref. 4. Since neither of these possibilities have as yet been considered by the machine designers, some further work is indicated, but a study of a dispersive crossing for the European ISR design revealed no particular problems.

At large $p_\perp$ near 90°, a large aperture spectrometer[5] can measure hadron yields out to 20 GeV/c at reasonable counting rates, if the CERN-Columbia-Rockefeller parameterization of high $p_\perp$ ISR data is correct. (For the Chicago-Princeton parameterization, yields are much less.)

Here we encounter a conspiracy in our favor with respect to particle identification: using atmospheric pressure Cerenkov counters as dictated by the large solid angle, one finds that π's, K's and p's can be simultaneously identified in the range 10 - 20 GeV/c. (A Freon counter and a CO_2 counter are a good combination.) One will not want to go higher in momentum because of the rates. At lower momenta, higher pressure is required for complete particle identification, and pressurized counters mean smaller solid angle; but then the rates are much higher. Thus complete 90° spectra are expected to be obtainable in a straightforward way.

The detailed study of the fascinating and totally unexpected phenomenon of large high $p_\perp$ hadron yields must rank as one of the highest priorities in particle physics.

A modification of this same apparatus can study the anomalous "direct" production of muons (expected at the level of 10^{-4} of the

---

5. C. Y. Chien, H. Gordon, A. Kanofsky, M. A. Kramer, J. Russ, "A Single Arm Spectrometer to Study High P Processes Near 90° at ISA", these Proc.

pion yield).[6] Another paper[7] discusses the possible use of the spectrometer at intermediate angles.

It should be entirely feasible to combine such a spectrometer with the 4π detector, or with a similar apparatus on the opposite side, and thus measure associated multiplicities in high $p_\perp$ events, or dihadron mass spectra in an entirely new range. (The numbers are such that measurable results are guaranteed.) With 2×10^4 counts/hour above $p_\perp = 5$ GeV/c, on one side,[5] and with 0.5 sr on the other side, a high coincidence rate will be obtained.

A possible arrangement (suggested by Grannis) combining several specific triggers with a 4π detector is shown in Fig. 1.

The difficult task of measuring particle yields at high $p_\perp$ as a function of x is very conveniently attacked by using the possibility of running at unequal beam energies, in such a way that $p_\perp$, the lab momentum detected, and the c.m. energy ($\sqrt{s}$) all remain constant, while only x is varied. This method was used in a large-aperture Pb glass array[8] to study particles decaying into γ's (e.g. π^0's) and again in a charged-particle spectrometer, with complete hadron identification.[9] At the present time, drastically different shapes for the x distribution at large $p_\perp$ are predicted by different models.

---

6. J. Kirz, "A Brief Comment on Large $p_\perp$ Muons near 90°", these Proc.

7. A. Kanofsky, "Experiments Using a Single Arm Spectrometer in the Intermediate Angle Region at ISABELLE", these Proc.

8. F. Grannis and D. Green, "High $p_\perp$ π^0 Detector at ISABELLE", these Proc.

9. M. L. Good, "Single Particle Spectra at High Transverse Momentum as a Function of x", these Proc.

5) New Particle Searches. Straightforward extensions of existing techniques can look for quarks[10] and for magnetic monopoles,[11] and if nature does not cooperate, can set limits more stringent than those of cosmic ray searches for these exotics. The possibility of studying threshold effects was also considered.[12]

Specific searches for charm or other new quantum numbers were not considered as such, since it is too hard to be specific; each possible decay mode is virtually a new experiment. It is here that one enters into multiparticle spectrometers, and a particular apparatus combining great flexibility and large solid angle was studied.[13]

It seems clear that multiparticle experiments with large aperture magnetic analysis and with at least partial particle identification will be performed; but here the possibilities are virtually endless, and an exhaustive survey is not possible. However, the high luminosity available, the tiny total dimensions of the beam intersection, the good access to the intersecting region, the flexibility provided by the separately variable beam energies, and the tendency to be able to use atmospheric pressure Cerenkov counters, all point toward a relative ease in attacking this difficult area of physics with good prospects of success.

---

10. K. J. Foley and B. T. Meadows, "Search for Fractionally Charged Quarks at ISABELLE", these Proc.

11. G. Giacomelli and A. Thorndike, "Monopole Searches at ISABELLE", these Proc.

12. A. Kanofsky, "On the Possibility of Searches for Particles by Threshold Effects Using Precise Determination of the ISA Energy", these Proc.

13. D. Cheng, K. Goulianos, B. Knapp, J. Rosen and P. Schlein, "A Versatile Central Spectrometer for ISABELLE", these Proc.

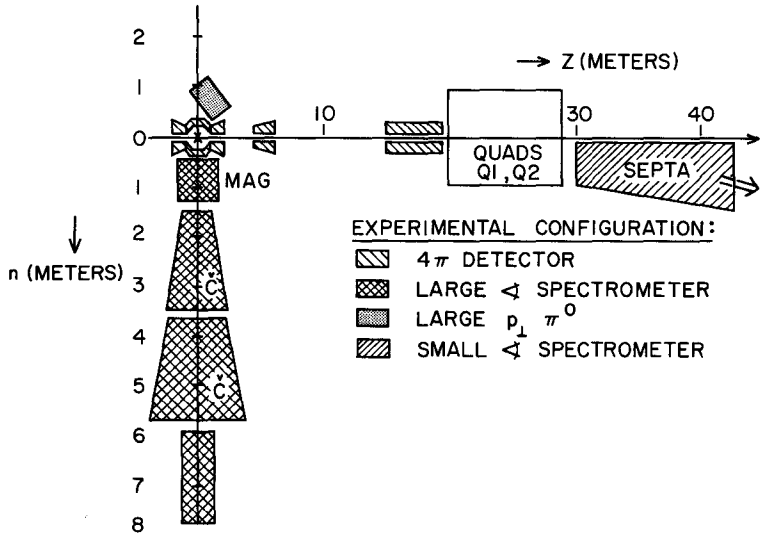

Fig. 1. Combined spectrometer configuration with 4π detector.

III. Conclusions

Two specific insights were gained during the study:

1) Very special, rather bizarre beam pipe shapes are needed for optimal performance in different experiments. It is hoped that expert design and construction of such pipes will be considered a routine part of the operation of the machine facility.

2) The systematic use of asymmetric beam energies, discussed in a report by Peierls,[14] adds an extra dimension of flexibility from which almost every experiment considered seems to benefit. Thus this style of running should be considered routine.

The overall picture that emerges from the work of this group is an exciting one, in which the broad general features of hadron collisions can be studied in a straightforward way over an enormous range (a factor of 50) in the variable s, lying at and above the presently highest available energy. At the same time, the presently known mysterious new phenomena, e.g., the high $p_\perp$ hadron yields and the anomalous "direct" production of leptons, can be pursued out to considerably higher transverse momenta then can now be achieved.

It seems almost certain by now that more new phenomena will turn up, either in the form of new massive particles, in the violation of hallowed selection rules, or in totally unforeseen ways. The proposed machine will enable us to discover if this is indeed so.

---

14. R. F. Peierls, "Advantages of Asymmetric Operation of ISABELLE", these Proc.

DESIGN OF A LEPTON DETECTOR FOR ISABELLE

Summary Report of Working Group*

R. Burnstein
Illinois Institute of Technology
W. C. Carithers
University of Rochester
M. Duong-van
Stanford Linear Accelerator Center
R. Imlay
University of Wisconsin
M. Kreisler
University of Massachusetts
U. Nauenberg
University of Colorado
C. Rubbia, L. Sulak
Harvard University
G. Snow
University of Maryland
H. H. Williams
University of Pennsylvania
and
E. Paschos, M. Sakitt, C. L. Wang, L. L. Wang
Brookhaven National Laboratory

I. Theoretical Background

A. Introduction

The most direct test of the underlying theory of weak interactions is the search for the intermediate vector bosons.[1] In addition to the long standing prediction of charged mediators of the weak force ($W^{\pm}$ particles), gauge theories require the existence of

---

* The summary talk at the review session was given by C. Rubbia

1. S. Weinberg, J. Phys. (Paris) Suppl. 34, c1 (1973).

neutral counterparts (W^o particles) which mediate the neutral currents. The observation of neutral currents in numerous neutrino experiments provides strong support for the existence of a triplet of intermediate vector bosons.

The most promising way of producing[2] them is with proton-proton colliding beams, where they can be identified by their leptonic decays. The discovery of J/Ψ resonances points out the type of experiments which can search for these fundamental objects. In any unified theory of weak and electromagnetic interactions, the expected masses are of 0 ($\sqrt{\alpha/G}$) or roughly 30 - 100 GeV/c^2. Such masses are within the reach of the ISABELLE colliding ring facility.

We first derive rigorous bounds[3] for the production of W's in terms of the reaction

$$p + p \rightarrow \mu^+ \mu^- + X.$$

For charged mesons the relations follow from the conserved vector current hypothesis, while for neutral mesons the bounds depend in addition on the particular gauge theory under consideration. The practical value of the bounds rests on the fact that we can relate the production of $W^{\pm}$ or W^o to the production of $\mu^+\mu^-$ pairs of the same dilepton mass and at the same center-of-mass energy. In the absence of measurements for the above reaction at very high energies, we investigate data at lower energies searching for the scaling limit of the reaction. A summary of existing results indicates that the data fall on a smooth curve suggesting that this may well be the scaling limit. Adopting the scaling law we can in turn calculate lower bounds for the production of W-bosons by virtue of inequalities.

---

2. A Proposal for Construction of a Proton-Proton Storage Acceleration Facility, BNL 20161 (1975).

3. L. M. Lederman and B. G. Pope, Phys. Rev. Lett. 27, 765 (1971); L. M. Lederman and D. H. Saxon, Nucl. Phys. B63, 315 (1973).

In a second approach, the previous results are reproduced via the quark-parton model,[4] since the general principles involved in deriving the bounds are naturally incorporated within the model. Using the quark distributions from the existing fits[5] to the lepton production data to give the best agreements with the electromagnetic production of $\ell\bar{\ell}$ in pp collisions, we calculate the $W^{\pm}$ production in both pp and $\bar{p}p$ reaction. The model predicts a larger production for W^{+} than W^{-} in pp reactions due to the fact that there are more positive quarks in protons. Finally we summarise the expectations for the decay widths.

B. General Bounds

In all the processes under consideration, we assume that the leptons couple directly to a weak or electromagnetic current, which in turn couple to the hadronic system. The lepton vertex is well determined by the theory of electromagnetic and weak interactions and the main interest is on the couplings of the currents to the hadrons shown in Fig. 1a. The conserved vector current hypothesis tells us that the cross sections for the production of W's with different charges are related to each other and also to the electromagnetic matrix elements. In the following discussion we neglect the vector-axial interference terms because such terms do not occur in the total production rate. Thus the W-production cross section is written as the sum of two positive terms, one arising from the vector term alone and the other from the axial term.

---

4. The literature of the parton model as it applies to this process is rather extensive. We mention some of the early papers here and refer to the recent articles at place where they are relevant. S.D. Drell and T.-M. Yan, Phys. Rev. Lett. 25, 316 (1970) and Ann. Phys. (N.Y.) 66, 578 (1971); P.V. Landshoff and J.C. Polkinghorne, Nucl. Phys. B33, 221 (1971), B36, 642 (1972); J. Kuti and V. Weisskopf, Phys. Rev. D4, 3418 (1971); S.M. Berman, J.D. Bjorken and J. B. Kogut, Phys. Rev. D4, 3388 (1971).

5. J. Pakvasa, D. Parashar and S.F. Tuan, Phys. Rev. D10, 2124 (1974), D11, 214 (1975).

$$d\sigma/d^3q = \left(\frac{d\sigma_W}{d^3q}\right)_{\text{vector}} + \left(\frac{d\sigma_W}{d^3q}\right)_{\text{axial}} \geq \left(\frac{d\sigma_W}{d^3q}\right)_{\text{vector}}$$

Relating the vector term in W-production to the isovector part of the electromagnetic current we can obtain a bound for W-production of the same mass and at the same center-of-mass energy

$$\frac{1}{3}\ \frac{d\sigma^-_{pp}}{d^3p} + \frac{d\sigma^+_{pp}}{d^3p} \geq \frac{3GM^3}{4\sqrt{2}\ \alpha^2}\ \frac{d\sigma_p^{\ell\bar{\ell},I=1}}{d^3q dM}$$

The peculiar combination of σ^- and σ^+ is required by isospin considerations. In the above inequality, the axial coupling of the intermediate vector boson has been dropped together with the isoscalar part of the electromagnetic current.

For the production of neutral vector bosons the results depend on the form of the weak neutral current. In Weinberg-Salam[6] type models

$$\frac{d\sigma^{W^o}}{d^3q} = (1 - 2\sin^2\theta_w)^2\ \frac{d\sigma^V}{d^3q} + \frac{d\sigma^A}{d^3q}$$

which implies the inequality

$$\sigma^{W^o} \geq \frac{3}{8}\ \frac{GM_W^3}{\sqrt{2}\ \alpha^2}\ (1 - 2\sin^2\theta_w)^2\ \frac{d\sigma^{\ell\bar{\ell}}}{dM}$$

provided that isoscalar terms of the electromagnetic and the weak neutral current are neglected.

If the electromagnetic cross section for the production of $\ell^+\ell^-$ pairs was known then the above equations would provide lower bounds for the production of W's. In the absence of such data at high energies it is noted that the function

$$\phi\ (Q^2/S) = M^3 \left(\frac{d\sigma}{dM}\right)_{\ell^+\ell^-}$$

---

6. S. Weinberg, Phys. Rev. Lett. 19, 1264 (1967); A. Salam in Elementary Particle Physics (N. Svartholm, ed.), Stockholm p. 367.

should scale in the limit S, $Q^2 \to \infty$ with Q^2/S = finite. Thus one can look at the available data at lower energies. A compilation shows that the data from three different experiments[7-9] fall on a smooth curve for $5.5 \le S/Q^2 \le 100$, which suggests that it may well be the scaling limit for the reaction. The curve is also reproduced by a model calculation. Figure 2 shows the data and the theoretical curve, both of which are explained in detail in the next section.

C. Parton Model Calculations

In this section we calculate the production of W mesons and $\ell\nu$-pairs in the quark parton model, see Fig. 1b. In terms of the u,d quark distribution of the proton, the $\ell\nu$ production cross section is given by

$$\frac{d\sigma^{\pm}}{dm_{\ell\nu}} = \frac{G^2}{3\pi} \cos^2\theta_c \, m_{\ell\nu} \, H^{\pm}(\tau)$$

where

$$H^{\pm}(\tau) \equiv \int_0^1 dx_1 \int_0^1 dx_2 \; \delta(x_1x_2-\tau) \; x_1x_2h^{\pm}(x_1,x_2), \quad \tau \equiv m_{\ell\nu}{}^2/s,$$

$$h^{+}(x_1,x_2) = u(x_1)\bar{d}(x_2) + u(x_2)\bar{d}(x_1),$$

$$h^{-}(x_1,x_2) = d(x_1)\bar{u}(x_2) + d(x_2)\bar{u}(x_1),$$

where u(x), $\bar{u}(x)$, d(x) and $\bar{d}(x)$ are the quark, antiquark distributions in the proton. The x is the fraction of the proton momenta carried by the quark. For $W^{\pm}$ production we have

$$\frac{d\sigma^{\pm}}{dm_{\ell\nu}} = \frac{G^2}{12\pi} \frac{m_{\ell\nu}^{\;3}}{(m_{\ell\nu}-m_W)^2 + \Gamma^2/4} \cos^2\theta_c \, H^{\pm}(\tau),$$

---

7. J. H. Christenson, G. S. Hicks, L. M. Lederman, P. J. Limon, B. G. Pope, and E. Zavattini, Phys. Rev. Lett. 25, 1523 (1970).

8. J. J. Aubert, U. Becker, J. P. Biggs, J. Burger, M. Chen, G. Everhart, P. Goldhagen, J. Leong, T. McCorriston, T. G. Rhoades, M. Rohde, S.C.C. Ting, S. L. Wu, and Y. Y. Lee, Phys. Rev. Lett. 33, 1404 (1974).

9. B. Knapp, W. Lee, P. Leung, S. D. Smith, A. Wijangco, J. Knauer, D. Yount, D. Nease, J. Bronstein, R. Coleman, L. Cormell, G. Gladding, M. Gormley, R. Messner, T. O'Halloran, J. Sarracino, A. Wattenberg, D. Wheeler, M. Binkley, R. Orr, J. Peoples and L. Read, Phys. Rev. Lett. 34, 1044 (1975).

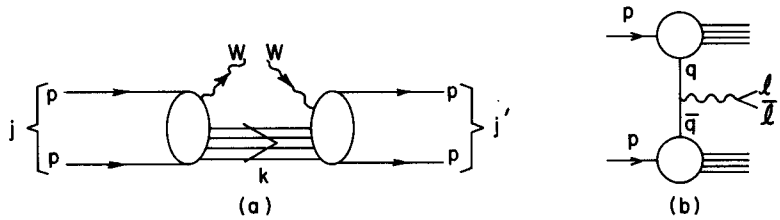

Fig. 1.(a) Lepton pair production in p-p collisions.
(b) Parton mechanism of the production of lepton pairs.

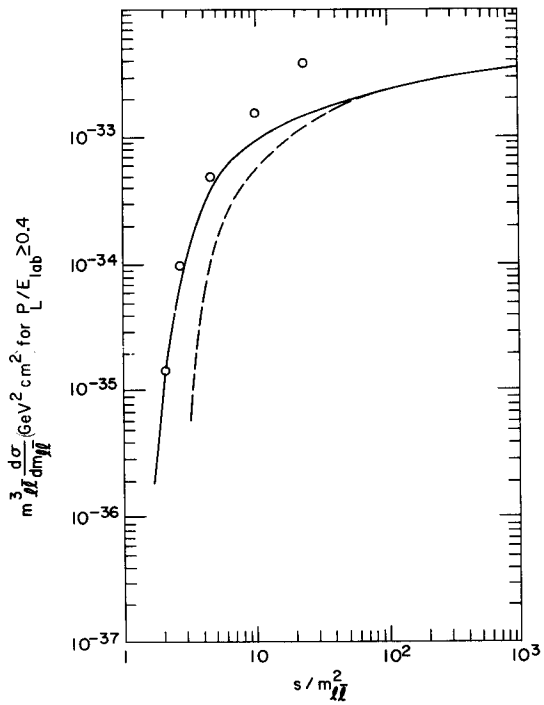

Fig. 2. The scaling function $\phi(Q^2/s)$. The experimental points from the BNL-Columbia experiment[10] are at limited values of Y. The distribution functions described in the text were used for the calculation of the theoretical curve.

where the notation is standard. The integrated cross section is

$$\sigma_W^{\pm} = \sqrt{2}\,\pi G\, H^{\pm}(\tau)\, \cos^2\theta_c .$$

In principle the quark distributions in the proton can be determined from lepton-induced reactions. As a check of the procedure, we compare the presently available $\ell\bar{\ell}$ production data with the predictions of the model. The electromagnetic $\ell\bar{\ell}$ production cross section in pp reactions is given by

$$\frac{d\sigma}{dm_{\ell\bar{\ell}}} = \frac{8\pi\alpha^2}{3m_{\ell\bar{\ell}}^3} \int_0^1 dx_1 \int_0^1 dx_2\, \delta(x_1x_2-\tau)\, x_1x_2\, f(x_1,x_2)$$

where

$$f(x_1,x_2) = \frac{4}{9}\,[u(x_1)\bar{u}(x_2) + u(x_2)\bar{u}(x_1)]$$
$$+ \frac{1}{9}\,[d(x_1)\bar{d}(x_2) + d(x_2)\bar{d}(x_1)\,]$$
$$+ \frac{1}{9}\,[\lambda(x_1)\bar{\lambda}(x_2) + \lambda(x_2)\bar{\lambda}(x_1)].$$

It is well known that the cross sections for lepton pair production in the large τ region are very sensitive to the quark and antiquark distributions at large x ($x \simeq 1$). Lepton induced experiments cannot determine accurately enough the antiquark distributions at $x \simeq 1$. For this reason the set of quark and antiquark distributions which give the closest agreement with available data for the production of $\ell\bar{\ell}$ pairs are chosen. We find that the distributions used by Pakvasa, Parashar and Tuan[5] give the best agreement with the data. The distinctive feature of their fit is that the antiquark distribution near x = 1 behaves like $(1-x)^{7/2}$, which gives a slower vanishing power than other fits. Assuming that the proton is made of valance quarks u_v, d_v and sea quarks,[5] which contain equal distributions of all different types of quarks, they obtained the following quark distributions

$$u(x) = u_v(x) + c(x), \quad d(x) = d_v(x) + c(x),$$
$$\lambda(x) = \bar{\lambda}(x) = \bar{u}(x) = \bar{d}(x) \equiv c(x),$$
$$u_v(x) = 1.79\, x^{-\frac{1}{2}}\, (1-x)^3\, (1+2.3x),$$
$$d_v(x) = 1.107\, x^{-\frac{1}{2}}\, (1-x)^{3.1},$$

$$c(x) = 0.1\ x^{-1}\ (1-x)^{7/2}$$

Using those distributions, we calculate the cross sections.

Figures 2, 3, and 4 show the comparison of the model prediction with the BNL-Columbia experiment,[10] the MIT-BNL experiment,[8] and the FNAL-Columbia-Illinois experiment,[9] respectively. In Fig. 2 we also include a dotted curve corresponding to a model[11] where the sea quark distribution is proportional to $(1-x)^9$. Figure 4 summarizes the results of a calculation with Y integrated over the entire range; it also shows the "experimental points" integrated over the Y range according to the model.

The model does give a reasonable agreement with the experiment. However, one needs more data at higher energies to check scaling. The main conclusions are: (1) The data from three different experiments seem to fall on a smooth curve, which suggests that it could be the scaling limit for the reaction; (2) The curve is close to the scaling curve obtained from the parton model with an antiquark distribution proportional to $(1-x)^{7/2}$.

Using the same quark distributions we can calculate the production cross sections for W^+ and W^- separately, as shown in Figs. 5 and 6. It is noted that the cross section for the production of W^+ is larger than that of W^- as is evident from the fact that there are more u quarks than d quarks in the proton. In the same figure we also show the corresponding cross sections for $\bar{p}p$ collisions. The cross sections for W^+ and W^- are now equal. The cross sections for $\bar{p}p$ beams[12] are at least an order of magnitude larger than the average cross section

---

10. L. M. Lederman, Columbia preprint, Dec. 6, 1974.

11. H. P. Paar and E. A. Paschos, Phys. Rev. D10, 1502 (1974). For still another parametric form see, G. Farrar, Nucl. Phys. B77, 429(1974).

12. This conclusion is also confirmed by G. Altarelli, N. Cabibbo, L. Maiani and R. Petronzio, Nucl. Phys. B92, 413 (1975).

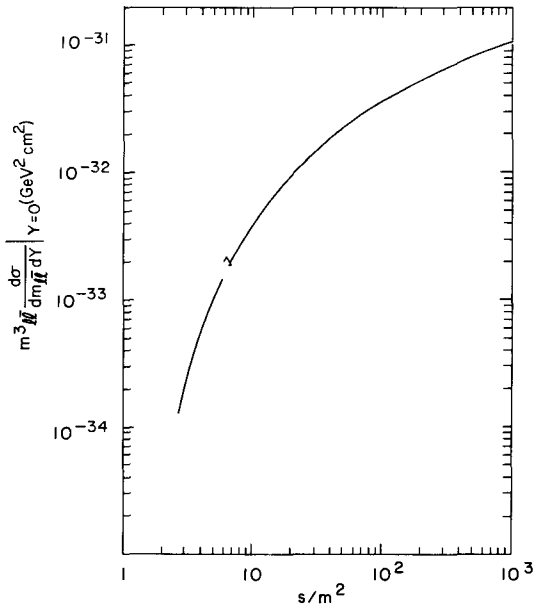

Fig. 3. The scaling function for the BNL-MIT experiment.

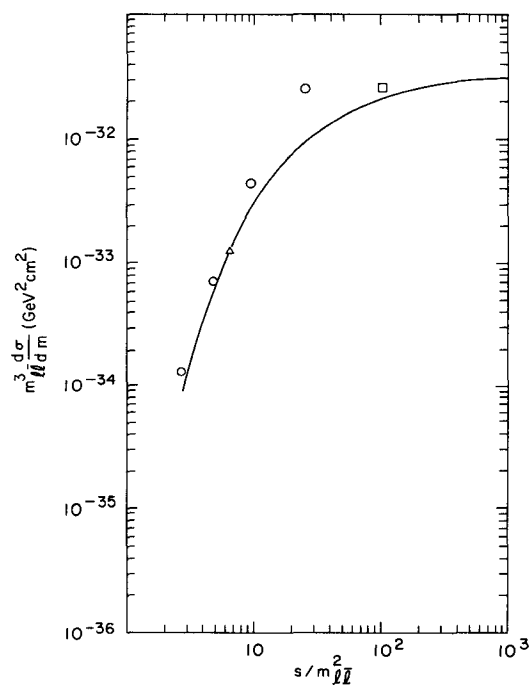

Fig. 4. The scaling function integrated over the entire region of Y. The experimental points involve an integration, according to the model, over the unobserved region of Y.

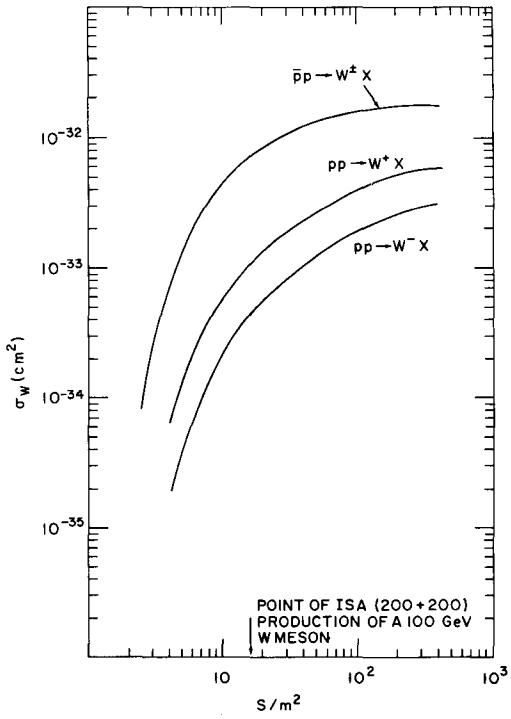

Fig. 5. Production cross sections for the reactions (a) $\bar{p}p \to W^{\pm}x$, (b) $pp \to W^{+}x$, and (c) $pp \to W^{-}x$.

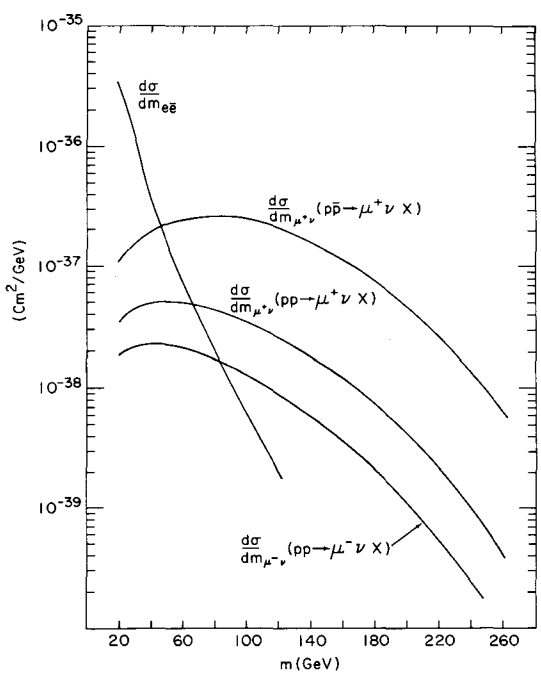

Fig. 6. Differential cross sections in the absence of a W for reactions. (a) $\bar{p}p \to \mu^{\pm}\nu x$,

$$\frac{1}{2}\,[\sigma(pp \to W^+ + x) + \sigma(pp \to W^- + x)].$$

This is a consequence of the fact that there are more antiquarks in the antiproton.

D. Decay Modes

The easiest signature for detecting W's uses its leptonic decay modes. To estimate the leptonic branching ratio we use the fact that its mass is heavy enough so that asymptotic limits hold. The hadronic width[13] for $W^{\pm}$ is given by

$$\Gamma(W \to \text{hadrons}) = \frac{GM_W^3}{3\pi\sqrt{2}}\ R$$

where

$$R = \frac{\sigma(e\bar{e} \to \text{hadr.})}{\sigma(e\bar{e} \to \mu\bar{\mu})}$$

and the axial contribution was set equal to the vector contribution. The branching ratio is

$$B = \frac{\Gamma(W \to \mu\nu) + \Gamma(W \to e\nu)}{\Gamma(W \to \text{hadrons})} = \frac{1}{R}$$

where $R \approx 5.5$ at $\sqrt{Q^2} = 7$ GeV. This is a sizable ratio for the experimental observations. But even a logarithmic rise in R, which is suggested by some theories, and is not inconsistent with the data,[14] gives $B \approx 0.08$ for an $M_W \approx 100(\text{GeV}/c^2)$. Thus the detection through the leptonic modes seems possible.

The unique signature for charged W-production is a peak in the perpendicular momentum of the produced muon (or electron). Figure 7 shows again a parton model calculation[15] with the momentum distributions described in the previous section. Two sharp peaks are

13. J. D. Bjorken, Phys. Rev. 148, 1467 (1966); L.-F. Li and E. A. Paschos D3, 1178 (1971).

14. J. A. Kadyk, et al., in Colloque de Neutrino at Haute Energie, Paris (1975), p. 17.

15. For similar calculations at lower energies see, R. L. Jaffe and J. R. Primack, Nucl. Phys. B61, 317 (1973).

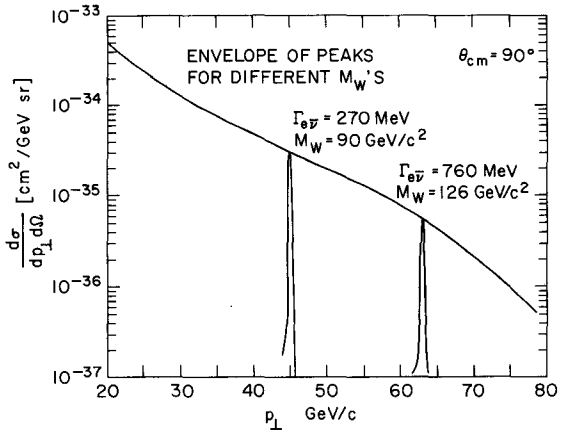

Fig. 7. The double differential cross section as a function of lepton transverse momenta.

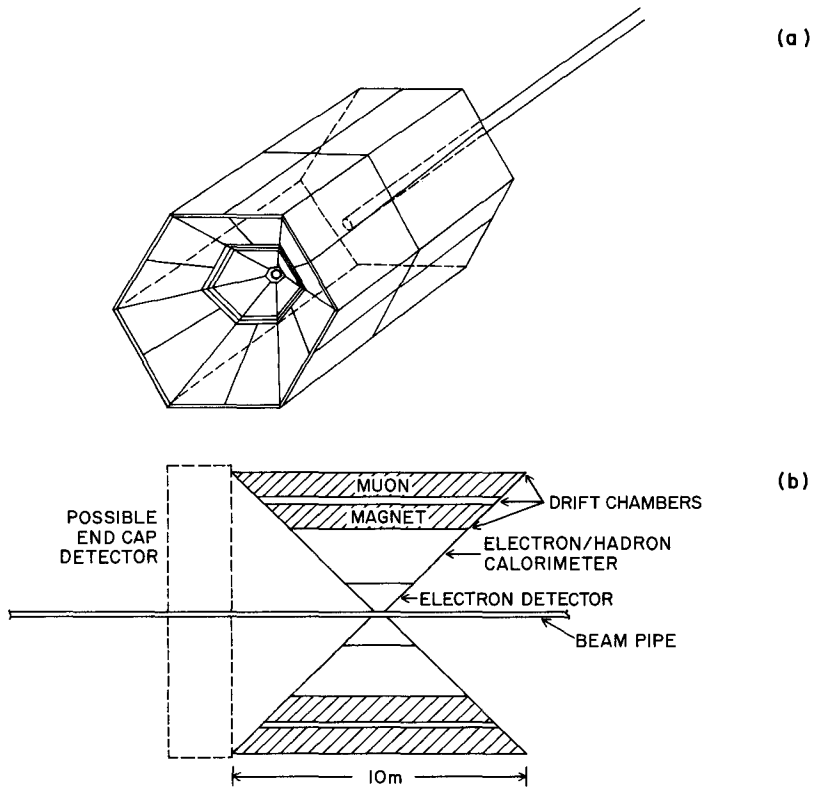

Fig. 8. General configuration of lepton detector.

shown at $p_\perp \approx 45$ and 63 GeV/c corresponding to W's of 90 and 126 GeV/c^2, respectively. The smooth curve is the envelope of the peaks of such curves for different W masses and for $S = (400)^2 (\mathrm{GeV})^2$.

The signature for Z^o is much better since one can measure the dimuon (dielectron) pairs and search for a peak in their effective mass. An open issue here is the distinction of an intermediate vector boson from an ordinary hadron. A signature in this case comes from a measurement of the leptonic decay width. For $M_W \approx$ 100 GeV the width is of the order of 100 MeV. In contrast, electromagnetic decay of an ordinary vector meson, i.e.,

$$V \rightarrow \gamma \rightarrow e^+e^-$$

can be estimated by vector meson dominance

$$\frac{\Gamma_V}{M_V} \approx \frac{\Gamma_P}{M_P} \approx \frac{\Gamma_J}{M_J}$$

to give a width of the order $\sim$ 1 MeV. Thus the difference in widths distinguishes between the two cases.

II. Experimental Apparatus

A. Introduction

We have designed a detector to look for the most characteristic signature of $W^\pm$ and Z^o production, high transverse momentum leptons. The device can be used for either single lepton or dilepton searches and has sufficient solid angle to be able to deduce the existence of a neutrino, from the $W^\pm$ decay, via the imbalance in transverse momentum. In addition, since this detector will be exploring a new region of physics, we felt that versitility was desirable and therefore it was designed with the capability of identifying both electrons and muons.

The general configuration of the lepton detector is shown in Figs. 8a and 8b. The purpose of the inner section of the detector

is to detect the electron from the W decay while at the same time reject with good sensitivity the presence of a hadron. The electron identifier in conjunction with the calorimeter should, at $p_\perp > 10$ GeV/c, discriminate against pions at the level of 10^{-4} while still detecting most of the leptons. This high rejection level was chosen to protect ourselves from "surprises" at very high energies.

The e-π separation of approximately 10^4 to 1 can be achieved by having an electron identifier which can detect leptons with less than 1% pion background while the calorimeter, occupying the middle section of the detector, can achieve another factor of 100 in the hadron-electron separation. Such a calorimeter can be designed with its front end built for maximum sensitivity to electromagnetic showers, while the rest of the module can be optimized as a hadronic calorimeter. The outer section of the detector, the muon identifier, is composed of magnetized iron. This should allow a measurement of muon momentum to an accuracy of roughly 12%.

A serious constraint on the design of the entire detector is the desirability of keeping transverse dimensions as small as possible to reduce the muon background in the outer muon detector as a result of π-μ decays. Another reason for size constraint is that the volume of the outer muon identifier goes as R^3 where R is the transverse dimension of the detector. A large R would lead to a rapid increase in the amount of iron in the muon detector, whose cost is already a dominant factor in the cost of the total detector. We should add that the electron detector is being designed as a "plug-in unit" that could be removed and replaced by shielding, making the overall apparatus a muon detector with an even better $\pi \rightarrow \mu$ decay rejection.

If the pion background turns out to be severe at the highest ISABELLE energy, one can reduce this background substantially by reducing the machine energy while not severely reducing the W decay signal for W masses below 100 GeV/c^2. This is because the continuum

pion production at large $p_\perp$ increases faster with center of mass energy then the W production cross section, which should not vary much with energy in the region starting a few GeV above threshold, and the peak in $p_\perp$ stays roughly at $M_W/2$.

In addition to the detector shown in Figs. 8a and 8b, one will have "end caps" composed of calorimeter modules, in order to catch missing transverse momentum. We have also considered an optional modification of the detector which uses a magnetic solenoid in the central region.

B. Electron Identification Module

1. Transition Radiation Detectors. Detection of the transition radiation produced when a relativistic particle passes through an abrupt interface between two materials of different electron densities has been proven to be a practical and very powerful tool for the detection of particles with high $\gamma[\gamma = (1-\beta^2)^{-\frac{1}{2}}]$. It is this technique that we propose to use as the primary element of the electron identifier.[16] An extremely efficient transition radiator that has been constructed consisted of stacks of a large number of thin lithium foils followed by a xenon-gas filled MWPC to detect the x-rays from the radiator.[17] Such a radiator-detector system has been extensively tested and is being used for electron identification in an experiment at the ISR with a very similar geometry to the one proposed here.

We determine the optimal performance of our electron identifier by extrapolating the performance of the ISR detector to our region of kinematic interest. The ISR detector is optimized for electrons in the 1 to 5 GeV/c range, while our detector needs to be optimized for the detection of electrons in the 10 to 50 GeV/c range, while

---

16. G. M. Garibian, Scientific Report EØH-27, Yerevan Physical Institute, (1973).

17. J. Fischer, S. Iwata, V. Radeka, C. L. Wang and W. J. Willis, BNL-20063, Nucl. Instrum. & Methods (in press).

providing good pion rejection in this region. The total energy radiated from a single foil increases linearly with γ so that in principle the x-ray intensity should increase linearly with the momentum of the particle. At particle energies above a few GeV/c, the limitation in the π-e separation is the Landau tail in the ionization energy deposited by the pions in the xenon MWPC. While an increase in the momentum of the pions increases the ionization energy loss due to the relativistic rise ($\sim$ 30% increase), we would expect a much larger increase in the x-ray yield (a factor of 10). Hence overall we would expect a large improvement in the π-e separation at higher energies. In practice, however, there are two factors which severely limit this improvement. One is the fact that as γ increases, the maximum frequency of the emitted x-ray radiation increases linearly, while the intensity at a particular frequency only increases logarithmically. Hence most of the additional energy comes in the form of high energy x-rays ($>$ 20 keV). Unfortunately these high energy x-rays are hard to detect with MWPC because the total photon cross section falls as a high power of the incident x-ray energy. The other limitation is due to the saturation in the production of x-rays due to existence of limiting distances between surfaces called formation zones.[16] The net effect of these two limitations is to allow the detection of only a window of x-ray energies. This is clearly seen in Fig. 9.

We have been able to optimize our detector for the energy regime between 10 and 50 GeV, by using a thickness of lithium foils of 1.25 mils and a foil separation of 20 mils. With this geometry we calculate that 500 foils will yield a detected x-ray intensity 40% larger than the ISR detector. This is sufficient to offset the 30% increase in the hadron energy deposition. Hence we expect the π-e separation to remain the same as in the ISR detector, namely about 200 to 1. In addition, the transition radiator can achieve better pion rejection if we lower slightly its electron detection

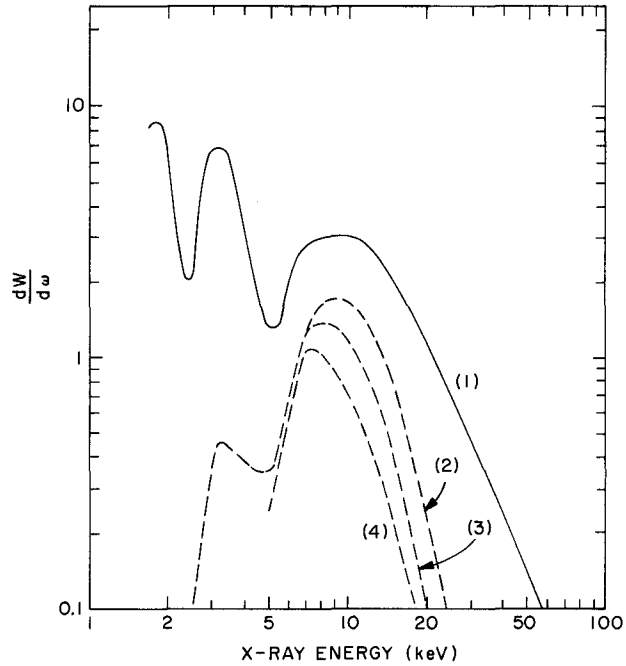

Fig. 9. X-ray spectrum from Transition Radiator, assuming no absorption in Li foils (curve 1). Curves 2 through 4 include absorption and detection efficiencies in 2.08, 1.04 and 0.52 cm Xe respectively.

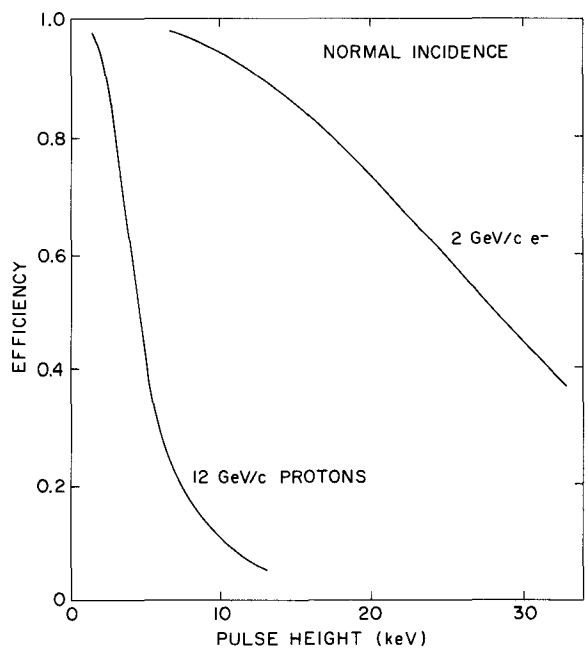

Fig. 10. Pion-Electron Discrimination in Transition Radiator.

efficiency. This can be seen clearly in Fig. 10 (Ref. 18), where the pion trigger can be reduced from 20% to 5% for a decrease in the electron trigger from 97% to 90%. This is the rejection level for 1 transition radiator unit. Hence for two units, the levels become 2.5×10^{-3} for pions and .80 for electrons.

2. Design Description. The electron detector will consist of a set of Li foil transition radiators (TR). In order to get better than 100 to 1 electron to pion separation, the energy deposited by the x-rays from two stacks of transition radiators is sampled. Each stack will consist of 500 1.25 mil Li foils separated by 20 mils, making each stack about 27 cm long. The spacing between foils will be accurately maintained by having dimples in the foils themselves. The boxes made out of sheet metal will be supported from the top and outer side with aluminum channel. In addition there will be a thin metal plate at the bottom of each stack to support the weight and a mylar window at the top thin enough to allow the x-rays to get through. Each stack will have dry helium flowing through it to keep the humidity out. The layout of these chambers is shown in Figs. 11 and 12.

Right outside the pipe will be a set of 2 PWC in an hexagonal arrangement around the pipe. These are followed by 6 TR units around the pipe as shown in Fig. 11. One Xe chamber will measure the x-ray energy from the electrons. Next there is a thin gold foil to stop the x-rays and another PWC to measure the ionization energy from the track coming through to make sure it is a minimum ionizing track. This group is followed by 24 TR units, four in each sextant as shown in Figs. 11 and 12. These are subdivided because for the outer TR the dimension of the foils would be 77×156 cm^2 and they could not support their own weight. This last unit is followed by a Xe PWC to sample the x-ray energy from this last unit.

---

18. This graph is taken from the report of W. J. Willis on Test Results of TR Detectors distributed at the 1975 ISABELLE Summer Study.

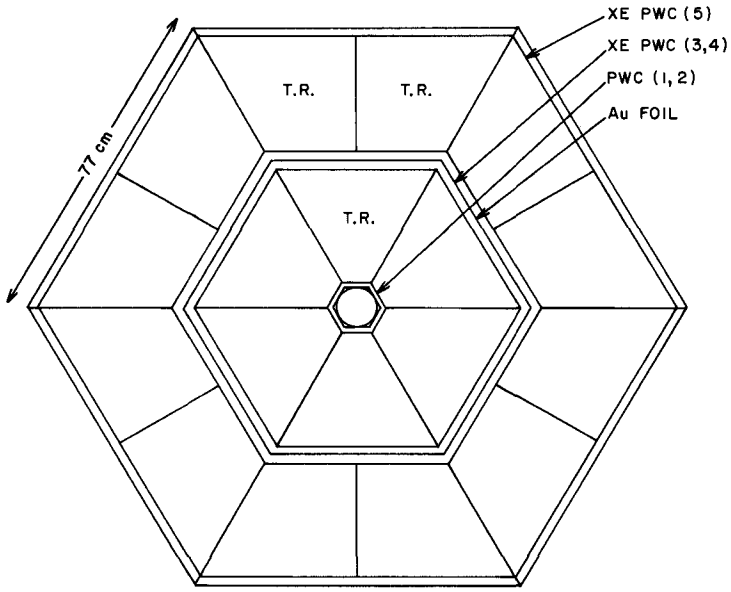

Fig. 11. Layout of Transition Radiator, beam view

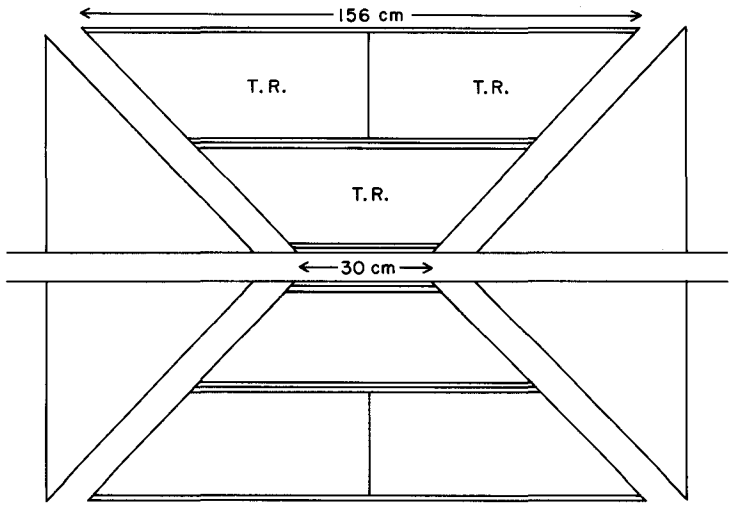

Fig. 12. Layout of Transition Radiator, side view

The PWC will have 2 mm wire spacings except for the innermost ones which will be 1.5 mm. The innermost chambers will have 50 wires each leading to a total of 50 $\times$ 12 = 600 readout wires. They cover a length of 30 cm. The middle chambers have 220 readout wires each giving rise to a total of 2640 readout wires. The outermost chambers have 385 readout wires each or a total of 2310 readout wires. This gives rise to a total of 5550 readout wires. Each wire will be read out at both ends to get rough track coordinates along the beam direction by using the method of current division. The innermost chambers will be run in the mode that will maximize its fast response since they are in a "hostile environment". The other chambers farther out will use Xe as the detecting gas.

An electron signal will consist of a charged track that gives a signal in every chamber, a large signal in chambers 3 and 5, and a minimum ionizing particle signal in chamber 4. The electron pion separation suffers because the ionization loss of the pions has a Landau tail which gives an energy deposition as large as that of the x-rays from the TR stack. One can decrease this effect by sampling the ionization from many stacks and hence reduce the Landau tail. If there is a constraint on size then increasing the number of stacks reduces the number of foils in each stack and hence reduces the x-ray output from each stack. We have compromised by using 2 stacks as a reasonable detector. Nevertheless, 3 stacks comprising the same dimensions but with reduced distances between foils is also adequate and might give a somewhat better π-e separation.

In Table I we give a rough cost estimate for the entire electron identification module.

C. Electron-Hadron Calorimeter

The middle section of the detector is a calorimeter, composed of two cylindrical units, one optimized for electrons and the outer one for hadrons. Figure 13 shows the calorimeter position relative to the inner section, described previously.

TABLE I. Cost Breakdown

Item	Chamber Cost	Readout Cost
1. 12 Inner PWC's 1.5 mm wire separation 600 readout wires[a]	$10 K	$30 K
12 PWC's after the first T.R. stack 2 mm wire separation 2640 readout wires[b]	12 K	66 K
6 Outer PWC's 2 mm wire separation 2310 readout wires[b]	16 K	58 K
	$38 K	$154 K
2. Li Foils[c]	13 K	
3. Miscellaneous	10 K	
TOTAL		$215 K

a. Each wire has readout on both sides with a current division method. We calculate costs based on $25/readout = $50/wire. This cost includes amplifier, transformer and one ADC every eight wires.

b. Adjacent wires are connected together so that the number of electronic elements is reduced by a factor of 2.

c. Based on 30 μ foils at $450 per pound.

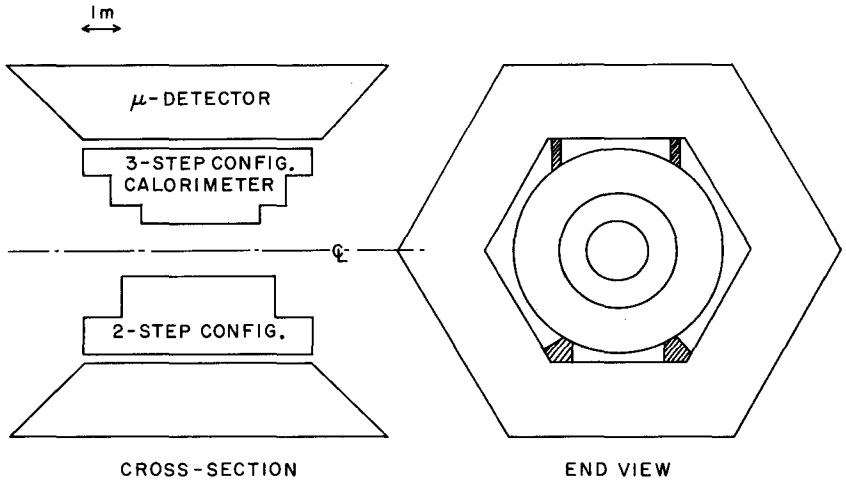

Fig. 13. Layout of calorimeter module in lepton detector.

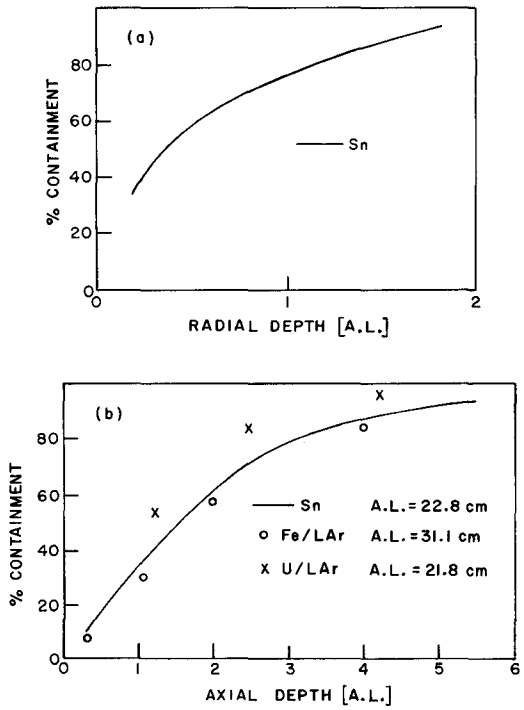

Fig. 14. Hadronic shower containment

The calorimeter is a liquid argon ionization chamber which will measure the ionization without any electron multiplication.[19] The active medium liquid argon, a condensed material ($1.4 g/cm^3$) which does not attach electrons, has a high electron mobility (5 mm/μs at 1 kv/mm). The electronegative impurities are frozen out in the liquid argon (86^oK).

We propose a calorimeter with large number of thin plates to minimize the sampling fluctuations while keeping the average density high. For the electron section, the number of radiation lengths of steel (or lead) needed is 20, which has a total thickness of 20 $\times$ 1.8 cm = 36 cm of steel (or 11 cm of lead). The problem of hadronic shower containment has been studied[20,21] and some of the results are shown in Fig. 14. For the hadronic section we need an additional 8 interaction lengths, to what exists in the first section, giving a total of 10.5 interaction lengths. This will be composed of 100 plates of steel, 1 cm thick, separated by .5 cm. The total thickness of the calorimeter will be 2 meters. Details of the mechanical support of the steel plates are shown in Fig. 15. The construction does not introduce any significant dead spaces.

The charge collection will be done by using mylar with copper evaporated on both sides. The mylar will be divided into 5 cm $\times$ 5 cm sections for the electron unit and 30 cm $\times$ 30 cm sections for the hadron unit. These sections are chosen with the requirement that the probability of a high transverse momentum π^o being associated with a charged $\pi^{\pm}$ (thereby interpreted to be an electron) in one cell is roughly 1 / 800. The detailed characteristics of one hadron cell are shown in Table II.

---

19. W. J. Willis, V. Radeka, Nucl. Ins. and Methods, 120, 221 (1974).

20. C. W. Fabjan and W. J. Willis, Physics Limitations of Calorimetry, Proceedings of FNAL Workshop on Calorimeters, May 9-10, 1975.

21. J. Engler, W. Flager, B. Gibbard, F. Monning, K. Runge and H. Schopper, Nucl. Ins. and Methods, 106, 189 (1973).

TABLE II. One Hadronic Calorimeter Cell:

1 cm Steel + .5 cm Liquid Argon

	Steel	Liquid Argon	Average in Chamber
ρ, g/cm^3	7.9	1.4	5.7
dE/dX, MeV/cm	11.6	2.2	8.5
Rad. Length, cm	1.77	13.5	2.5
E Crit., MeV	21	30	21
Rad. Length/Cell	.57	.036	.61
Int. Length, cm	12.9	65	17.5
Dielectric Const.		1.6	

dE(Liquid Argon)/dE(Liquid Argon + Steel) = .11;

Drift time = 180 ns/mm

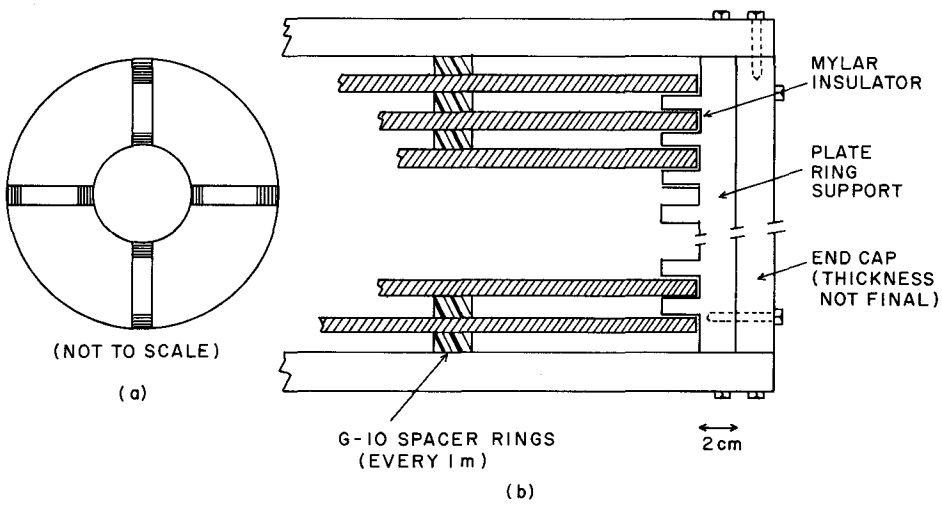

Fig. 15. Mechanical Support for Calorimeter Plates. (a) End cap and plate ring support. (b) Side view.

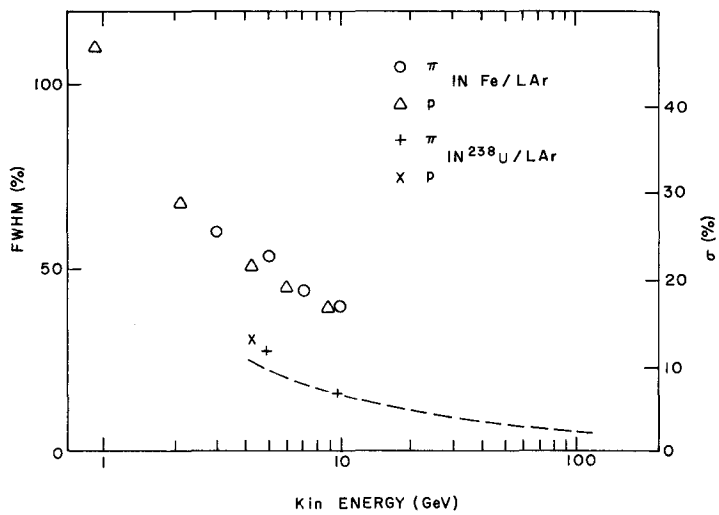

Fig. 16. Energy Resolution for an Argon Calorimeter.

From Table II, one sees that the sampling is acceptable since a single cell represents roughly 1/5 of the radiation length, and the energy loss across a cell is less than the critical energy. For this configuration, .61 picocoulomb per GeV of the energy converts into showers.[19] The energy deposit necessary to give a signal corresponding to one electron is 264 eV,[19] while the rms noise is typically 18.2 MeV. The noise contribution to the linewidth, or the "electronic resolution" is FWHM = 43 MeV.[19] The expected electron energy resolution is then $2\%/\sqrt{E}$ while for the hadron, it will be $20\%/\sqrt{E}$, with E in units of GeV (see Fig. 16). The decrease in accuracy for hadrons is the result of the nuclear binding effect. While the use of uranium decreases this effect, we only considered steel for simplicity.

The approximate cost of the calorimeter is between .75 and 1 million dollars.

D. Muon Identification

1. Resolutions and Backgrounds. The outer section of the detector uses magnetized iron, both as a shield against hadrons and as a momentum measuring apparatus for muons up to 50 GeV/c. A rough sketch of the apparatus is shown in Fig. 17.

The momentum resolution ($\Delta p/p$) for muons transversing the magnetized iron is shown as a function of thickness in Fig. 18. We have assumed a magnetic field of 20 kG and a measurement error of $\sim \pm$ 0.25 mm. As can be seen, the resolution is dominated by multiple coulomb scattering and is roughly momentum independent. For the size of our detector, roughly 2 meters thick, $\Delta p/p$ = 12%. Notice that although the resolution improves like $\sqrt{\ell}$, the costs increase like ℓ^3 so muon resolutions better than 10% are prohibitive. Moreover, if one insists on an electron/calorimeter core followed by a muon shell, then costs dictate that the calorimeter provide some of the magnetized iron for muon measurement. We will now show that the above resolution is adequate.

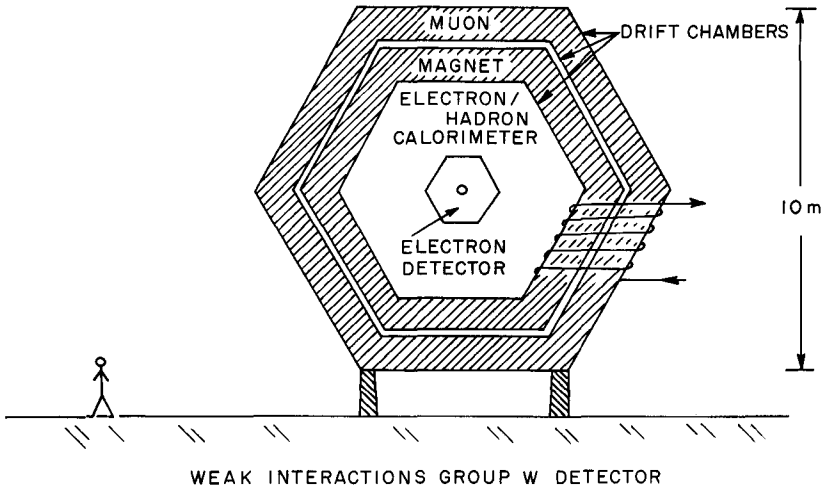

Fig. 17. Muon Magnet Layout.

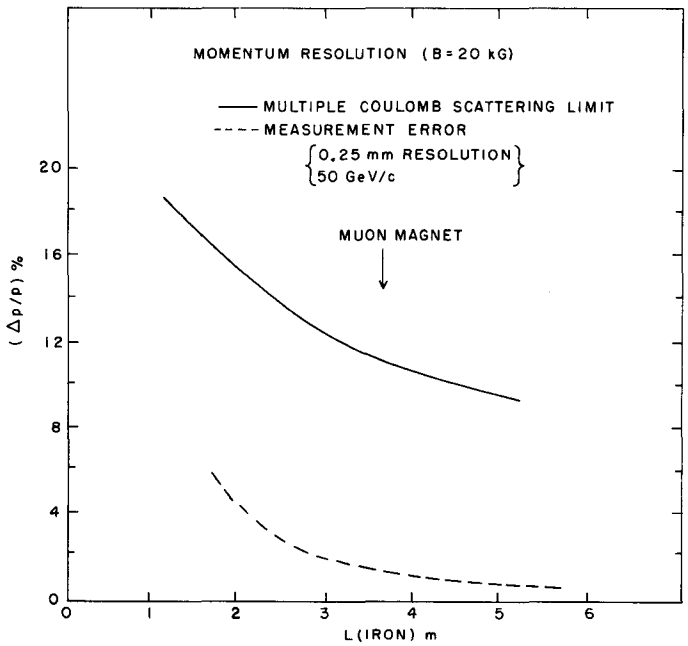

Fig. 18. Momentum Resolution in Muon Detector.

The minimum scale for the resolution is set by the natural line width of the W, which is expected to be no larger than a few percent. A second fundamental smearing comes from the transverse momentum distribution in the production of the W. The first order effect for production of mass M_w and transverse momentum $p_\perp^w$ is:

$$\frac{\Delta p_\mu}{p_\mu} = \frac{p_\perp^w}{M_w} \quad \text{for } p_\perp^w \ll M_w .$$

Therefore, if the W is produced with transverse momentum less than 10% of its mass, then the muon resolution is limited by the measurement error. Assuming that such is the case, we estimate the signal-to-background for three processes:

a. $\pi \rightarrow \mu$ decay from high $p_\perp$ pions

b. Direct production of high $p_\perp$ muons

c. π punchthrough.

For $M_w < 100$ GeV, $\pi \rightarrow \mu$ decay is the dominant process. The π spectrum in $p_\perp$ is expected to be of the form:

$$\frac{d\sigma}{dp_\perp} = \frac{\text{Constant}}{(p_\perp)^n} .$$

The effective cross section for μ's from π decay with momenta within one resolution width of $M_w/2$ can then be calculated:

$$\sigma_{eff}^{\pi} = \frac{4\alpha p_d}{(n-1)(n-\alpha)^{n-1}} \; p_\perp \frac{d\sigma}{dp_\perp} \Bigg|_{p_\perp = M_w/2}$$

where

α = muon momentum resolution = 12%

p_d = π decay probability.

We have then calculated σ_{eff}^{π} under two different assumptions. In the first case we use the CCR parameterization

$$\frac{d\sigma}{dp_\perp d\Omega} = \frac{1.54 \times 10^{-26}}{(p_\perp)^{7.24}} \, e^{-26.1 \, p_\perp/\sqrt{5}} \; \frac{cm^2}{GeV.sr}$$

and assume that it is valid over the entire region of interest. In the second case we only have the CCR parameterization out to $p_\perp$ = 10 GeV/c and then assume a "worst" case that n = 7.4 is correct for $p_\perp$ < 10 GeV and then changes suddenly to n = 3, for higher $p_\perp$. Table III shows the results for σ^{π}_{eff} as a function of $p_\perp$ for these two different cases.

Since the cross section for W production is expected to be of the order of 10^{-33} cm^2, with a leptonic branching ratio of 1/3, the signal-to-background should be greater than 10^3 for M_W > 30 GeV.

One can also use the Table III to estimate the sensitivity to weak muon production in the <u>absence of a W</u>. This cross section is estimated to be:

$$\frac{d\sigma}{dp_\perp} = 10^{-37}\ cm^2/GeV.$$

If the CCR parameterization is correct, then the weak muon production is greater than the $\pi \rightarrow \mu$ background for $p_\perp \geqslant 20$ GeV. Of course, the signal-to-background improves enormously if one demands an imbalance of transverse momentum as a neutrino signature. Reducing the π decay length by filling the central core (at the expense of electron identification) would improve this by a factor of about 5. If there were no measurement error on the muon momentum, the ratio would improve by another factor of about 8.

The apparatus has approximately an 8 GeV cutoff when both ionization energy loss and bending in the magnetic field are considered. Assuming a luminosity of 10^{33} cm^{-2} sec^{-1}, $d\Omega$ = 8 and a decay space of 1.5 m we obtain a rate for pions decaying into muons with p_T > 8 GeV/c of 10^{-2}/sec. The rate clearly would be reduced substantially if the electron detector was replaced with an absorber. Hadron penetration drops exponentially with an absorption length of 20 cm in iron. In the first few absorption lengths secondary hadrons are produced which might penetrate the iron but most of these will be below the 8 GeV cutoff. Making reasonable assumptions, the hadron penetration rate with 16 absorption lengths is smaller than the rate

TABLE III. Background Estimates: $\sigma^{\pi}_{eff}(cm^2)$

$p_\perp = M_W/2$ (GeV/c)	CCR	$n = 3$ for $p_\perp > 10$
2	4.3×10^{-30}	
5	4.6×10^{-33}	
10	2.2×10^{-35}	
15	8.4×10^{-37}	8.1×10^{-36}
20	7.6×10^{-38}	2.5×10^{-36}
30	2.1×10^{-39}	3.6×10^{-37}

of muons from pion decay even with a substantially shorter decay path then assumed above.

2. Muon Magnet. The design shown in Fig. 17 consists of a hexagon with an overall height of 10 m. The first 3 meters from the beam pipe will be occupied by the electron detector and the hadron calorimeter. It is assumed that the hadron calorimeter is = 75% iron which is magnetized and therefore constitutes part of the magnetic path for the muons. Along the beam line, the magnet is pyramidal in shape to allow coverage from $\theta = 90 \pm 45^{\circ}$.

a. Effect on Large Lepton Hall. This device cannot be accommodated in the present design of the experimental building, and we therefore make the following suggestions:

i. The minimum clearance in all directions around the beam centerline be 7 meters. (We note that the current "yellow book" shows the beam only 4.5 meters from the floor).

ii. The crane coverage should have at least a 40 ton capacity. Clearly, a larger crane would be desirable, but not essential.

iii. Since this device will weigh in excess of 5000 tons (see below), care should be taken in considerations of floor loading design.

b. Construction Considerations. The muon magnet consists of 580 m^3 of iron, with a total weight of approximately 5000 tons. In addition to the floor loading problems, this mass presents some difficulty in assembly. We envisage this device being welded from some 200 pieces, all of which would be less than 40 tons.

The current cost of scrap iron is \$100/ton. A conservative estimate indicates that this cost will triple when shipping is considered. Thus, the cost of the iron will be $\sim$ 1.5 million dollars. We estimate that the manufacture of the device, including the winding of the coils will cost $\sim$ \$800,000 (based on experience at NAL). Therefore, the muon magnet can be completely installed for 2.3 million dollars. It may be possible

to obtain surplus iron or iron currently on site.

c. Power Requirements. The momentum resolution varies linearly with the magnetic field B and only as the square root of the length of iron. Therefore, it is desirable to obtain as high a magnetic field as possible. For B = 20 kG at a radius of 5 meters, approximately 10^6 amp turns are required. This results in 4 megawatts with 20 tons of copper coil. A lower field = 16 kG can be obtained with only 0.8 megawatts and 4 tons of copper coil. In either case, water cooling is necessary.

d. Magnetic Field and Momentum Acceptance. Assuming that the magnet will be run at 20 kG and that a muon travels through a field length of $\sim$ 350 cm, the minimum momentum muon which can reach the outside of the muon magnet is 7.8 GeV/c, when effects of dE/dx and bending in the magnet are considered. This momentum cutoff insures a relatively clean trigger from π decay backgrounds as discussed above.

3. Detectors. The error in momentum arising from multiple scattering in the iron decreases only as the square root of the length. Limits on momentum resolution also arise from the accuracy with which tracks can be measured. The tracks should be measured with sufficient accuracy, approximately 0.5 mm at 50 GeV/c, so that the error in momentum is dominated by multiple scattering. Furthermore, plural scattering and other nongaussian effects can lead to large momentum errors and thereby cause low momentum particles to appear to have high momenta. To detect these effects it is necessary both to over-constrain the momentum determination and to measure tracks with an accuracy of approximately 0.25 mm. In the present design the muon is measured in four places with a position and angle measured at each plane. This results in approximately 700 m^2 of surface to be covered by chambers (1400 m^2 of planes).

These detectors are drift chambers. Assuming that we design chambers based on current technology (4-m $\times$ 4 m chambers with 10 cm wire spacing), this necessitates $\sim$ 8000 wires at a cost of \$30/wire for a detector cost of \$240,000.

We anticipate being able to use the chambers themselves as the triggering device rather than having to use an additional bank of scintillation counters.

E. Optional Central Detector: A Magnetic Solenoid Spectrometer

An alternative central detector, which is complementary to the transition radiator device discussed earlier, is a magnetic solenoid spectrometer. In fact, one might design the outer electron-hadron calorimeter to accept either i) the transition radiator detector, ii) a steel core for purely muonic experiments, or iii) the magnetic solenoid.

The strengths of a magnetic spectrometer are the ability to determine the sign of charged particles in particular electrons, and measure their momenta for $p \leqslant 50$ GeV/c. The specific goals of the design discussed here are to obtain: i) $e^{\pm}$ sign (a unique feature of this detector) and momentum determination, as well as separation of Dalitz pairs, ii) electron-pion separation (a rejection factor of roughly 10^4) against π's via the correlation between momentum measurement in the magnet and energy measurement in the shower detector, iii) $\mu^{\pm}$ sign and momentum, which is redundant with muon identifier, and iv) information on the interaction topology, which is especially useful should the W decay hadronically into multiple, isotropic, high $p_{\perp}$ hadrons ($\sim$ 10 particles each with $\sim$ 5 GeV/c).

1. Required Fields and Resolutions. The scale (a radius of L = 0.75 m) of the solenoid detector is set by space and cost constraints of the outer detector. Obtainable magnetic fields are on the order of 10 kG. For 50 GeV/c particles, this implies a sagitta of

$$\sigma = \frac{R\theta^2}{8}$$

$$R(m) = \frac{33\ p\ (GeV/c)}{B\ (kG)}$$

$$\theta = \frac{L}{R} = \frac{0.75\ m}{R\ (m)}$$

$$\sigma = \frac{R\theta^2}{8} = \frac{R(.75)^2}{8R^2} = \frac{0.07}{R}$$

$$\sigma = \frac{.07 \times 10\ (kG) \times 1000}{33\ p\ (GeV/c)} = \frac{21.3\ mm}{p\ (GeV/c)}$$

Note that σ is proportional to L^2. The best spatial resolution obtainable today is $\sim 100\ \mu$ with drift chambers. Figure 17 shows the momentum resolution for this spatial resolution. Note that with 10 kG a 50 GeV/c particle is measured with $\Delta p/p = 20\%$, which is certainly sufficient for a sign measurement.

2. Central Detector Design. The design and discussion of the solenoidal magnet follow closely Report #148 of the 1974 PEP Summer Study.

The main requirements on the solenoidal detector are:

a. Small radial dimensions of the magnet so that it fits into the electron-hadron calorimeter and muon identifier discussed earlier, i.e., so that the volume and cost of the entire detector is kept to minimal values.

b. Accurate position measurements inside the magnet in order to obtain optimal momentum measurements for charged particles.

c. Thin magnet coils to minimize the energy deposited by showers in the coils.

d. Incorporation of coils and flux return into the electron calorimeter and muon identifier so as to minimize their interference with the overall detector.

e. Little material in position location devices to minimize photon conversion.

Figure 20 shows a side view of the detector, while Fig. 21 shows cross sectional view.

3. Charged Particle Detector. Five cylindrical two-dimensional wire chambers are placed inside the solenoid to provide momentum measurements for the charged particles. It might be advantageous to insert scintillation counters before the first wire chamber to identify photon induced showers. Drift chambers without electric field shaping have achieved spatial resolution better than $\pm$ 75 μ even in a magnetic field as high as 15 kG.[22]

Figure 19 shows the uncertainty in the momentum of the charged particles calculated for B = 5 kG and 10 kG, including multiple scattering in the chambers, and assuming Δx = 0.1 mm and Δx = 0.2 mm for the position measurement. A total of 0.027 radiation length of material including styrofoam, aluminum, mylar, glue, wires, chamber and interchamber gas was assumed. The magnet radius is 0.75 m. It appears that 5 kG is a reasonable value for the magnetic field, and with Δx = .1 mm provides sign determination to 50 GeV/c.

4. Conventional Magnet. The design of a normal magnet involves considerations of power consumption and the number of radiation lengths in the coil wall. A tradeoff between these factors leads to a coil thickness of 5 cm of aluminum. This needs 1.2 MW of power at full field (5 kG). About 35% of the γ's will convert in this coil (0.5 rad lengths) which will serve as the first radiator of the shower detector-hadron calorimeter. The parameters for this design are shown in Table IV.

The iron return yoke is designed to leave the end regions open for additional particle detectors (see Fig. 20). The return path at a radius of 2.5 m is 10 cm thick. Several plates of the hadron calorimeter could serve as this path, or, at a larger radius, the flux return could be completed through the thick iron of the muon

---

22. A. Sadoulet and A. Litke, LBL Report #3316.

TABLE IV. Solenoid Magnet Parameters[a]

	Superconducting Coils		Conventional Coils
Magnet field (kG)	5	10	5
Radius (m)	.75	.75	.75
Length (m)	2	2	2
Acceptance angle	45-135°	45-135°	45-135°
Solid Angle	70%	70%	70%
Thickness coil (cm)[b]	0.445	0.89	5
$L_{radiation}$	0.3	0.5	.5
$L_{absorption}$	0.05	0.06	.13
Magnet force/(area of coil)	1 atm	4 atm	1 atm
Iron flux return thickness (cm)	5	10	5
Power[d] (MW)	.15	.15	1.2
Weight (m tons)	35	70	35
Cost of cryosystem	$100 K	$220 K	
Cost of S. C. Cable[c]	50 K	80 K	
Total cost[e]	150 K	300 K	$35 K
Electricity cost			$100 K/yr

a. Scaled from Report #148 of the 1974 PEP Summer Study.

b. Includes dewar.

c. At Summer 1974 prices.

d. Including compensating coils.

e. Assumes 3 - 4¢/KWH, 20% duty cycle.

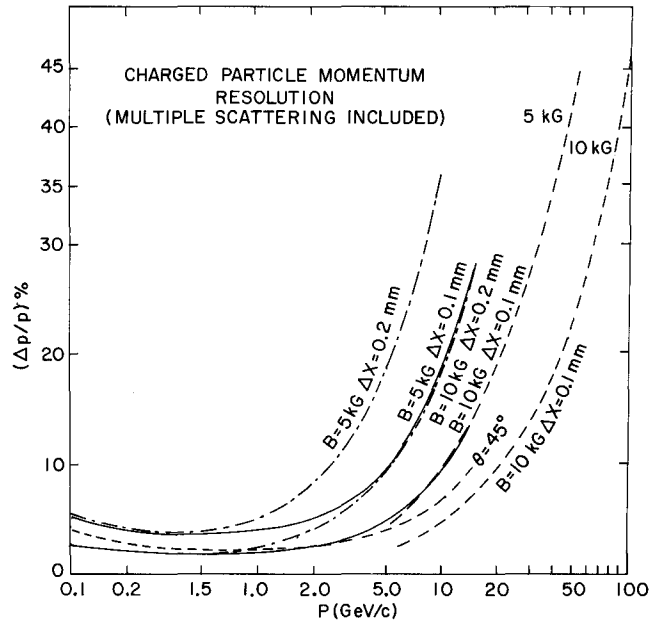

Fig. 19. Momentum resolution of charged particles for different values of magnetic field, B. Also different position resolution in the drift chambers $\Delta x = 100\mu = 200\mu$ are considered. All curves, except one, refer to normal incidence, $\theta = 90^{\circ}$.

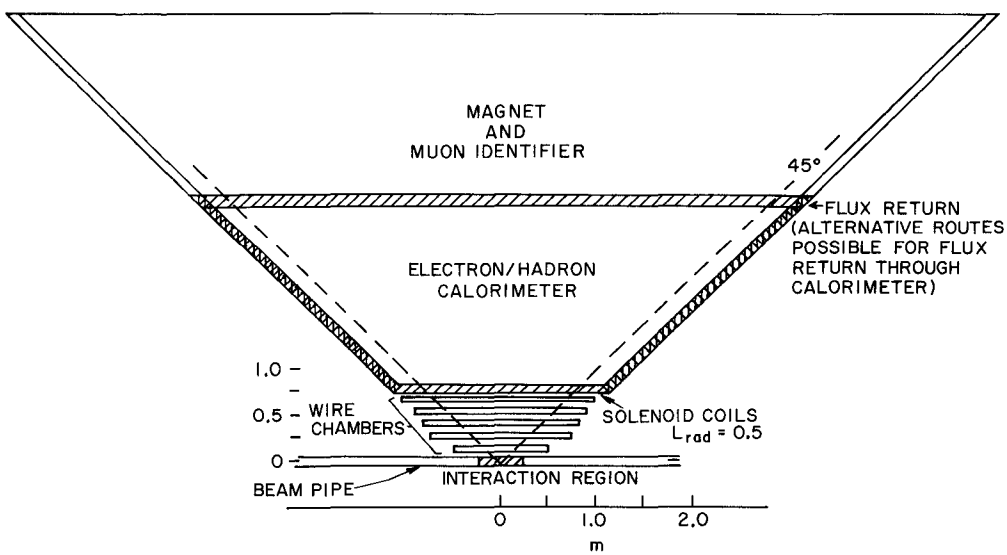

Fig. 20. A side view of the detector with optional solenoidal magnet.

identifier. In either case, the B field direction in the iron is perpendicular to that anticipated for the design with a transition radiator central detector.

5. Superconducting Magnet. A superconducting coil for the solenoid may be desirable, especially for obtaining the highest possible field. Niobium-titanium alloy has been considered for the superconductor, and it is proposed that it be embedded in an aluminum matrix to minimize the γ conversions. At present only a copper matrix has been used in production, but there seems to be no apparent reason that aluminum would not work as well. The properties of these cables are shown in Table V. The NbTi alloy will carry about 1.5×10^5 amps/cm^2 at 50 kG. The effect of loop stress on the stability of the properties of the superconductor, etc., suggest a safety factor of 40. Thus, a current density of 1.0×10^4 amps/cm^2 was used in the design outlined in Table V.

6. Charged Particle Rate in Position Location Devices. The charged particle rate in the proposed detector is $R = L(d\sigma/dy)(\Delta\phi/2\pi\ N_c$ where y is the rapidity, L the luminosity, N_c the average charged multiplicity. The maximum value of y in ISABELLE is $\pm$ 8 (as compared to $\pm$ 4 at the ISR). For the solid angle subtended by our detector, $\Delta y = \pm 2$, $\Delta\phi/2\pi = 1$. Thus, $R = 10^{33} \times 4 \times 10 = 1.6 \times 10^8$/sec assuming no s dependence in σ and N_c. For the worst case of a cylindrical chamber at a radius of 10.0 cm, the circumference is 600 mm, i.e., if this first device is an MWPC with 1 mm wire spacing, 600 wires are exposed to the particle flux. The number of particles per wire is:

$$\frac{1.6 \times 10^8}{.6 \times 10^3} = 2.5 \times 10^5/\text{ sec-wire.}$$

The maximum flux of charged particles consistent with efficient chamber operation has been determined by several groups. In J. Peoples' report,[23] 1.4×10^5/sec wire is the suggested limit. Experience at

---

23. ISABELLE Report, BNL 17522, p. 358, (1972).

TABLE V. Properties of Superconducting Cables

NbTi:	Density	$\sim$ 6 g/cm^3 (54% Nb by weight)
	Radiation Length	$\sim$ 10 g/cm^2 = 1.67 cm
	Absorption Length	$\sim$ 150 g/cm^2 = 25.0 cm
	(Z_{Nb} = 41, Z_{Ti} = 22)	
NbTi-Al:	Density	$\sim$ 4.8 g/cm^3
	Radiation Length	$\sim$ 2.4 cm
	Absorption Length	$\sim$ 28.4 cm

CERN, Aachen, Munich, Harvard collaboration at the ISR[24] shows a limit of $10^4/mm^2$-sec. Beam counter studies at SLAC show that chamber efficiency starts to drop at 1.2×10^5/sec-wire. This implies a rate of $6 \times 10^6/2.5 \times 10^3 = 2.5 \times 10^3/mm^2$-sec consistent with the ISR number. The area of our first chamber is 600 mm $\times$ 400 mm = 2.4×10^5 mm^2, implying a rate of $1.6 \times 10^8/2.4 \times 10^5 = .8 \times 10^3/mm^2$-sec, well within the ISR and SLAC limits.

We conclude that even the inner most vulnerable chamber is adequate to handle the charged particle rates with current technology. At larger radii, drift chambers with wire spacing increasing as the radius would provide the required spatial resolutions in this flux of particles.

7. Electron-Pion Separation. Charged pions and electrons shower differently in the high Z material at the electron calorimeter. However, charge exchange and δ-ray production of pions can enable them to simulate electrons. By sampling the energy deposited at different depths in the shower detector, a high rejection ratio (10^2) can be achieved against pion contamination in the identification of electrons. Further, if the incoming particle is momentum analyzed, an additional rejection factor of $\sim 10^2$ can be achieved.[25] For example, Fig. 22 shows how events populate a plot of energy deposited in the first half vs. that deposited in the second half. A more efficient separation is obtained by sampling the shower 3-4 times and requiring a transition curve characteristic of an electron shower.

---

24. C. Rubbia, private communication.

25. D. C. Cheng, private communication; P. Limon, private communication.

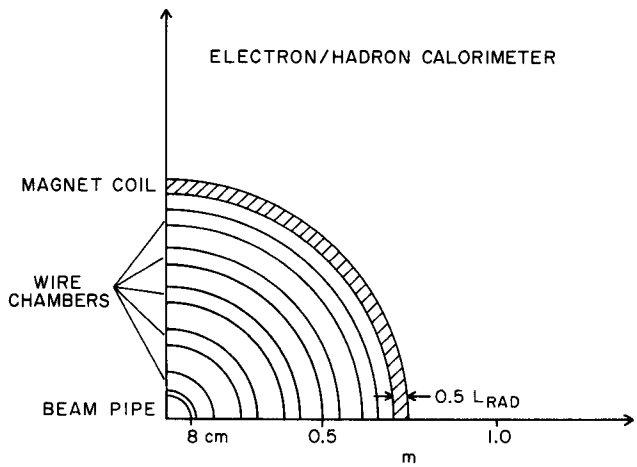

Fig. 21. Cross section of the central detector with optional solenoidal magnet.

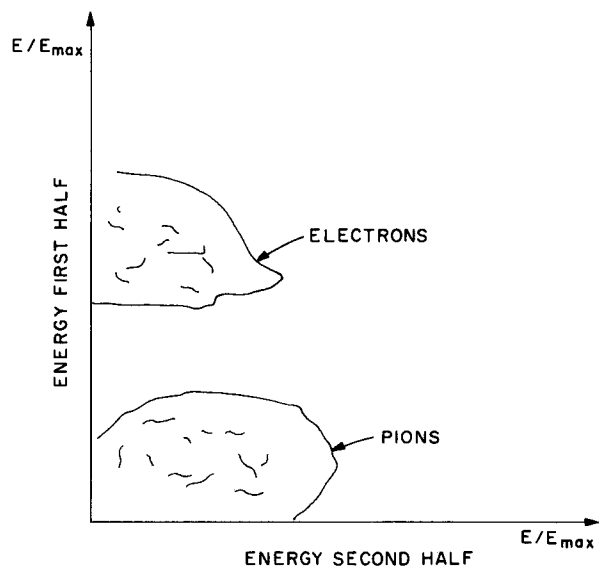

Fig. 22. Scatter plot of Energy Deposited in Shower Detector.

III. Conclusions

Based upon our present understanding of the weak interactions, the study of high transverse momentum leptons promises to be one of the most exciting aspects of the physics that will be done with ISABELLE. The question of the existence of an intermediate vector boson is fundamental to high energy physics and a search for that particle seems quite practical as an early experiment for the ISABELLE program. After having considered the construction and utilization of the proposed detector, we have come to the conclusion that the detector should be constructed simultaneously with the ISABELLE ring itself, with at least the muon magnet section, participating in the first round of the physics program.

The availability of the muon magnet would enable searches for W's or other processes yielding high p_T muons to be explored. For initial operation of the detector in the "muon only" mode, the electron identification and the hadron calorimeter need not be operational initially. Rather a "plug" of iron could fill the first 3 m, both to reduce π-μ decays and to raise the low energy cutoff for muons slightly.

Experience at the ISR indicates that backgrounds near the machine are worse during the initial phases of operation. The initial program proposed would neither be significantly affected by such backgrounds nor require the beam stability needed by many other experiments. Also since the mass of the muon magnet is considerable, early construction of the magnet would minimize the pertubation of the magnet on the alignment of the ring magnets due to floor loading. In addition, the suggested early construction scheduling would eliminate interference with the running schedule of ISABELLE.

As the physics program progressed, we could gradually add sections of the inner modules and end caps. If we were optimistic and believed the theoretical estimates literally, we would be able to

detect the existence of the W even running with low luminosity. That chance, plus the desire to test the inner sections initially at low rates, leads us to recommend installing these sections rapidly after the initial muon search, rather than waiting until the machine comes up to its design luminosity.

LARGE EQUIPMENT AND FACILITIES

Summary Report of Working Group*

L. Rosenson and S. Ting
Massachusetts Institute of Technology
J. Russell†
Southeastern Massachusetts University
W. Selove
University of Pennsylvania
and
S. Lindenbaum, W. Love, R. Louttit,
S. Ozaki, F. Paige, E. Platner, S. Protopopescu
Brookhaven National Laboratory

I. Introduction

The Large Equipment and Facilities group of the 1975 ISABELLE Summer Study addressed itself primarily to considering a general purpose modular multiparticle spectrometer system for studying many hadronic interactions including, A) high mass resonances, B) inclusive, C) various exclusive reactions, D) various correlation experiments, E) some particular investigations of an unusual nature which appear in the "strong" interactions such as strangeness violation and other violations of various conservation laws, and F) investigation of large $p_\perp$ events and jet phenomena.

A) The recent discovery of the J/ψ particles supports to a considerable extent the theoretical proposal of a fourth or charmed quark which carries a charm number +1 or -1 (i.e. the anticharmed quark). From the foregoing one would expect charmed particles produced in pairs each of which has a very narrow mass width and decays by weak interactions. From a study of the $\bar{p}$ and K^- (i.e. other particles which are produced

*The summary talk at the review session was given by S. Ting.

†With support from the National Science Foundation.

in pairs), it is expected[1-3] that the threshold for charmed particles would be in the region s = 2000 - 5000 and they would have a relative abundance in the central region (of a rapidity plot) of the order of 0.01 - 0.05 times the pion production for each member of the fundamental representation.

Furthermore, one might expect new higher mass particles similar to the J/ψ particles which decay hadronically.

Finally one cannot rule out the existence of even heavier quarks than the charmed quark or alternatively (speaking independently of any model) massive hadronic objects (i.e. $\geqslant$ 10 GeV mass) which could become abundant at s $\geqslant$ 50 000. Thus multiparticle spectrometers of good resolution and large solid angle would be required to detect such particles.

B) A study of various inclusive reactions such as those given in Table I would be of considerable interest. The rapidity dependence of their cross sections would be of particular interest, especially since at the ISR $\Delta y = 4$ for the length of the central plateau whereas at ISABELLE $\Delta y = 8$ for the central plateau.

C) Various exclusive reactions, some examples of which are given in Table I, will be of considerable interest in testing various dynamical models.

D) Correlations: The very high energies available at ISABELLE should be very useful in studying correlations between particles. In particular in the central region it is useful to distinguish long range and short range correlations.

---

1. M. Antinucci, A. Bertin, P. Capiluppi, M. D'Agostino-Bruno, A. M. Rossi, G. Vannini, G. Giacomelli, and A. Bussiere, Lett. Nuovo Cimento, 6, 121 (1973).
2. T. Gaisser and F. Halzen, Wisconsin Preprint, COO-435.
3. BNL 20161, ISABELLE (June 1975), pg. 17. See also other parts of the physics discussion relevant to this spectrometer study.

TABLE I. Various Examples of Inclusive and Exclusive Reactions of Interest

INCLUSIVE		
1.	$p + p \to c + X \to c_1 + c_2 + \ldots$	— e.g. $c = \Lambda$, K_s^o, $\emptyset$
2.	$p + p \to c$ + n prongs	— "semi-inclusive".
3.	$p + p \to c + d + X$	— Correlations in central region vs y, $p_\perp$, $\emptyset$ with particle identification.
4.	$p + p \to p\ (x \approx 1) + c + X$	— Structure of large M^2 diffraction.
5.	$p + p \to c$(large $p_\perp$) $+ X$	— Look for jets, i.e. several particles with large $p_\perp$.
6.	New particle searches	— e.g. decays with large $p_\perp$.
EXCLUSIVE		
7.	$p + p \to p + N^* \to p + \pi^+ + \pi^-, \ldots$	
8.	$p + p \to N^* + N^*$	
9.	$p + p \to \Delta^{++} + n$	

E) It may well be that the usual strong interaction invariance principles will break down at high energies (i.e. ISA energies). This could be due to a great increase in the strength of weak interactions where they become sizeable compared to the strong or could be a phenomenon purely connected with the increase in energy.

Therefore searches for exclusive interactions which exhibit strangeness violations or violations of isotopic spin, etc., should be of interest.

It is the opinion of this study group that the investigation of these processes, in particular those with multiparticle final states, requires a large solid angle magnetic spectrometer system with reasonable momentum resolution. A separation of the spectrometer system into two high momentum arms straddling the outgoing proton beams to detect relatively high momentum small-angle particles, and one large solid angle spectrometer for large angle particles with relatively low momentum, is expected to be a natural way to build this detector. The capability to identify outgoing particles is also considered to be essential.

The general purpose modular multiparticle spectrometer system we shall propose is expected to be able to study many aspects of the above described phenomena and others we have not enumerated or in many cases (perhaps the most important ones) not even thought of.

II. Spectrometer Systems

The spectrometer systems we considered had to meet several criteria:

1. Their net effect on the ISA beams was to be made negligible.
2. Their solid angle coverage, resolutions, and particle identification characteristics, were to be optimized within the constraints of space available, ISA constraints, and, of course, reasonableness of overall cost.

III. Spectrometer With Analyzing Magnet Over the Intersection Region

Figure 1 shows an elevation view of a spectrometer with a dipole magnetic field transverse to the crossing beams located so that its center is at the intersection region. The magnetic field is positioned so that vertical deflection of charged particles takes place,* in order to avoid as much as possible the higher expected background near the horizontal plane, and provide a symmetric insertion.

The central magnet C (4 meters in diameter, 2 meter pole separation) around the interaction region has a field integral of 60 kG meters. It is excellent for momentum analysis up to 20 GeV/c and angles $\gtrsim 6^{\circ}$, and a momentum resolution of 2-3% should be possible. Except very near 90° almost 2π azimuth coverage should be possible. The large central magnet and the ones surrounding it will probably be filled with proportional wire chambers and other detectors (possibly drift chambers, calorimeters, etc.).

In order to compensate for the ISA beam deflection in magnet C two other magnets, D and E (see Fig. 1), on each side of the intersection are required, one to bring the beam back to the required trajectory and the other to change its angle to the required angle.

The magnets D and E are located symmetrically at 8 and 16 meters from the crossing point. The 60 kG m field integral of D returns the ISA beams to the appropriate accelerator horizontal plane and the E magnet restores the beam direction to the horizontal beam direction so that the vertical beam paths look like Fig. 2.

---

* If mechanical problems make it desirable to have horizontal deflection, the magnets can be rotated 90° around the beam axis, however in this case the insertion will no longer be symmetric.

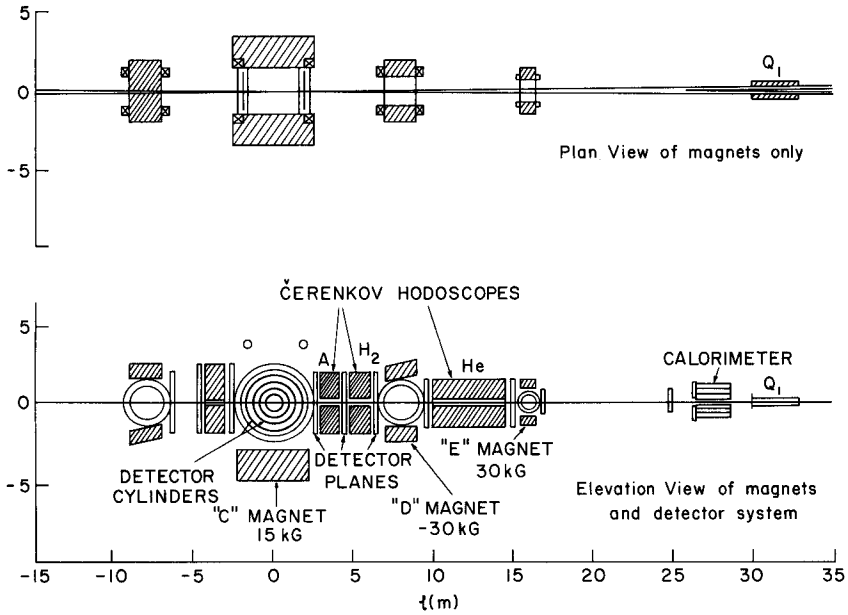

Fig. 1 Plan view of magnets only and elevation view of magnets and detector system.

One should note that in this system the crossing of the intersecting beams is approximately at the point of tangency of two circles in the vertical plane which may make the luminosity of this section more difficult to control. One will, of course, have to turn the magnets on or off in careful synchronism in order not to lose the beam. However, once this synchronism is accomplished, the magnets can be turned on or off at any time and at any level of excitation since the system is nondispersive for small deflections. These magnets form high momentum spectrometer arms so that charged particles emitted at angles less than 6° can be analyzed down to the smallest angle practicable ($\approx$ 3 mrad).

The particles that are emitted in the range from 2° to 6° can be brought out of the beam pipe and very well analyzed (better than 0.25% at 60 GeV/c) by detectors in the field free space in front of and behind the D magnet. Since the D magnet proposed has a 2 meter gap approximately 2π azimuthal coverage is also available in this region. As one detects smaller angles some loss of azimuth coverage occurs due to the beam pipe. However, it is estimated that for angles down to $\sim$ 8 mrad or so about half of the azimuth can be extracted into detectors well ahead of the D magnet and thus analyzed with substantially the full resolution (better than 1% to nearly the full machine energy). From $\sim$ 3 mrad to 8 mrad the particles leave the beam pipe behind the D magnet and would be analyzed (2-3% at 20 GeV/c) by the E spectrometer. Below 3 mrad the particles reenter the beam pipe at Q_1 and cannot be detected and analyzed with this spectrometer. Particles with momentum up to 20 GeV/c will, however, receive sufficient deflection by the central magnet so that detection down to zero mrad is possible. One should note that for an angle of 3 mrad $p_{\perp} \sim 600$ MeV/c at 200 GeV/c. These results are summarized in Fig. 3.

Should a solenoidal magnet with field parallel to the beam direction containing detectors (or a detector system with no field at all) be desired over the interaction region, the sign of one

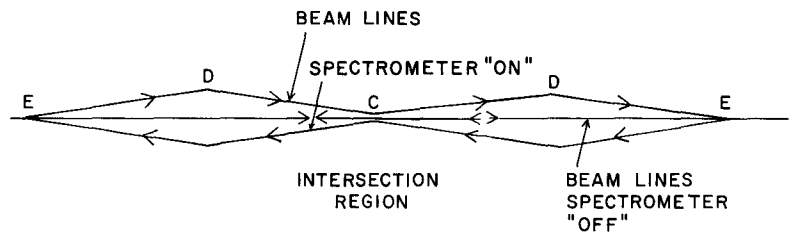

Fig. 2 Elevation view of colliding beams in the spectrometer insertion of Fig. 1.

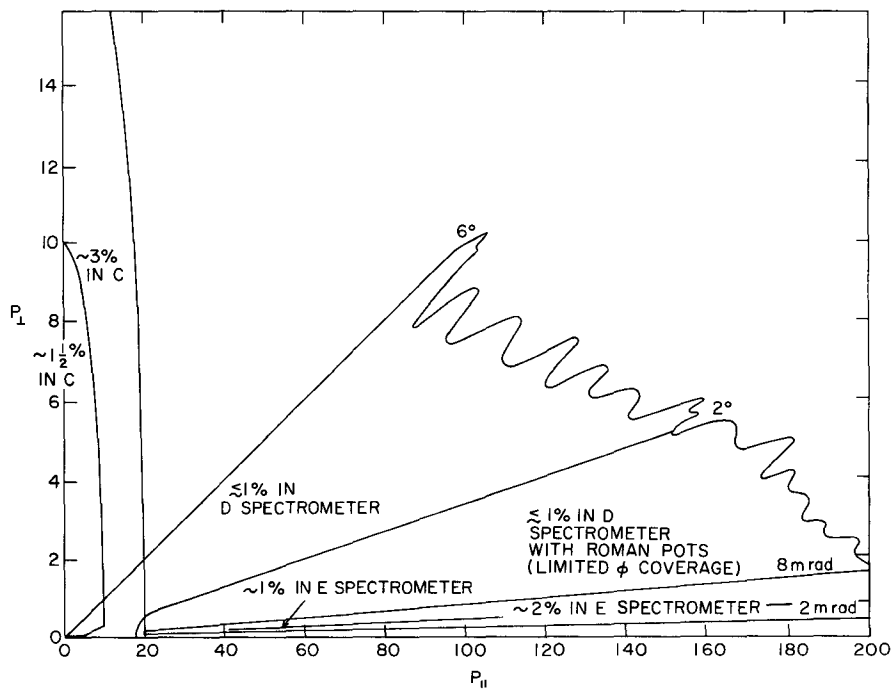

Fig. 3 A plot of the various regions of $p_{||}$ vs $p_{\perp}$ covered by the different spectrometer magnets and the corresponding angular ranges and momentum resolutions.

pair of D and E magnets may be reversed, producing a 9 mrad vertical crossing angle and an otherwise similar operation of the D and E spectrometers. A solenoid detector could be filled with a basic set of cylindrical drift or PWC chambers and many other associated detectors. The resolution of the D spectrometer could be pushed to $\sim$ ¼% at 200 GeV by pushing the quads and the E magnets to (say) 30 meters from the intersection, or alternatively, increasing the dipole field integral will increase the resolution.

The configurations we have considered are particularly simple from the track reconstruction point of view. Most of the high momentum tracks need be measured only in field free regions. The vertex spectrometer is a simple cylinder and could have quite a uniform field for the first meter or so of radius. Depending on the choice and layout of detectors, pattern recognition and track fitting can be greatly speeded up. This is a very important consideration for keeping the computer costs within manageable bounds since the average multiplicity at s = 160 000 is expected to be high.

As an effective mass spectrometer the D magnet is capable of detecting narrow resonances of masses 5 - 10 GeV/c^2 or greater if they have "all charged" particle decay modes. Consider a neutral particle with a two-body decay and a 5 GeV/c^2 rest mass produced with 100 GeV/c momentum. The opening angle of $\sim 6^o$ fits very well into the D magnet window and the effective mass resolution would be in the neighborhood of 5 MeV.

The configurations are particularly open. Calorimeters for the detection of neutrals could be located beyond the E spectrometer (± 60 mrad fits between the E magnet yokes) and over very large angles around the C magnet.

As noted above the device is unable to detect high momentum particles below about 3 mrad, which is a substantial part of the diffractive region at 200 GeV/c. For detection of these particles one

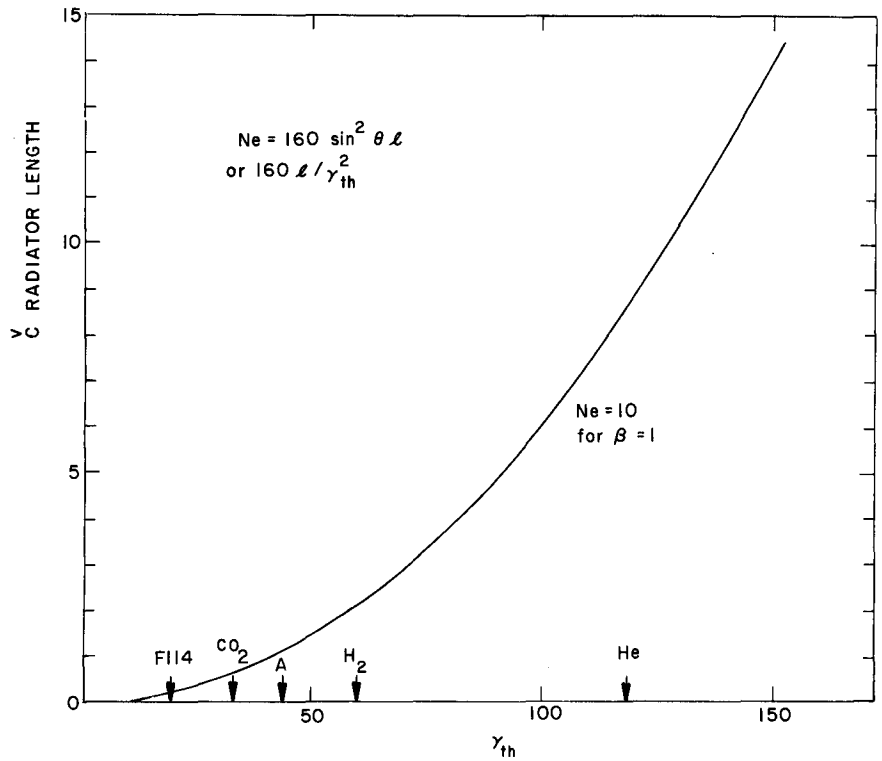

Fig. 4 Cerenkov counter radiation length versus $\gamma_{threshold}$.

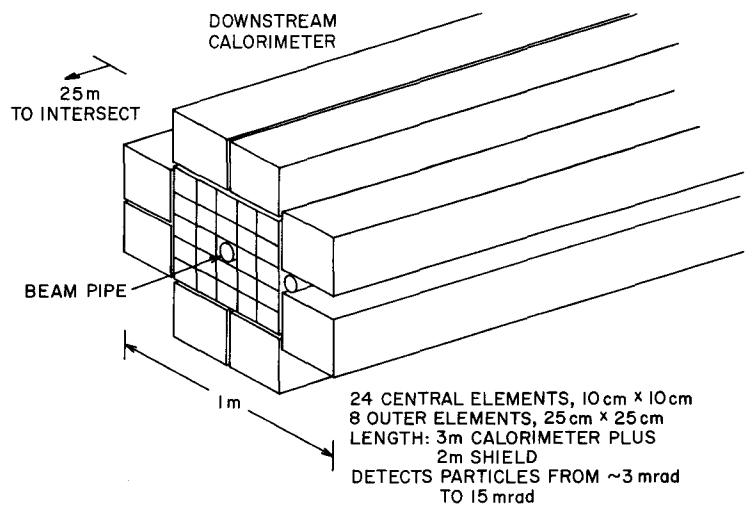

Fig. 5 Downstream calorimeter.

would need a considerably longer straight section than presently contemplated or else a special setup. Two possibilities have been described by the working group concerned with initial and low-luminosity experiments.[4,5]

Cerenkov counter hodoscopes can also be employed for particle detection in, for example, positions as shown in Fig. 1 which is a schematic of a possible arrangement of this spectrometer. The Cerenkov radiator length estimated as required as a function of the particle is given in Fig. 4.

IV. Detectors

The expectation of reaching luminosities of $\sim 10^{32} - 10^{33}$ means that event rates (assuming $\sigma \approx 40$ mb) could be $\sim 4 \times 10^6$ to 4×10^7 per second (i.e. one event every 250 to 25 nanoseconds). The particle multiplicity of an event can also be expected to be rather high. Thus it is clear that the detectors most worth considering are:

1. Scintillation counters and scintillation counter hodoscopes.
2. Proportional wire chambers.
3. Drift chambers.
4. Cerenkov counters and Cerenkov counter hodoscopes.
5. Calorimeters of many cells (i.e. hodoscopic arrangements) so that the rate in each cell is tolerable.

Since detectors of the types 1 - 4 have been operating in many systems for some time, we will not discuss these in any detail. One should note, however, that the drift chambers will be used in a new high rate environment and located in a magnetic field and there-

4. R. M. Edelstein and M. Zeller, "Elastic Scattering and Diffraction Dissociation in the Angular Range 1 - 50 mrad", these Proc.

5. C. Y. Chang, E. Engels, M. Kramer, R. Lanou, and L. Pondrom, "Small Angle Single Particle Spectrometer for ISABELLE", these Proc.

fore special techniques will have to be incorporated for their use.

The question of calorimeters will be discussed briefly as this instrument is still in its early stages of application. The two types of calorimeters currently in use are the scintillation type and the liquid argon ionization chamber type. The liquid argon type has a resolving time ($\sim$ 400 nsec) which is more than an order of magnitude longer than the scintillation type (with a pulse shape $\sim$ 15 - 20 nsec) and thus will limit the usable luminosity to an order of magnitude lower. However, the liquid ionization chamber has advantages in uniformity, and in the case of fine sampling, and gets better energy resolution.

One should note that if one is looking for single particle high $p_\perp$ events, such as in a search for the two-body leptonic decay mode of W's then the event rates are low enough so that the liquid argon calorimeter resolving time does not restrict use of full luminosity. Such a lepton detector is described in another summary.[6]

An $\sim 4\pi$ calorimeter system is not envisaged for the spectrometer described in the early stages of ISABELLE due to cost and other considerations, such as interference with the other detector systems in the magnetic spectrometer. What is now contemplated are forward and backward calorimeter units and also large angle detector units covering only portions of the solid angle. In particular an attempt is made to design a calorimeter to detect jets, i.e. a situation where two or more particles have a relative transverse momentum of $\sim 1/3$ - $\frac{1}{2}$ GeV/c and are proceeding forward (or backward) together with energies the order of 50 - 100 GeV each. Such a pair of particles will separate with a relative angle 5 - 10 mrad. We therefore consider a calorimeter array whose segments are

a. 5 - 10 mrad apart,

---

6. R. Burnstein, W. Carithers, M. Duong-van, R. Imlay, M. Kreisler, U. Nauenberg, C. Rubbia, G. Snow, L. Sulak, H. Williams, E. Paschos, M. Sakitt, C. L. Wang, and L. L. Wang, "Design of a Lepton Detector for ISABELLE", these Proc.

b. are each large enough in area to give reasonable containment of a shower.

For the higher energies we are dealing with segment size which could be as small as $\sim 4'' \times 4''$ to satisfy condition (b). Then condition (a) suggests putting the calorimeter 20 meters away from the intersection. The calorimeter also has to be $2\frac{1}{2}$ to 3 meters thick and it therefore seems desirable to be able to accommodate an arrangement within the straight sections with at least 30 meters between the intersection point and the first quadrupole.

A sketch of such a proposed downstream calorimeter is given in Fig. 5 which can detect particles from $\sim$ 3 mrad to 15 mrad.

Calorimeters for high $p_\perp$ jets (i.e. a group of 2 or more high $p_\perp$ particles with relatively small relative transverse momentum) were also studied and seem commercially feasible provided only a part of the solid angle (sufficient to contain the jet) is built. These hodoscopic calorimeters would have a shape such that the particles incident on the first face would find $2' \times 2'$ area segmented into $6'' \times 6''$ calorimeter cells and would flare along the direction the particles travel so that 4' further down (i.e. the exit face) the calorimeter is $5' \times 5'$.

It was concluded that a pair of such devices could study the gross rate of high $p_\perp$ particles when in close, and after being backed off sufficiently could study the internal structure of the jets (i.e. ratio of jets of singles).

Other uses in studying high $p_\perp$ events not necessarily of the jet variety are obvious.

V. Vacuum Chamber Requirements

A general schematic of the type of vacuum chamber we envisage for this spectrometer system is shown in Fig. 6.

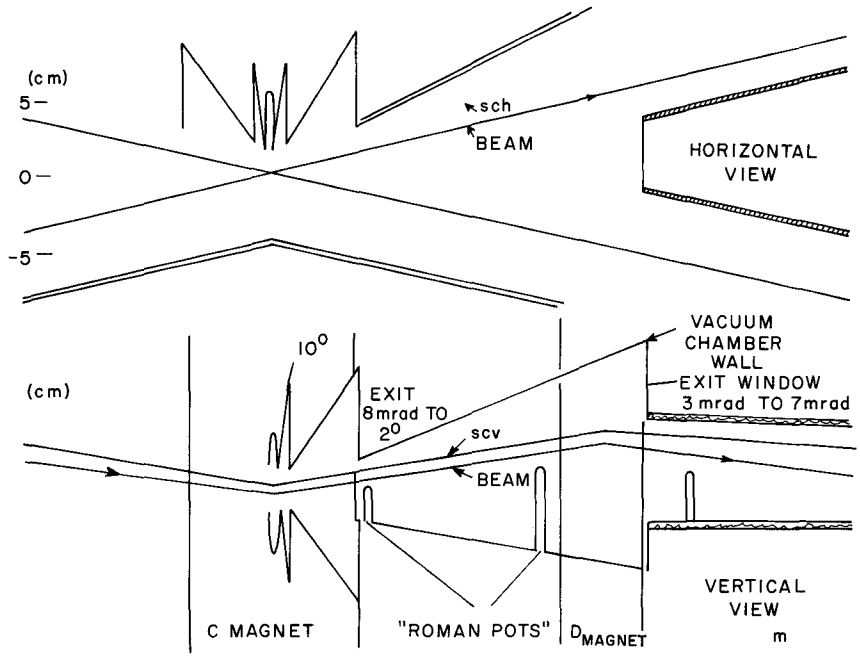

Fig. 6 Horizontal and vertical views of the vacuum system (note different distance scales in the two views).

One should note that the vertical scale is in cm (to show detail) while the horizontal scale is in meters so that wiggles and angles are amplified in this schematic.

VI. Detector Costs

Detector costs are very difficult to estimate as the technologies of the detectors are rapidly changing and the ideas of experimentalists on the detector arrays required are also a rapid function of time. Nevertheless we have made some ball-park guesstimates of costs:

1. A drift chamber detector system with a proportional wire chamber trigger system: estimated cost ~ $600K.
2. Downstream and side calorimeter pairs discussed: estimated cost ~ $500K.
3. Cerenkov hodoscopes: estimated cost ~ $400K.

Thus we can see that the magnets are the main cost of the spectrometer system.

VII. Magnets and Costs

Central Magnet

60 kG-m	(4 m diam 15 kG)
~ 3.0 M$	(+ ~ 0.5 M$ for refrigerator)

"D" Magnets

60 kG-m

~ 1.1 M$

x 2 = 2.2 M$

"E" Magnets

30 kG-m

~ 0.12 M$

x 4 = 0.5 M$

VIII. Solenoidal Magnet

The solenoidal magnet at the intersection has not been discussed yet and a proposed version is shown in Fig. 7. It is shown containing a liquid argon calorimeter with a trigger system. Figure 8 shows a side view of this solenoid magnet vertex detector system. Some of its capabilities are listed below:

Kinematic range ≡ Central Region

$$\frac{p_\perp}{p_{||}} < \tfrac{1}{4}\ , \qquad p_\perp < 20\ \text{GeV}, \qquad \frac{\Delta p_\perp}{p_\perp} \approx 0.06 \left(\frac{p_\perp}{20} \right)$$

Physics:

1) "High" $p_\perp$ ($\sim$ 10 - 15 GeV/c):

   Jets and corrections over large solid angle
   Back-to-back jets?

2) "Low" $p_\perp$ ($\lesssim$ 1 GeV):

   Correlations, effective masses, etc.

3) In association with forward spectrometer:

   Semi-inclusive reactions with associated multiplicity
   Correlations

The cost of such a solenoidal magnet system with detectors is crudely estimated to be $\sim$ 5 million dollars. Alternatively, one could include a cylindrical drift chamber system inside the solenoidal magnet.

IX. Summary

In this report we have briefly described and discussed various elements, and general considerations pertaining to a general purpose modular multiparticle spectrometer system. Although one has emphasized the study of hadronic interactions, obviously the solenoidal magnet vertex detector system can be used in a search for W bosons and other weak interaction processes.

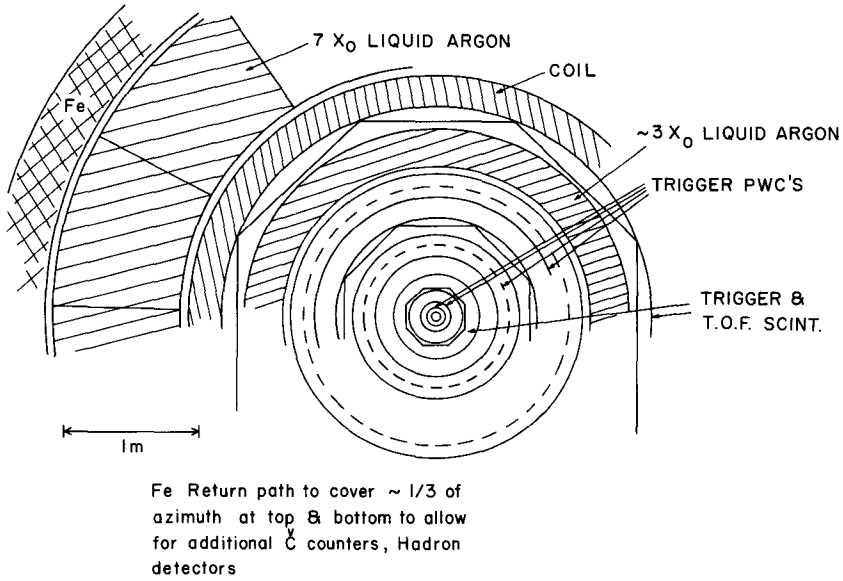

Fig. 7 Solenoidal vertex magnet with a particular detector system viewed along the beam.

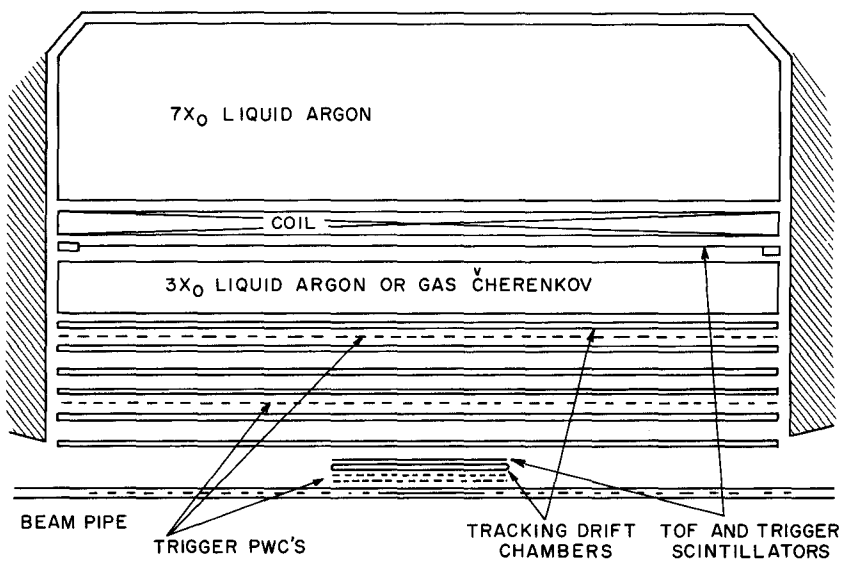

Fig. 8 A side view of Fig. 7.

In conclusion, a useful spectrometer system, which can do many different types of experiments, seems compatible with the requirements on the ISA straight sections.

EXPERIMENTAL INSERTIONS

Summary Report of Working Group*

J. Sandweiss
Yale University
T. F. Kycia
Brookhaven National Laboratory

The plan is to start up ISABELLE like the ISR with eight identical insertions. The arrangement of the elements is shown in Fig. 1. Four sets of quadrupole doublets are used to match the β functions in the insertions to the values in the cells. The total free space available at the crossing point is 40 meters. Space outside the outlines of the dewars would also be available. These standard type insertions would have a performance that's shown in Table I. For a current of 10 amperes, a β_v function of 4 meters at the interaction region and a standard crossing angle of 11.38 mrad we obtain a luminosity of 2.65×10^{32}. The interaction length is only 38 cm. With only minor perturbations, the low-β and high luminosity insertions would be made available. The low-β insertion can be obtained by a minor adjustment of the strength of the quadrupole doublets. The luminosity is increased by a factor of two but β_{max} increased from 100 to 400.

The high luminosity insertion can also be obtained by only a minor perturbation. That is accomplished by reducing the crossing angle by a factor two. It is shown schematically in Fig. 2. Four common bending magnets are used within the 40 meters of free space, reducing the available free space to 26 meters which should in general be adequate. One of the basic restrictions on the design of the insertions is that no dispersion be introduced within it.

---

* R. Burnstein, A. Carroll, C. Chien, T. Kycia, R. Lanou, R. Majka, A. Mann, J. Marx, P. Mazur, L. Rosenson, J. Russ, J. Sandweiss, P. Schlein, A. Thorndike.

TABLE I. ISABELLE Performance - Initial Phase

	Standard	Standard Low-Energy	Low-β	Low-β Low-Energy	Hi-Luminosity
Luminosity (cm^{-2} sec^{-1})	2.65×10^{32}	1.02×10^{32}	5.31×10^{32}	1.44×10^{32}	1.06×10^{33}
Tune Shift	1.74×10^{-3}	4.53×10^{-3}	8.68×10^{-4}	3.20×10^{-3}	1.74×10^{-3}
Crossing Angle (mrad)	11.38	11.38	11.38	11.38	5.69
Free Space (m)	± 20	± 20	± 20	± 20	± 13
$\ell_{INTERACTION}$ (m)	± 0.19	± 0.50	± 0.19	± 0.50	± 0.38
β_v^* (m)	4.0	4.0	1.0	2.0	1.0
$\beta_{v,max}$ (m)	~100	~100	~400	~200	~400
β_h^* (m)	20	20	20	20	20
σ_v^* (mm,rms)	0.243	0.632	0.121	0.447	0.121
σ_h^* (mm,rms)	0.543	1.414	0.543	1.414	0.543
Energy (GeV)	200.0	29.4	200.0	29.4	200.0
Current (A)	10	10	10	10	10

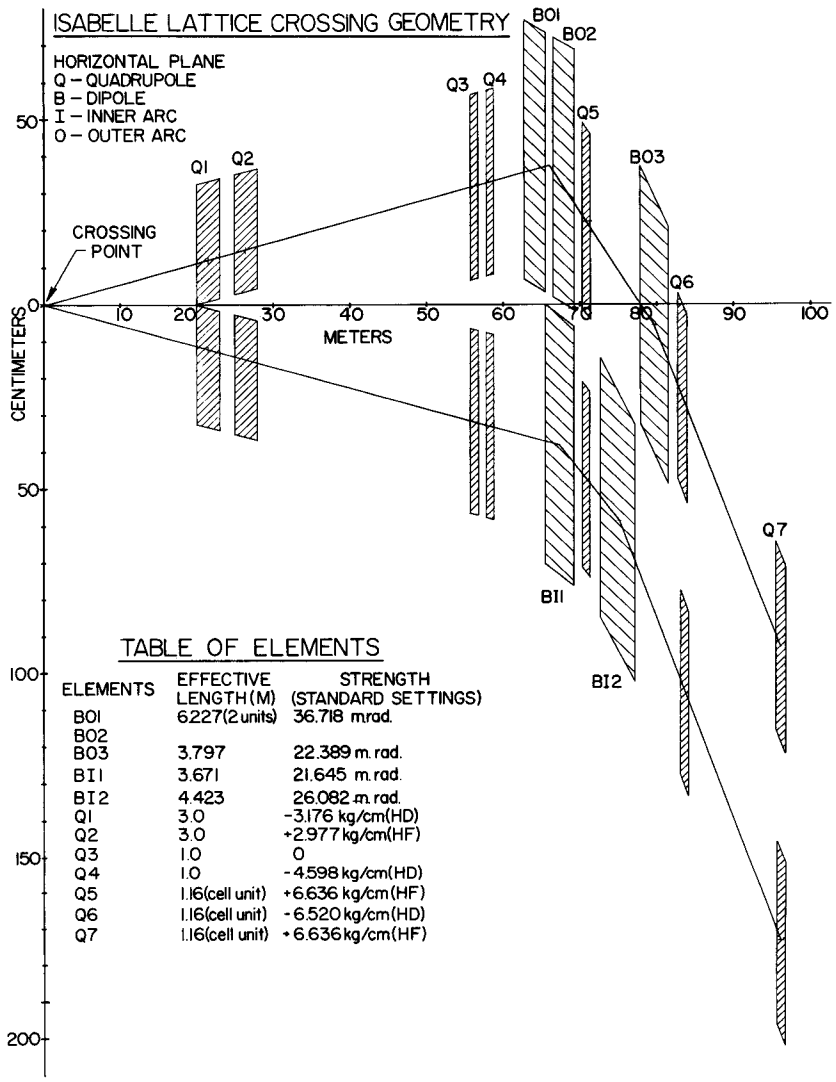

TABLE OF ELEMENTS

ELEMENTS	EFFECTIVE LENGTH (M)	STRENGTH (STANDARD SETTINGS)
B01	6.227 (2 units)	36.718 mrad.
B02		
B03	3.797	22.389 m. rad.
BI1	3.671	21.645 m. rad.
BI2	4.423	26.082 m. rad.
Q1	3.0	-3.176 kg/cm(HD)
Q2	3.0	+2.977 kg/cm(HF)
Q3	1.0	0
Q4	1.0	-4.598 kg/cm(HD)
Q5	1.16 (cell unit)	+6.636 kg/cm(HF)
Q6	1.16 (cell unit)	-6.520 kg/cm(HD)
Q7	1.16 (cell unit)	+6.636 kg/cm(HF)

Fig. 1 Beam trajectories and arrangement of lattice elements in the crossing region.

There is no net dispersion introduced by the four bending magnets since there is no net change on the proton beam line.

From Table I we see that a luminosity of 10^{33} can be achieved with a current of 10 amperes. The tune shift is only 1.7×10^{-3} and the interaction length is only 76 cm.

After the initial phase of operation, the plan would be to change one at a time to the specialized insertions as their need arises. Examples of these are the high-β insertion for studying small angle p-p scattering in the Coulomb-nuclear interference region and insertions which require more free space.

During this summer study, the possibility of a lattice consisting of seven standard insertions and one low-β insertion had been investigated. It was demonstrated that this arrangement is completely feasible.

The goal of the group working on Experimental Insertions has been to verify that the current plan for insertions is viable and that the fundamental insertion design as given in the Yellow Book[1] is a good basis for going ahead. The way in which that was done was to select a large number of experiments and determine from the detailed layouts whether they could be incorporated in the current design. For that reason the insertion group was organized to have representatives from nearly all the experiments. It became, therefore, a fairly large and slightly amorphous, but effective group. By looking at all these detailed experiments, the group has tried to identify the limitations which the Yellow Book design imposes on the experimental utilization of the machine, with particular emphasis on trying to find any particular problems or limitations which would be serious enough to require fundamental change in the design. There was a secondary goal, which was to provide a kind

---

1. A Proposal for Construction of a Proton-Proton Storage Accelerator Facility, ISABELLE, Revised June 1975, BNL 20161.

of first-round feedback for the refinement of the design, to review the sort of popularity contest for the different types of insertions, to look for special hardware which might be necessary to use the insertions, and then finally to get refined information on the sizes of the halls. The outcome of this investigation is that the insertion design does indeed satisfy all the experimental requirements.

The proposed experiments are described in detail by other groups and specific references given elsewhere in these Proceedings. We shall concentrate on the features of the experiments which are particularly relevant to the insertion design, and to show the kind of insertion that's required. The first experiment is the measurement of total cross sections, and the second one is the study of charged particle angular distributions, multiplicity, rapidity, etc., at low $p_\perp$. That could be done with the 4π detector in which charged particles are detected in the absence of any magnetic field, and that fits right into a standard insertion. The next experiment would be a set of studies which could be carried out by a small-angle, small-aperture spectrometer of the classical design with good particle identification with Cerenkov counters. It would be possible to study inclusive spectra, search for new stable particles, and look at diffraction dissociation by essentially the missing mass technique. That fits into the standard insertion, but it requires some new hardware. In particular, it requires a quadrupole with a hole in it, which appears to be a feasible development, and it also requires some extension of the experimental hall. In the study of diffraction dissociation, large errors are introduced into the missing mass resolution because of the intrinsic spread of the beam, and one idea which came up was to use a dispersive crossing rather than the nondispersive crossings which are typical in the current design, and then to use a vertical bend spectrometer. By knowing where the interaction took place horizontally, the precise momentum can be known, and thereby, the resolution

tion on missing mass can be improved. That would be a nonstandard insertion and that has not been, but could be, designed. And then finally, one might look at diffraction dissociation by decay products. For this experiment there are various multiparticle spectrometers which would be suitable and they all fit into the standard insertion.

Next on the list is elastic scattering. The arrangement for the Coulomb-nuclear interference region basically involves detectors near the beam pipe, and that fits into an insertion, as we'll see later, which has a standard shape geometrically, but it has a new tune. This was referred to by Lloyd Smith as a realistic high-β design. It works out very well and nothing needs to move physically; simply a new tune is required for the quadrupoles in the insertion. For elastic scattering at larger t, a dipole spectrometer has been studied and that fits nicely into the standard insertion. For the large $p_\perp$ hadrons inclusive and semi-inclusive study, there were two designs made of large $p_\perp$ spectrometers with modest changes of the hall. It would need to be slightly wider, but otherwise they fit easily into the standard insertion. The search for jets with lead glass and calorimetry also fits into the standard insertion.

There is a whole class of experiments which will be carried out in a large general purpose multiparticle spectrometer. They consist of studies of multiparticle hadronic physics, resonances, clusters, jets, correlations, etc. This spectrometer will fit in the early days into the standard insertion, but it would benefit from a planned modification of the insertion design. That is one of the modifications which are natural in the context of the design, namely moving back the first pairs of quadrupoles in order to increase the free space in the crossing region. Furthermore, there is a second general purpose detector for lepton-studies which consists of a very large piece of apparatus to discover the W, study μ pairs, leptons and various kinds of weak interactions. It would require the highest luminosity, but that's available in one of the

standard designs and would not present any problems. The various methods of searching for quarks, monopoles, etc., have also been incorporated within the standard insertion without difficulty.

In the category of previously unthought of experiments, three have been looked at in some detail, namely, a new object detector, some K^o-type studies, and multilepton detection. In these we shall have various arrangements, some using equipment mentioned above such as the large lepton device. Again, all of the previously unthought of experiments fit nicely into the standard insertion. The reason for having such a long list of experiments was to make certain that there is no important experiment which could not be done with the basic insertion design.

Experiments with storage rings which are particularly challenging are those in which particles must be detected at small angles relative to the crossing proton beams. Two experimental arrangements in that category are the small angle spectrometer and the set-up for studying Coulomb-nuclear interference. We shall describe in more detail how both of these arrangements would be accommodated within the current design.

In the case of the small-angle spectrometer, the idea, developed during the summer study, was to use for the first quadrupoles the design shown in Fig. 3.[2] It's a standard quadrupole,but with the yokes pulled back so that there is a gap in the median plane for particles emitted at small angles and the vacuum chamber. Although this quadrupole has not been designed, it looks like a project which is well within the scope of the hardware development. As far as the circulating beam is concerned, it is exactly the standard insertion. The experimental arrangement for the small angle spectrometer using these quadrupoles is shown in Fig. 4.

---

2. C. Y. Chang, E. Engels, M. Kramer, R. Lanou and L. Pondrom, "Small Angle Single Particle Spectrometer for ISABELLE", these Proc.

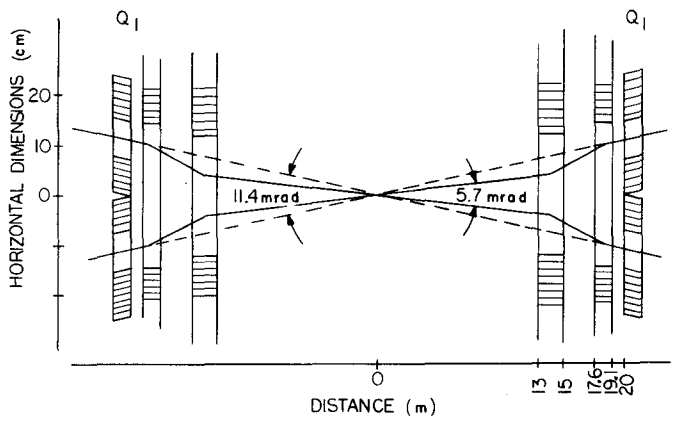

Fig. 2 Beam trajectories for the hi-luminosity configuration. The crossing angle is reduced by a factor of two.

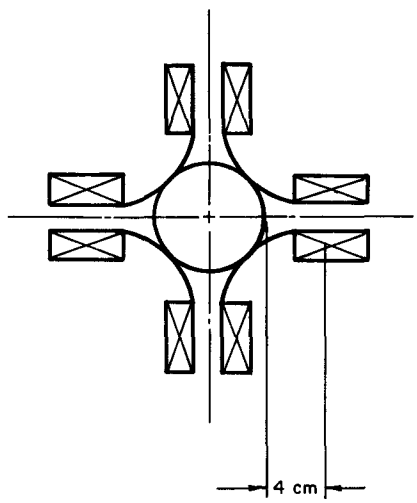

Fig. 3 Standard quadrupole but with a gap in the median plane for particles emitted at small angles.

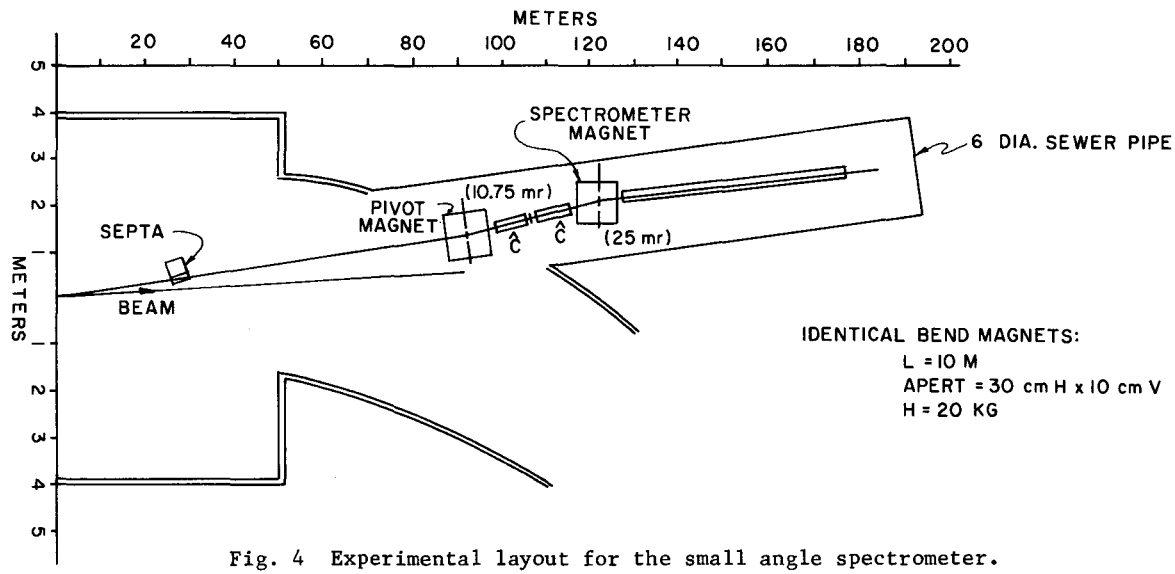

Fig. 4 Experimental layout for the small angle spectrometer.

After the small angle beam passes through the hole in the quadrupoles, it enters the septum magnets. Particles emitted at the desired angle and momentum are selected by the septum magnets and directed to the pivot magnet which redirects them to the spectrometer. It consists of a spectrometer magnet with particle detectors and three Cerenkov counters. This arrangement permits particle detection from a production angle of 8 mrad down to 1.5 mrad The experiment would be situated in the samll angle hall which is 100 meters long and for which a 6'-wide extension would be required.

An experiment which has established a need for long insertions in the past studies and which required the longest insertion is the Coulomb-nuclear interference experiment.[3] In the present design, the β function would be tuned at the crossing to about 60 or 70 but physically the section is the same as the standard insertion. It is shown in Fig. 5. Detectors are situated within 3 cm of the beam in front of the first quadrupoles and within 0.5 cm of the beam in front of the second quadrupoles. They would probably need to be moved in after the full energy has been reached. The phase advance doesn't reach 90° but is actually about 70°. It is of no consequence, however, since the resolution error induced by this is not important in the experiment. There is an interesting point here about the ranges of t_{min} and t_{max} at the different energies. At 200 GeV, the downstream detectors are the principal ones and they cover the t range from 3×10^{-3} to 0.09 $(GeV/c)^2$, which is a fine interference region. At 30 GeV the upstream detectors are the relevant ones and cover the t range from 0.002 $(GeV/c)^2$ out to large values since, in fact, there is no obstruction. Of course, these are matched by the detectors on the other side for the other scattered particle. The point here is that if one beam is maintained at say 200 GeV and the other is varied, then the downstream detector for the scattered 200 GeV proton has exactly the same t

3. R. D. Majka and J. N. Marx, "Measuring Coulomb-Nuclear Interference as a First Round ISA Experiment", these Proc.

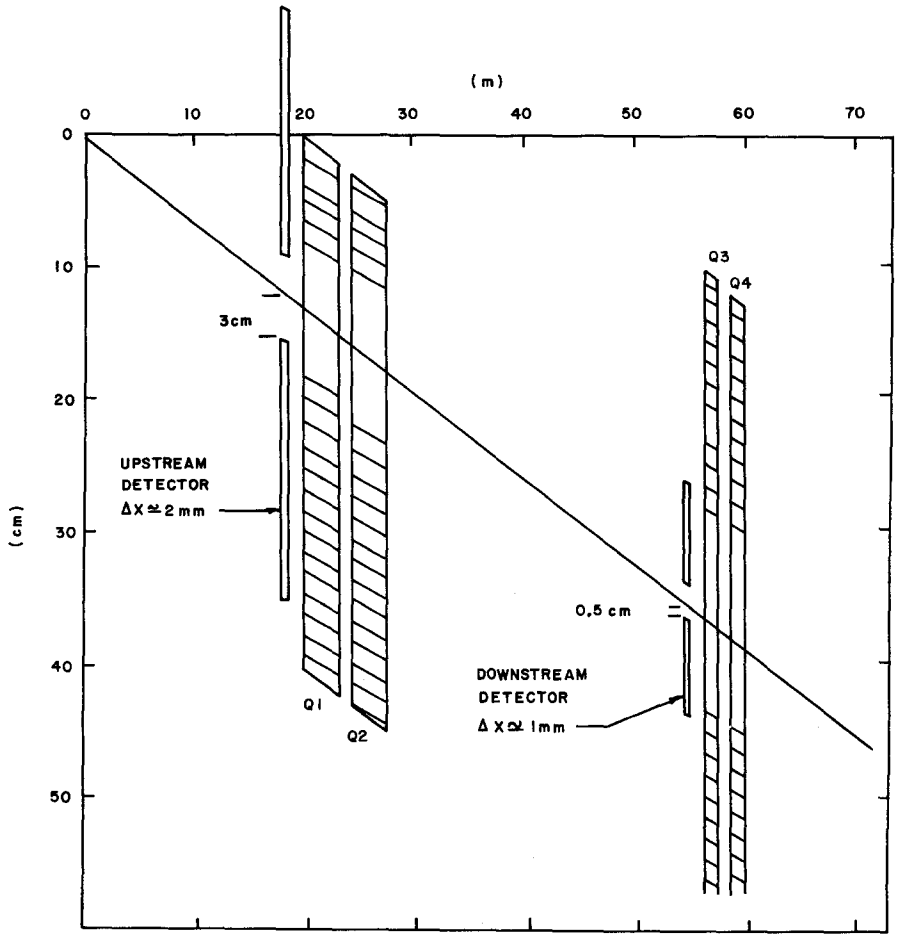

Fig. 5 Experimental arrangement for the Coulomb-nuclear interference experiment.

resolution as s is varied. In fact, it is clear that with either set of detectors, by varying one beam or the other beam, it is possible to cover the whole t range. The theme that has come out of the study is that there are a number of cases where it is very useful to be able to run the machine with asymmetric energies. Another theme that runs through all of these discussions is the importance of having great virtuosity with vacuum chambers. The experiments will really be very much affected by the ability to make unusual shapes so normal incidence can occur, thereby minimizing interactions in the walls.

The conclusions of our group are that the basic insertion design works very well and that it is a good basis for going ahead. The asymmetric beam energy operation is surprisingly useful in a number of cases, namely the total cross section, the elastic cross section, the real part and the small angle spectrometer experiments. We did find that in order to fit some experiments into the experimental halls minor modifications, that were typically a meter or two, were required. As mentioned above, another theme that ran through this study is the fact that it is desirable to have the maximum vacuum virtuosity.

There are also some topics for future study, which we mention briefly. Some of those are refinements of the design, which we didn't consider. We gave primary importance to trying to check out the design against the greatest number of possible experiments, so we didn't look into areas such as rooms for assembling equipment, working space, shielding, counting areas, etc. Also, in the refinements of the experimental design luminosity measuring and monitoring devices will need to be incorporated.

Finally, in summary, we attempted to make up, as an exercise, the first year of the ISA schedule. It was necessary to reject a number of experiments since they just did not fit into the schedule. In making out a typical ISA first year schedule, we discovered that the halls had to be slightly changed around because one of the

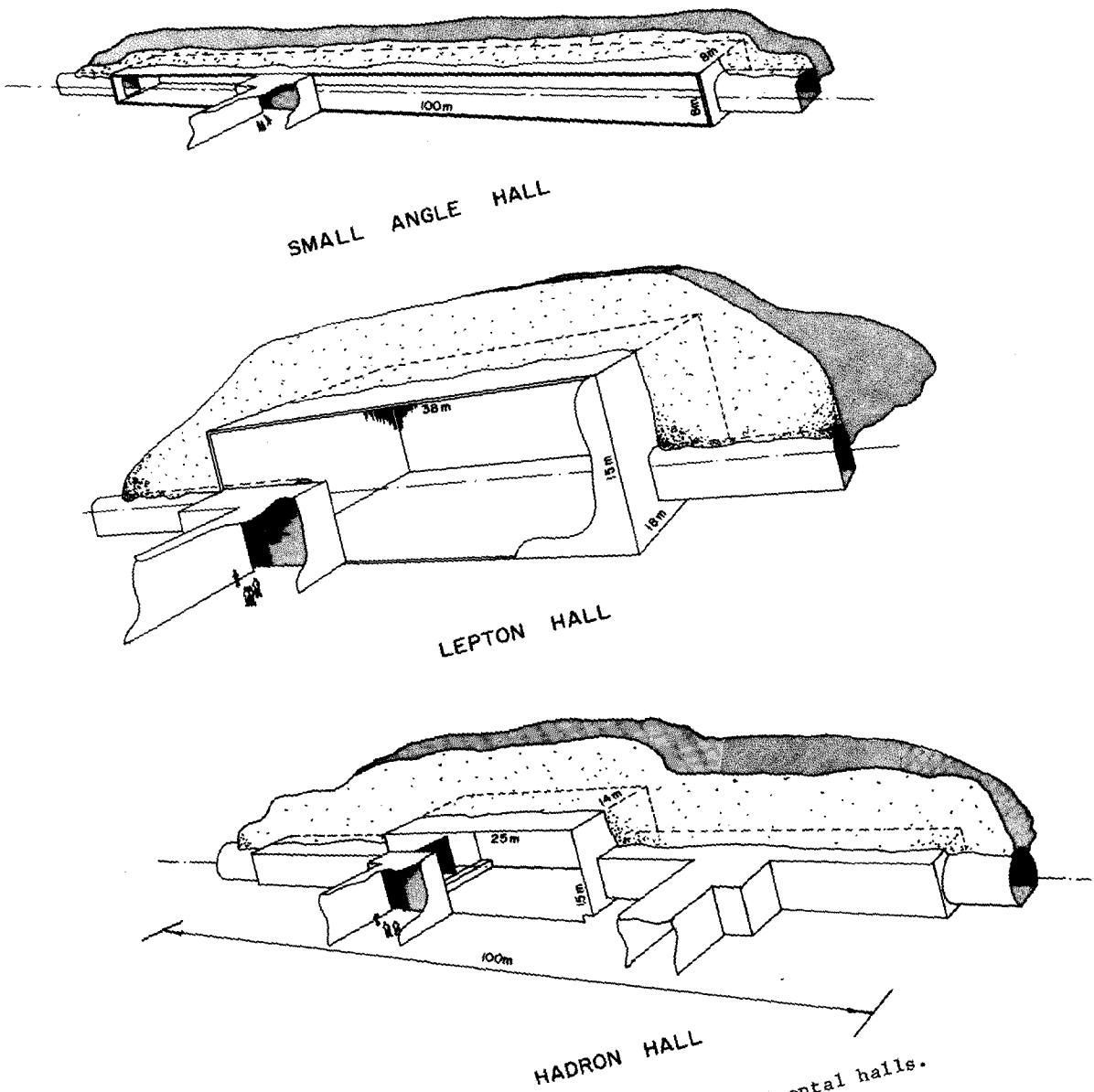

Fig. 6 Three classes of experimental halls.

experiments, the small angle spectrometer, required the center of mass to move radially outward. That required moving around which were hadron halls, and which were lepton halls, (shown in Fig. 6), and this was trivial. In hadron hall number 1 we put the large $|t|$ elastic scattering experiment in which presumably would be discovered the second, third, etc., minima and who knows what else. Small angle hall number 2 would be assigned to inclusive studies with the small angle spectrometer, looking for, among other things, new stable particles. In lepton hall number 3 would be discovered all the intermediate bosons; in hadron hall number 4, multiparticle studies with the large spectrometers; they get to discover jets, etc. Then, in hadron hall number 5, it would be shown whether the total cross sections continue to rise and, if so, in what way. Using the same apparatus, they would have the first look at correlations, etc. for charged particles, without magnets. In small angle hall number 6, they might have a bit of a slow start while they learn how to make the new tune for the high-beta insertion, but perhaps that would go since it wouldn't need very much in the way of luminosity. And then in lepton hall number 7, one would look at large $p_\perp$ hadron production and for the "question mark" among other things. After the first year, one can get on with other important experiments which, of course, are yet unthought of.

NEW AND UNTHINKABLE IDEAS

Summary Report of Working Group*

L. M. Lederman

Columbia University

1. Introduction

Colliding protons at 200-400 GeV each provides an initial state with a fantastic excitation energy--so far removed from our experience as to encourage the widest degree of speculation as to what new phenomena may now take place. Since a great deal of thought has already gone into extrapolations of "conventional" HEP to 400 GeV, it seemed appropriate to invest some time in thinking about processes that have, until now, not been investigated and described in the rich literature of ISABELLE, POPAE, and the European proton storage (LSR) ring study groups. We set out to study the reaction

$$p + p \rightarrow \text{something new.}$$

To give this process its largest possible rate, we should seek the inclusive channel:

$$p + p \rightarrow \text{something new} + \text{anything.}$$

In a well attended preliminary session, many suggestions were made[1]:

---

* W. C. Carithers, C. Y. Chang, L. M. Lederman, U. Nauenberg, C. Rubbia, and N. P. Samios.

1. Under the theorem that all truly novel ideas are totally obvious, no credit (or blame) will be given to physics ideas presented below.

A. New Symmetry Violations

e.g. 1. $p + p \rightarrow$ nothing.

This implies a search for violations of baryon number, charge, or both. Again, the inclusive channel is preferred:

$$p + p \rightarrow \text{nothing} + \text{anything}.$$

2. It is conceivable that the old symmetry violations could, in the intense fields of the 400 GeV collision, change their character, the $K^o - \bar{K}^o$ particle mixture could show interference effects of opposite sign.

3. Other properties of particles may change due to the environment at birth, e.g., mass, charge, etc.

4. Lorentz invariance breakdown at very small distances should be suspected.

B. Search for New Objects

1. Particles of high mass that are stable, perhaps because they are the ground states of new families carrying new conserved quantum numbers.[2] A particular example of this would be a sudden vast increase in the production of antiparticles perhaps suggested by some cosmological problems.

2. Particles that have very long lifetimes, that require: i) a K_L^o-type detector or ii) search for high-energy decay products after the machine is off (or before

---

2. Quarks, monopoles, etc., are defined as old, familiar objects for this discussion.

it's turned on) or iii) search for neutral massive leptons through thick shields.

3. Particles of very high mass and short lifetime which decay hadronically could be sought via the unique signature of $\Sigma P_{\perp} \approx M/2$.

The burden of the study would be to think of the instrumental things that would bear on these "totally obvious" problems. Clearly what is done in this study will surely be improved by the relentless advance of instrumental technology. In the following sections, we present some approaches to the problems presented above.

2. Baryon Conservation

(Analysis contributed by U. Nauenberg, University of Colorado)

One might dare to ask the question whether baryon number is conserved in very high energy collisions. This question becomes somewhat reasonable when you note that conservation laws of this type may exist not only as a basic law of nature, but also as a result of the existence of a very strong binding force which keeps the basic baryon core from being dissociated in medium energy collisions. For example, the fact that strangeness is an element in elementary particle interactions did not become apparent until enough energy was available in the collisions to produce these new states.

Once we embark on such an experiment we must determine which is one of the most likely final states that may be produced in a baryon non-conserving collision. Here we must separate two pos-

sible types of non-conservation:

1. Baryon non-conservation that occurs because of the dynamics of a collision and hence may only occur when there is a "quark, antiquark annihilation." In such cases any number of final states may occur without a baryon in the final state. These may contain lepton pairs in addition to a large number of mesons, or just a large number of mesons.
2. Baryon non-conservation that occurs because the actual baryon core is disintegrated in the collision and the element of the core that carries the baryon number disappears. Then conservation of angular momentum requires the final state derived from the disintegration must have half integer angular momentum and hence an odd number of leptons must be present (the only fermion with baryon number zero). Of course this or these leptons can be accompanied by any number of mesons.

An experiment for ISABELLE that tries to observe such a reaction must be able to determine that two baryons are missing. As far as we can determine there is no detector that at these energies can distinguish a pion or kaon from a proton sufficiently well. Hence such an experiment must be designed to determine that the reaction occurred with no strongly interacting particles (charged or neutral) going through the detector. Hence all particles going through the detector must be either leptons or photons (either by themselves or from pi-zero decay). In addition we must determine that no baryons are escaping along the beam direction. Hence the

detector must be capable of measuring the electromagnetic (muons excluded) energy deposited in the detector to such accuracy to determine that less than 1.88 GeV is missing. This implies measuring the energy deposition to better than 2 out of 400 or ½%. Such an accuracy cannot be achieved on an event-by-event basis. Hence the signal must consist of a statistically convincing number of events all with energy depositions in the detector within a few percent of 400 GeV and all indicating that no hadrons were present in the final state.

Possible Detecting Arrangement. A good device to detect the presence of electrons is a transition detector.[3] Hence we would surround the interaction region with two stacks of transition radiators like the inner region of the "W Search Device" described in the lepton detector summary report.[4] It is shown in Figs. 1 and 2. Each stack would consist of 500 Li foils (~ 1 ¼ mils thick) with 20 mils spacing between foils. This set would give a π/e separation of better than 10^{-2}. Hence if our trigger is the requirement that no charge track be a hadron, we get a very good discrimination against typical events. This arrangement is then surrounded by an array of lead counters to measure the electromagnetic energy generated in the collision. The lead glass arrangement is shown in Fig. 3.

The central region would consist of 30 transition radiator units and 180 lead glass counters. Each of the end pieces would

---

3. J. Fischer, S. Iwata, V. Radeka, C.L. Wang, and W.J. Willis, BNL 20063. Submitted to Nuclear Instruments and Methods.

4. R. Burnstein, W. Carithers, M. Duong-Van, R. Imlay, M. Kreisler, U. Nauenberg, C. Rubbia, G. Snow, L. Sulak, H. Williams, E. Paschos, M. Sakitt, C.L. Wang and L.L. Wang, "Design of a Lepton Detector for ISABELLE", these Proc.

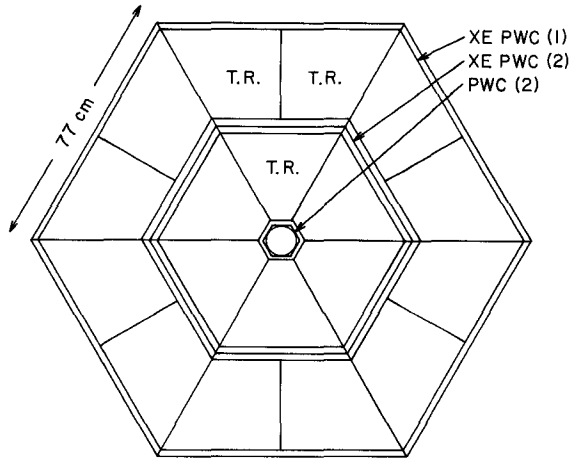

Fig. 1. Transition radiation detector system, cross-section through central region, view along beam direction.

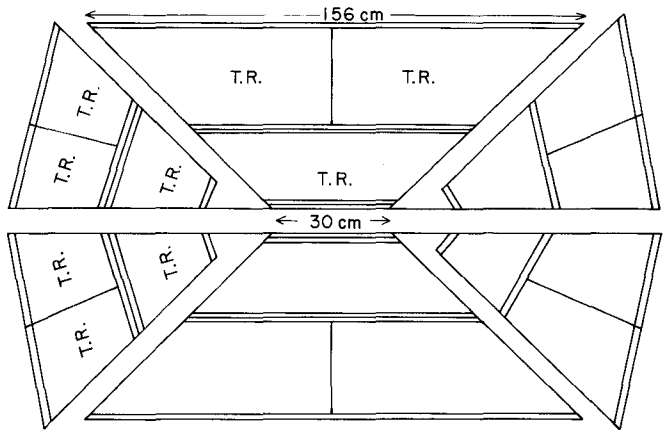

Fig. 2. Transition radiation detector system, vertical section through central region and end pieces.

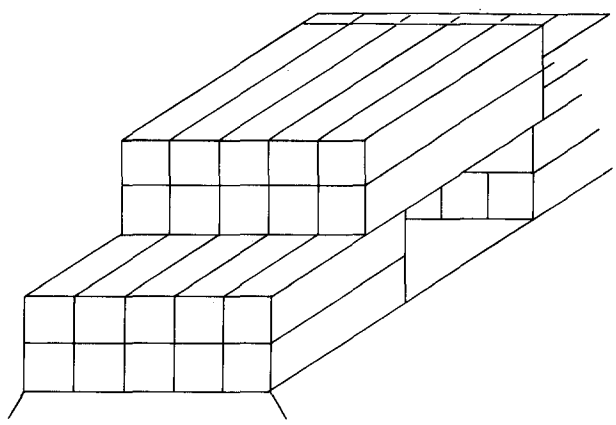

Fig. 3. One unit of lead glass arrangement for the central region.

have five transition radiators and about 10 lead glass counters. The number of MWPC wires is about 15,000 at a cost of about $15.00/wire. We could read wire combinations by tying wires/readout reducing the price substantially. The cost of the lead glass counters is about $800.00/unit. Roughly the cost of this device is about $400 K.

Rates. Because of the high counting rates, this experiment would not use the full luminosity of 10^{33} sec^{-1} cms^{-2}. A luminosity of 10^{32} sec^{-1} cms^{-2} leads to a counting rate in the forward modules of $\sim 10^5$ counts/sec/module which is manageable.

3. New Object Detector

(Analysis contributed by L. M. Lederman, Columbia University)

Consistent with the introductory charge to the "New Ideas" group, we outline here the conceptual design for a new object detector (NOD) with the following desired properties:

1. Wide angular acceptance.
2. High rate capability.
3. High mass resolution over a large range of masses.
4. Flexible triggering arrangement.
5. Measure charges of all objects.
6. Study interaction and decay properties of new objects.

We must keep in mind the fact that an ISA with 10^{33} luminosity will produce no more than $\sim 5 \times 10^{13}$ interactions per year. Any detector which can define a signal at say one event per 20 hours of high luminosity running is sensitive to no less than $\sigma \sim 4 \times 10^{-36}$ per one percent of overall efficiency.

The NOD makes use of many ideas picked up in the corridors of the ISA summer study, principally the new gas Cerenkov counter ideas of Sandweiss and Fitch, hadron calorimeter ideas of Willis, etc., etc.

We divide the system into its subsystems proceeding from the interaction ring outward. We refer to Fig. 4. We opt for 90° CM as the place where background to signal may be optimum--certainly the most favorable, geometrically.

A. Gas Cerenkov Counter

This makes use of the old idea that the observation of the Cerenkov angle θ_c via the radius of illumination in the focal plane of a spherical mirror is a sensitive measurement of β. Since for $\beta \approx 1$, this is the most difficult part of the problem, we note that, for negligible error in Δp,

$$\frac{\Delta m}{m} = \gamma^2 \frac{\Delta\beta}{\beta} = \gamma^2 \frac{\Delta\theta_c}{\theta_c} \quad .$$

We adopt a momentum range of 1 - 20 GeV/c and argue that new objects of low mass are adequately searched up to $P_\perp \lesssim 10$ m, i.e., $\gamma \lesssim 10$. Thus, if we insist that the worst mass error is $\lesssim 10\%$, we need

$$\frac{\Delta\theta_c}{\theta_c} \lesssim 10^{-3}$$

(very ambitious!).

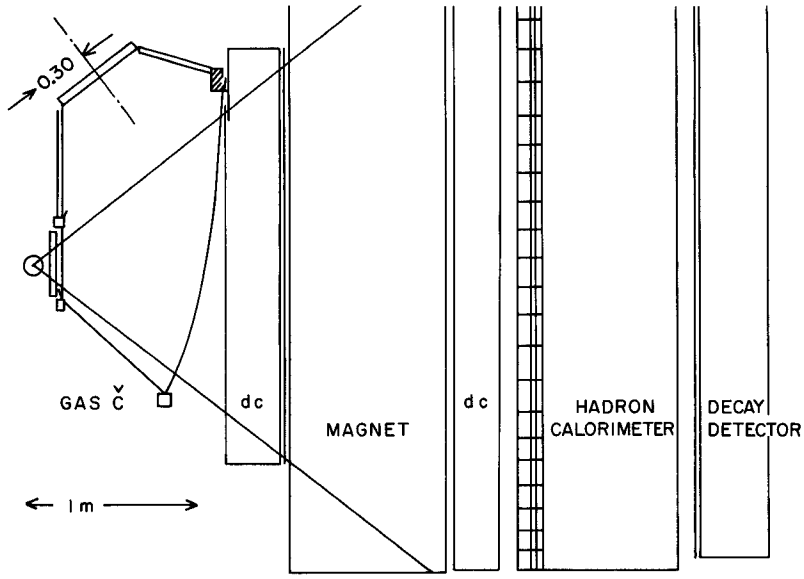

Fig. 4. Overall arrangement of the New Object Detector.

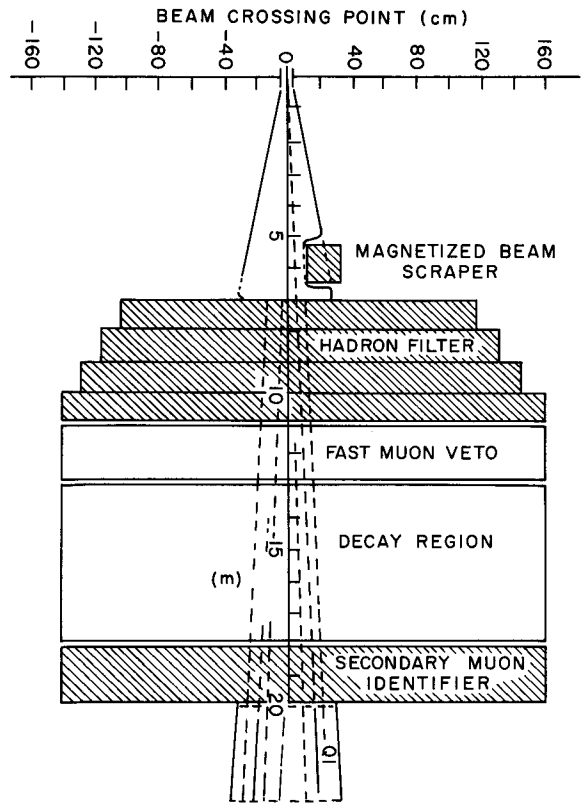

Fig. 5. Overall detector arrangement for K_L^o - type experiments to search for heavy leptons.

Radii may be measured by a Channel Electron Multiplier array (Sandweiss), by calculations from PM sampling of various sections of the focal plane (Fitch), perhaps by Xenon MWPC. We require $\gtrsim 5$ photoelectrons for good averaging--and a spatial resolution obtained from the following:

$N_{phe} \approx 100\ L\theta_c^{\ 2}$ Photoelectrons

$\theta_c \gtrsim .03$ in order to have $\sim$10 photoelectrons in one meter of gas

$f \sim$ one meter

Radius $R_c = f\theta_c \gtrsim 3$ cm.

(For a lethargic object of $\beta = .95$, $\gamma^2 = 10$ the radius is 30 cm which we take as an absolute upper limit for the Cerenkov aperture.)

Thus for $\Delta\theta/\theta \sim 10^{-3}$, we need a Δr of 30 μ. The total area of the photoconverter will be 60 x $\sim$100 = 6000 cm^2. If all of this were to be subdivided into 30 μ cells, would require:

$$\frac{6000}{\pi(.003)}\ 2 = 2 \times 10^8\ !$$

Since this is probably too much, we note that the larger radii require less detail--but we are left with about 10^7 elements and the need for a clever serial readout system which does not require the location of 10^7 preset addresses as in PWC's.

The optics are probably such as to focus the line source of the interaction region into a line. Dispersion and aberrations, etc., are assumed correctable to the required precision.

(Several suggestions for improvements have been made: i.e., i) clever optics that would convert the "DISC"--a zero acceptance Cerenkov that measures $\Delta\beta/\beta \sim 10^{-5}$ to a wide acceptance device,

ii) use a laser-driven shutter in synchronism with laser induced bunching in the machine for time-of-flight with picosecond resolution. In view of this, we believe a wide acceptance device at $\Delta\beta/\beta \lesssim 10^{-3}$ is in the bag.)

B. Magnet System

This is a simple track-magnet-track system. We are dealing with momenta from 0 to $\sim$20 GeV/c and we are backed up by a hadron calorimeter. Thus, we set a criterion of negligible contribution to the mass error:

$$\left(\frac{\Delta m}{m}\right) = \frac{\Delta p}{p} \lesssim .05 \quad .$$

A one-meter 10^4 gauss bend gives $p\theta = 0.3$ GeV

i.e., 10 GeV/c bends 30 mr .

In general for ≥ 4 on hits per track $\Delta p/p \sim \delta/L(0.3)p$ where δ is the resolution and L the track length. We chose L = 20 cm, δ = 0.2 mm and have

$$\frac{\Delta p}{p} = 3 \times 10^{-3}\, p \quad .$$

The biggest problem in this system is the rate in the PWC system which may go to $\sim$100 kcps per wire.

C. Hadron Calorimeter

This has several functions: to confirm the momentum measurement for hadrons, identify non-hadrons, hopefully improve the energy measurement at very high $P_\perp$, act as a mass measurer for shorter

lived neutral objects which decay hadronically via the effective mass of the secondaries.

Calorimeters of the Willis type using uranium and liquid argon have resolution

$$\Delta E \sim \frac{0.20}{\sqrt{E}}$$

but the integration time may pose a serious problem at the ISA rates. Nevertheless, at an integration time of ~ 30 ns, this would be a powerful addition. We visualize this as subdivided finely soon after the evolution of the electromagnetic part of the cascade in order to separate fairly small angle γ's. This might be done with PWC after ~ 1 rad length of uranium plates. In this way, π^o's could be identified up to ~ 5 GeV, η^o's to 8 GeV, etc.

D. Decay Detector

This is a large device, perhaps a streamer chamber or optical spark chamber (magnetized plates?), which looks, for ~ 2 m, at decays of long-lived objects. Candidates are heavy neutrinos or new K_L^o-type objects. This device is duplicated so that the one behind the hadron calorimeter looks at leptons or other non-hadrons. The duplicate sits on the far side of the vacuum pipe. See the K^o detector of Carithers for details.

E. Scintillation Counters, Triggering System and Charge Measurement

This is used for making roads in the track chambers at nanosecond resolution, for providing a fall back time-of-flight system for low β objects, for providing the trigger logic. The triggering

problem is difficult but will rely on the Cerenkov counter which, when blind to pions, will have a manageable intensity. We should also be aware of the possibility of fractional charge and include, if possible, a charge measurement to ±10%. This could most straightforwardly be done by a series of pulse height recordings, perhaps 4 in scintillation counters and also 6 in the PWC gas, acting in the proportional mode. After all, it makes no sense to measure a strange mass via β and p without verifying charge.

F. Summary

The main new point here is a fast, large acceptance mass spectrometer. The conceptual design tries to measure mass via β and p to $\gamma \cong 10$, to check or look for curious masses via the decay modes and to study the interaction properties of the new objects.

4. Search for Heavy Leptons via K_L^o-Type of Experiments at ISABELLE

(Analysis contributed by C. Y. Chang, University of Maryland, and N. P. Samios, Brookhaven National Laboratory)

Searching for new particles produced in a new energy region of PP collisions is of fundamental theoretical interest. In this note we propose to look for the production of long lived heavy leptons via K_L^o-type of experiments in the fragmentation region of PP collisions at ISABELLE. The new particle which we have in mind, might be characterized by:

1. Lack of strong interactions.
2. With a mass bigger than a few GeV/c^2 (e.g., > 5).
3. Possessing new quantum number, hence, a long lifetime.

4. Having a "0" or integral charge (M^o, $M^{\pm}$).

5. Decaying into ordinary leptons on the lowest leptonic states of its own kind, and some hadrons.

As shown in Fig. 5, the detecting system is located at the down stream end surrounding one of the crossing beams. It consists of a hadron filter, a fast muon veto device, and a decay region for the heavy leptons. The design is supposedly optimized to the following facts: i) covering the smallest possible P_t and highest $X = 2P_\ell/\sqrt{S}$ region for the new particles, ii) largest possible solid angle, iii) smallest decay path for high energy π's and K's into muons, and iv) largest decay probability of the heavy lepton.

The hadron filter is mainly a four meter deep Fe block. It provides more than twenty absorption lengths for the hadrons to interact. We assume that the $\lambda_\pi \simeq 130$ to 150 gm/cm^2, hence, the probability of hadron punch-through is $\simeq 10^{-9}$. For weakly interacting particles, such as muons and heavy mass charged leptons, dE/dx is $\simeq$ a constant due to ionization alone, essentially all of them should penetrate through the absorber with 6 - 7 GeV energy losses. Figure 6 shows the expected $\mu^{\pm}$ spectrum from the $\pi^{\pm}$ and $K^{\pm}$ decay in flight in the intersection region where 6 GeV energy loss into the four meter Fe block stopping material has also been taken into account.

Since muons are unwanted, they must be efficiently vetoed. For M^o, the fast muon veto device can simply be a scintillation counter which vetoes all charged particles that penetrate the hadron filter. For charged heavy lepton search, we can either use a gas threshold Cerenkov counter or some transition radiation detectors to veto the particle of high γ.

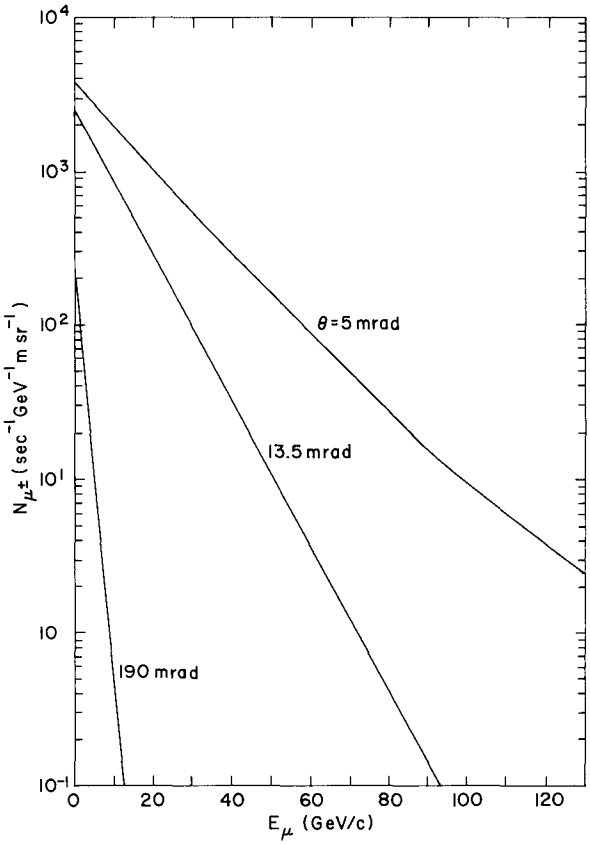

Fig. 6. Expected muon spectra after hadron filter, at various angles to the beam. θ is the angle between the muon and the primary beam direction.

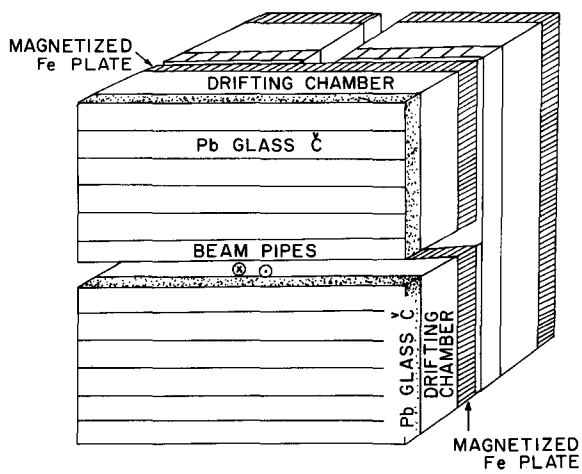

Fig. 7. Detector module arrangement for the decay region, which consists of five secondary particle detection modules, three in horizontal planes and two in vertical planes.

The decay region consists of five secondary particle detection modules. Each module, as shown in Fig. 7, consists of an array of Pb-glass Cerenkov counters (~ two radiation lengths thick), a drift chamber, and a magnetized Fe plate. The Pb-glass Cerenkov counters serve two purposes: i) making sure that the incoming $M^{\pm}$ has a muon pulse shape, and ii) serving as a π^{o} converter and e,μ identifier after the heavy particle decays. The drift chamber measures the decay vertex and the tracks of the decay particles of the heavy mass particle. The magnetized Fe plates provide a momentum analysis for the charged secondaries and also identify the μ's and π's, because pions may shower through the Fe plates. In order to cover smaller P_t regions, the detection modules are symmetrically located in all sides of the beam pipe. In addition, a magnetized beam scraper in the upper stream of the absorber is also under consideration. Such a scraper may serve as an ∞ aperture septum to the heavy leptons, but a beam scraper to the hadrons.

Behind the decay region, we may put a five interaction length μ-identifier there. Hence, the decay leptons can be identified.

Summarized below, the main features of this detection system are:

1. $\Delta\Omega \sim 0.0314$ str.
2. Smallest $P_t \simeq 0.28$ GeV/c or much lower if the magnetized scraper works,

   $X \simeq 0.25$ assuming $(P_L) \simeq 50$ GeV/c.
3. The decay detection efficiency is $\simeq 0.128$.
4. The most sensitive life time of the heavy particle depends

on the M/P ratio, i.e., $\simeq 48/\gamma$ for this particular arrangement. Therefore, it is sensitive to a 5 GeV/c^2 particle of momentum ranging from 10 to 100 GeV/c and life time ranging from 25 to 5 nsec. (proper life time), where for a 50 GeV/c^2 particle, the sensitive life time would be $\sim$230 to 50 nsec.

5. Since $\Delta\Omega^*$ decay detection efficiency $\simeq 4 \times 10^{-3}$, for luminosity = 10^{32} cm^{-2} sec^{-1}, we obtain: $10^{32} \times 4 \times 10^{-3} \times 10^{-33}$ event/nb-sec = 4×10^{-4} event/nb-sec $\approx$ 400 event/nb-300 hr.
6. Triggering rate and background.

5. Identifying Super-Massive Particles Decaying Solely into Very Many Hadrons

(Analysis contributed by C. Rubbia, Harvard University)

Assume that new particles exist with masses in the order of many tens or even hundreds of GeV/c^2. Except in some fortunate circumstances, like in the case of weak vector mesons ($W^{\pm}$, Z^o) where the two-body leptonic decay might be detectable, a standard multihadronic decay in many prongs is expected. Since these particles are likely to be produced with a very tiny cross section and with a large associated inelasticity, the question of how to separate between the decay prongs and the remaining particles, it is not completely trivial.

We shall define "massive particle" an object having the following basic properties:

i) a mass M comparable to the center-of-mass energy, $\sqrt{s}$,

ii) a lifetime longer than the collision time,

iii) definite quantum numbers, and in particular a (small) spin value,

iv) multihadronic decay with $\sim \log M$ type of multiplicity. This law is approximately verified by almost all multihadron final states with no leading particles.

Since the mass of the particle is comparable with the available center-of-mass energy, the particle will generally be very slow. In a first approximation we shall assume that it is actually at rest. The multiplicity assignment (iv) specifies the average momentum of the decay particles:

M (GeV/c^2)	$\langle n \rangle$	$\langle p \rangle$ (GeV/c^2)
50	15.2	3.27
100	18.0	5.5
150	19.7	7.6
200	21.0	9.65

Now, the basic idea is that because of assignments (ii) and (iii), there is no way by which the particle can "remember" (to an order $\cos^s \theta$) the direction of the incoming particles. Therefore, with respect to this direction, while the ordinary debris is strictly limited in $P_\perp$, this cannot be the case for the decay fragments of the particle, for which one expects:

$$\langle P_\perp \rangle \simeq \frac{1}{\sqrt{2}} \langle p \rangle \quad .$$

Therefore, the production of the new particles will be characterized

by an unusual "firework" of prongs which have all an "apparent" very large transverse momentum with respect to the incident beam line. This offers both an effective way of selecting for such events and a first crude handle on the mass, since large p particles carry the leading contribution in the expression of the invariant mass.

A way of illustrating the ideas is via a Peyrou plot, where $P_{\parallel}$ is plotted versus $P_{\perp}$. While ordinary fragments are expected to be confined to a very narrow region around $P_{\perp} \simeq 0$, the decay products of the massive particle are invariant with respect to rotations over the Peyrou plot. In such a plot it is also easy to see the effect of the slow motion of the decaying particle. The circle just becomes an ellipse.

Finally this method must not be confused with the "rapidity cluster" which is often suggested as a way of identifying massive objects since this last method, which works on "longitudinal" variables is very sensitive to particles produced with very large cross sections.

Likewise, this object is not a "fireball" or a jet which is characterized by a large conspiracy of particles in a given direction.

This is just one more of those unthinkable ideas.

6. Production of Anti-Nuclei at ISABELLE

(Analysis contributed by W. C. Carithers, University of Rochester)

As often noted, ISABELLE offers a considerable extension of the central plateau in rapidity (about 4 units). We have a high energy

density with no orientation toward particular quantum numbers. It is intriguing to identify this energy density as a microscopic model of the primordial "big bang," and to contemplate the possibility of cosmological experiments probing the hadronic era of the universe.

One particular model will serve to illustrate the possibility. There is as yet no cosmological model which can account for the observed non-homogeneous matter distribution in the universe on the basis of statistical fluctuations. A universe that begins as a homogeneous sphere will not evolve into the observed galaxies and clusters of galaxies as the result of statistical density fluctuations. Omnes has pointed out that this problem might be overcome by introducing a matter-antimatter phase transition near the end of the hadronic era of the universe. Crudely the idea is that antimatter (and matter) would "condense" locally like small droplets. The droplets are stable in the sense that if antimatter drops collide, they coalesce as do matter droplets. However, if a matter droplet approaches an antimatter droplet, the annihilation pressure pushes them apart. The model has the additional esthetic advantage of producing a universe which is charge conjugation symmetric.

Could one hope to observe a matter-antimatter phase transition? A naive approach might be simply to look for unexpectedly large production of light anti-nuclei $\overline{He}$, $\overline{Li}$, $\bar{C}$. Of course light nuclei would also suffice except for the background from nuclear spallation from beam-gas interactions or interactions in the wall of the vacuum chamber.

We present a simple argument based on quark-counting for calculating the expected yields of antinuclei. Consider the quark content of π^-, $\bar{P}$ (antiproton), and $\bar{D}$ (antideuteron):

	Quark Content	
π^-	$n\ \bar{p}$	$\bar{u}\ d$
$\bar{P}$	$\bar{n}\ \bar{p}\ \bar{p}$	$\bar{d}\ \bar{u}\ \bar{u}$
$\bar{D}$	$\bar{n}\ \bar{p}\ \bar{p}\ \ \bar{n}\ \bar{n}\ \bar{p}$	$\bar{u}\ \bar{u}\ \bar{d}\ \ \bar{d}\ \bar{d}\ \bar{u}$

The $(\bar{P}/\pi^-)$ ratio is a crude measure of the probability of picking up an extra antiquark. Call this probability x. Then the $\bar{D}/\bar{P}$ ratio should be proportional to x^3. Then

$$\left(\frac{\bar{D}}{\bar{P}}\right)\Big/\left(\frac{\bar{P}}{\pi^-}\right) \approx \frac{x^3}{x} = x^2 = \begin{cases} (5.0 \pm 1.2) \times 10^{-3} & \text{ISR} \\ (4.0 \pm 1.0) \times 10^{-3} & \text{Serpukhov} \end{cases}$$

$$x \approx 0.07$$

(The double ratio was chosen since it is the same at ISR and Serpukhov.)

We can then calculate the individual ratios

	Calculated	Measured (ISR)	p = 0.7 GeV
$\bar{P}/\pi^-$	.07	.10	
$\bar{D}/\pi^-$	2.4×10^{-5}	$5 \pm 1 \times 10^{-5}$	
$\bar{H}_3/\pi^-$, $\overline{He}_3/\pi^-$	8×10^{-9}		
$\overline{He}/\pi^-$	3×10^{-12}		
$\overline{Li}/\pi^-$	1×10^{-22}		

The cross section for large angle $\overline{He}$ production is then roughly:

$$\sigma_2 = 4(40 \text{ mb})\ (3 \times 10^{-12}) = 4.8 \times 10^{-37} \text{ cm}^2$$

$$\text{Counting rate} = (10^{33} \text{ cm}^{-2} \text{ sec}^{-1})\ (4.8 \times 10^{-37} \text{ cm}^2)\ \Delta\Omega/4\pi$$

$$= 41\ (\Delta\Omega/4\pi) \text{ counts/day}$$

Thus we might hope to detect $\overline{He}$ through ordinary production mechanisms. Detection of heavier antinuclei (e.g. $\overline{Li}$) would be strong evidence for a new process.

7. Metastable Neutral Particle Arm

(Analysis contributed by W.C. Carithers, University of Rochester)

A. Scope

Along with other bizarre objects which lack compelling theoretical motivation, one might contemplate a new neutral object which is stable enough to travel macroscopic distances before decaying. It might be a singlet ground state of a new quantum number such that it could decay only weakly. Even though possibly massive, it may have a substantial branching ratio to leptons, either exclusively, or along with a large number of hadrons. The basic signature would be the appearance of an n-prong vee whose vertex was a meter or more from the interaction region. One might also see large angle, high momentum muons from such a vertex. Secondaries in the forward direction (90° with respect to the interaction region) would be measured precisely in a traditional K^o spectrometer. One could obtain crude measures of the mass and hence lifetime from the

secondary particle momentum spectrum. Known objects such as Ξ^o, Λ, K^o, $\bar{K}^o$ provide convenient calibrations.

Implicit in all of the "novelty shop" proposals is the hope that the regime of large s, large $P_\perp$ is indeed a new territory full of new physics. We should not presume that even familiar objects retain their standard properties when born in such an unusual environment. The $(K^o,\bar{K}^o)$ system has proven to be an extremely sensitive interferometer capable of measuring miniscule effects. For example, the CP violating parameter ε might go to zero, or grow, or reverse its sign as a result of a different production mechanism for $K^o,\bar{K}^o$. Perhaps even Δm, the $K_L - K_S$ mass difference, will change as a result of tampering with the higher order weak process at production. By repeating the K^o interference experiments at ISABELLE we could check the stability of effects as small as $\Delta m/m = 10^{-14}$.

B. Detector

The apparatus is intended to search in $P_\perp$ collisions for:

1. Production of new and probably massive neutral, metastable objects.
2. Symmetry violations or changes in known symmetry violation in the $(K^o,\bar{K}^o)$ system.

The detector is situated at 90°. It should provide a sweeping field to remove soft charged particles, a decay region, large angle chambers to detect n-prong vees, and a forward spectrometer for the K^o studies. Moreover the detector should be compact in order to maintain a reasonable solid angle. One approach to the problem is shown in Fig. 8. Here the same superconducting coils provide both

sweeping and momentum analysis for the forward arm and large angle muons.

The design parameters can best be fixed by considering the minimum requirements for the K^o experiment, known in the trade as a "vacuum regeneration" experiment. Neutral K^o ($\bar{K}^o$) produced as eigenstates of strangeness decay as coherent combinations of K_L and K_S. Because of CP violation, the K_L and K_S decays interfere in the 2π channel. The 2π intensity as a function of the proper time, t, is a typical interference pattern:

$$I_{2\pi}(t) \propto \left(e^{-\Gamma_s t} + |\eta_{+-}|^2 + 2S(p)\,|\eta_{+-}|\, e^{-\frac{1}{2}\Gamma_s t} \cos(\Delta m t - \phi_{+-})\right)$$

Γ_s, η_{+-}, ϕ_{+-}, Δm have the usual meanings. S(p) is the momentum-dependent "dilution factor."

$$S(p) = \begin{cases} +1 \text{ for pure } K^o \text{ production} \\ -1 \text{ for pure } \bar{K}^o \text{ production} \\ \dfrac{\sigma(K^o) - \sigma(\bar{K}^o)}{\sigma(K^o) + \sigma(\bar{K}^o)} \text{ for incoherent production of both } K^o,\ \bar{K}^o. \end{cases}$$

Note that the experiment covers the 2 - 10 GeV K^o momentum range and is thus identical to our decade of experience at AGS and PS energies. Estimates of resolutions, detection efficiencies, and measurement errors are directly transferable. The one exception is the dilution factor, S(p). Because of the egalitarian production of particles in the central region, we should expect S to be substantially smaller at ISABELLE and our sensitivity to the interference term will diminish.

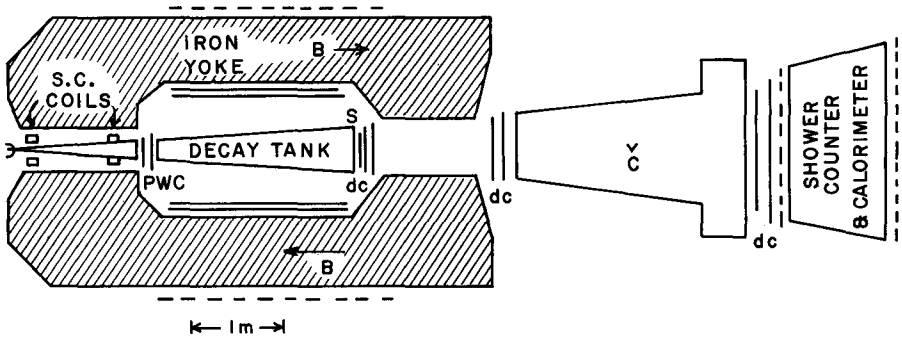

Fig. 8. Overall detector arrangement for metastable neutral particles such as the $(K^o, \bar{K}^o)$ system.

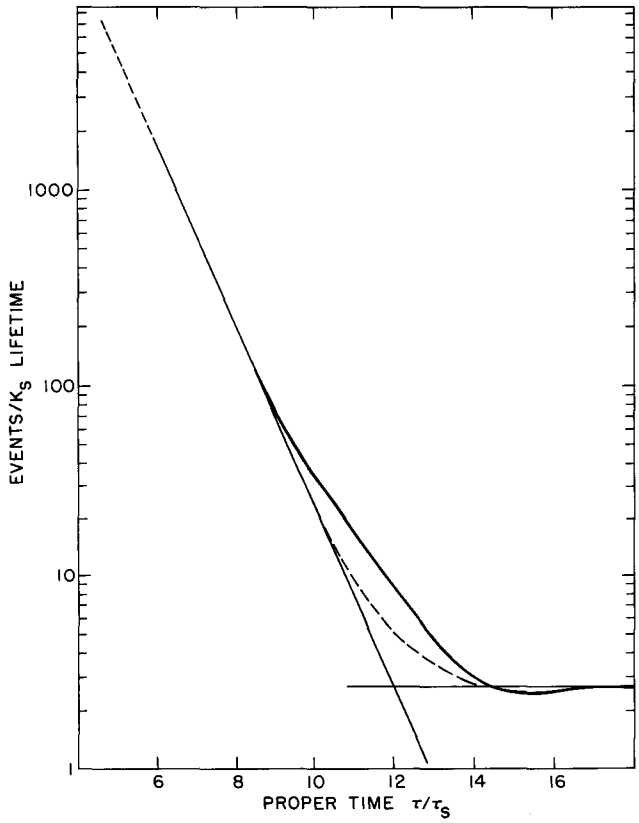

Fig. 9. Number of $K \rightarrow \pi^+ \pi^-$ events expected for a 100 hour experiment for typical dilution factors.

The superconducting coils provide approximately 1 GeV of bending power to sweep out soft charged particles. The length of the decay tank is fixed by the size of the interference region. The maximum sensitivity to the interference term occurs when interfering terms have equal amplitude. This occurs in the middle of the vacuum tank in Fig. 8 for a 5 GeV K_S, (i.e., 12 K_S lifetimes). The broad K^o momentum spectrum then sweeps out the interesting region in proper time.

PWC's precede the decay tank to tag remaining charged particles. Drift chambers just downstream of the decay tank measure the trajectory angles before entering the analyzing magnet. Drift chambers after the magnet complete the momentum analysis. A gas Cerenkov counter separates (π, μ, e) from heavier particles. Electrons are identified in the high z, thin plate front end of the shower counter/calorimeter. Muons are identified by their ability to penetrate the calorimeter while depositing minimum energy in the calorimeter. The detailed lepton identifications are important for measuring the leptonic charge asymmetries from K decays. The charge asymmetry gives an independent measure of Δm, S(p), and the $\Delta S = \Delta Q$ rule.

The decay tank is surrounded by drift chambers to detect an n-prong vertex. Since any long-lived object must decay weakly, one might expect a reasonable branching ratio to muons. Muons are bent in the magnetized iron of the return yoke. The muon momentum could be determined to about 25%.

C. Rates

Rates are based on the CCR parameterization of pion inclusive cross section at 90°:

$$\frac{d\sigma}{dP_\perp \, d\Omega} = \frac{1.5 \times 10^{-26}}{(P_\perp)^{7.24}} e^{-26.1 \, P_\perp/\sqrt{s}} \frac{cm^2}{GeV \, .sr} \quad .$$

Figure 9 shows the number of detected $K \to \pi^+\pi^-$ events expected for a 1000-hour experiment. The easiest way to characterize the sensitivity is to note that we expect

$$3 \; K_L \to \pi^+\pi^- \text{ events}/K_S \text{ lifetime} \quad .$$

This should result in a 25% measurement of $|\eta_{+-}|$. The phase of η_{+-} is less well determined because of the dilution factor. One could probably do no better than localizing the phase to a quadrant.

The singles rates in the front PWC will be less than 10^6/sec which could be easily tolerated. The detector of Fig. 8 is sensitive to new metastable neutral objects with lifetimes greater than 10^{-8} sec. If we assume that the object is produced with transverse momentum = 5% of its mass, then a limit at 90% confidence of 3.7×10^{-33} cm^2 could be placed on the production cross section if the lifetime were 10^{-8} sec.

LATTICE

Summary Report of Working Group*

L. Smith

Lawrence Berkeley Laboratory

Variants on the Standard Lattice

The lattice presented in the Yellow Book seemed reasonable and no attempts were made to improve on it.

Early in the study period, interest was expressed in using higher field magnets (for the same energy) and in a possible reduction in scope in order to save construction cost. Somewhat later, it appeared desirable to increase η, the rate of change of rotation frequency with momentum, in order to alleviate the requirement on wall impedance to avoid exciting a longitudinal instability. Although these motivations waned in importance by the end of the study, we had constructed a number of variants on the basic lattice, which are described in Table I.[1] The procedure was to remove cells from the normal part of the lattice and juggle the lengths of magnets, cells and insertions in order to maintain a rational relation of circumference to that of the AGS and approximately the same dispersion, which quantity directly affects the required aperture. One can see the general trend from the Table; as the field increases and the number of insertions decreases, the circumference and required number of magnets decrease whereas η increases. The two (5 T, 6 INS) columns show the effect on η of changing the dispersion, X_p. Although these trends are favorable with regard to both cost and the instability problem, it should be remembered that even at 5 T a new and more expensive magnet design would be required[2] and a reduction in the number of insertions would drastically reduce the scope with only a small saving in initial cost. Moreover, the increase in η, which is almost proportional to aperture divided by circumference

*A.W. Chao, D. Edwards, J. Gareyte, J.P. Gourber, A. Garren, J.C. Herrera, M. Month, L. Smith.

1. M. Month and L. Smith, private communication.

2. D.B. Thomas, "Magnets and Cryogenics," these Proc.

TABLE I. Lattice Variations

	4 T 8 INS	5 T 8 INS	5 T 6 INS	5 T 6 INS	6 T 8 INS	6 T 6 INS
Circumference	2959.5 m (3-2/3 C_{AGS})	2623.2 m (3¼ C_{AGS})	2421.4 m (3 C_{AGS})	2421.4 m (3 C_{AGS})	2421.4 m (3 C_{AGS})	2017.8 m (2½ C_{AGS})
L_{cell}	25.4 m	24.0 m	23.0 m	24.56 m	23.6 m	23.6 m
ℓ_B	4.09 m	3.74 m	3.49 m	3.88 m	3.64 m	3.64 m
L_{INS}	115.9 m	111.9 m	127.6 m	133.4 m	113.9 m	100.3 m
No. "B" cells	64	56	60	54	48	48
No. "E" cells	16	16	12	12	16	12
Sagitta	1.25 cm	1.31 cm	1.14 cm	1.41 cm	1.49 cm	1.49 cm
$X_{p,max}$	1.64 m	1.77 m	1.58 m	1.88 m	2.03 m	2.03 m
No. B (1 ring)	256	224	240	216	192	192
No. Q (1 ring)	216	200	186	174	184	162
γ_T	21.6	19.57	19.91	18.25	17.56	16.03
η_{INJ}	1.129×10^{-3}	1.597×10^{-3}	1.508×10^{-3}	1.988×10^{-3}	2.229×10^{-3}	2.877×10^{-3}

is not sufficient to justify a major change in these fundamental parameters for that reason alone.

II. Special Insertions

Two problems were addressed in this area — the design of a high-β (60 - 70 m) insertion and a study of the orbit-dynamical consequences of replacing one standard insertion by a low-β insertion. The high-β insertion was completed and used by the experimental insertions group[3] in their experiment to study elastic p-p scattering in the nuclear-Coulomb interference region, requiring the measurement of small scattering angles. The work on the low-β insertion consisted of matching it to the rest of the lattice for on-momentum particles, finding sextupole strengths to reduce the chromaticity to zero, examining the variation of tunes and β-values at each interaction point as a function of momentum and considering the impact of the 3rd integer resonance at 25-2/3 which is excited by the chromaticity correcting sextupoles when the periodicity of the lattice is reduced to unity. The results, described in Ref. 4, show that the momentum aperture is reduced, but perfectly adequate for collision conditions. Also, the excitation of the 3rd integer resonance is found to be quite weak.[5]

III. Correction Windings

In conjunction with the magnet group, recommendations were established for a configuration of correcting windings. With regard to systematic effects, we believe the dipoles should be made as uniform as possible by removing the known sextupole and decapole components, and that the duo-decapole component in the quads should also be removed. Each of these corrections would involve a single circuit, programmed in time during acceleration. The linear and quadratic chromaticity should be controlled by sextupole and octupole windings in the quads. For the standard configuration, two circuits for each should be sufficient to control the vertical and horizontal tunes

3. J. Sandweiss and T.F. Kycia, "Experimental Insertions," these Proc.
4. A. Garren, "ISABELLE with One Low-β Insertion," these Proc.
5. M. Month, private communication.

independently; however, during operation with special insertions it might be desirable to have a more complicated circuitry to reduce local β variation with momentum should it be required.

In addition, the beams should be separated vertically at the interaction points during stacking and acceleration. A set of four dipoles located in each insertion is suggested for this purpose. This is discussed in Ref. 6.

With regard to random dipole errors, there should be independently powered dipoles in each of the normal cell quads, alternating vertical and horizontal, in addition to the set of dipoles in each insertion whose function it is to make the beams meet properly.[6] Closed orbit errors of several millimeters are tolerable, except at the interaction points, where the insertion dipoles should provide a vertical accuracy of better than 0.1 mm.

Skew quads are needed to control coupling and vertical dispersion; these quads could go in the cell quads, powered to give a zero-harmonic control for coupling and two or three nonzero harmonics for vertical dispersion.[7] Since the dispersion is of major concern at the crossing points, where it would increase the effective beam height, a system of local vertical dispersion correction might be more appropriate whereby the beam heights could be carefully and independently controlled at each crossing point.

IV. Working Line and Nonlinear Resonances

The region in the tune diagram which is considered most suitable for operation is that between the 5th and 3rd order resonances, i.e. between 25.60 and 25.67. From the point of view of transverse coherent instabilities, sufficient Landau damping is obtained with a tune spread,[8] $\delta\nu \approx 0.02$. In the coasting beam, a corrected working

6. D. Edwards, "Closed Orbit Adjustment", these Proc.

7. A.W. Chao, "Some Effects of Random Errors in ISA Magnets", these Proc.

8. E. Keil, "Performance Limitations", these Proc.

line of this magnitude can be obtained with the chromaticity correcting sextupoles and thus a 10 A beam comfortably fits into the available working space. The space-charge tune shift due to direct space-charge[9] in addition to image contributions was computed, taking proper account of β-variations and dispersion, to be ~ 0.015 units (at 30 GeV), with a variation of about 10% between center and edge of the stack. This is a small effect. In any case, it is correctable by proper variation of quadrupole settings and the settings of the chromaticity correctors (sextupoles and octupoles).

When the beam is bunched for acceleration, the space-charge effects change due to the beam bunching, while the tune spread due to chromaticity is also changed as the beam momentum spread increases. These effects cannot be fully compensated magnetically in the same manner as indicated above for the coasting beam. This is because when the beam is bunched a new phenomenon must be taken into account, the synchrotron motion. As an individual particle executes synchrotron motion, it changes its physical position in the bunch. For a particle with peak synchrotron amplitude, the motion during a synchrotron cycle is along the complete bunch length, from head to tail and so on. Now, when a particle is at the end of a bunch, it feels no space-charge tune shift since the longitudinal charge density must fall to zero; while at the center of the bunch, the particle feels the maximum tune shift, roughly the coasting beam value times the bunching factor. Thus, again using Ref. (9) and assuming a bunching factor of 2 (see Ref. 10), we obtain, at 30 GeV, $(\delta\upsilon)_{max} \simeq 0.03$. Now it should be pointed out that such an intrinsic spread in tune cannot be compensated for by conventional means.

Although this value of tune modulation of about 0.03 units is consistent with a placement of the beam along the main diagonal safely within the boundaries between the 5th and 3rd order resonances,

---

9. A.W. Chao, J.C. Herrera and M. Month, "Betatron Tune Change Due to Direct Space-Charge in the ISA", these Proc.

10. W. Schnell, "Stacking and Acceleration", these Proc.

it was still thought desirable to look at the consequences if the ISA was forced to operate across the 5th and even across the 3rd order resonances when the beam is initially bunched. After calculating the stopband widths on the basis of random errors in the placement of conductors, we concluded that the 5th order resonance widths even those due to the excitation of the systematic 5th order resonances were sufficiently small to require no corrections, while the 3rd order resonances are large enough so that correction elements would be necessary. However, only a limited number of elements located adjacent to two diametrically opposite insertions would be needed for this purpose. It should be noted that the space-charge effect discussed here has a characteristically rapid fall-off with energy; specifically, it goes like $1/\gamma^2$. Thus, as acceleration proceeds, the effect rapidly disappears. This implies, of course, that the sextupole resonance correction elements would only be required at low energy.

The conclusions of this section are considered in more detail in Ref. 11.

---

11. J. Gareyte and J.P. Gourber, "Control of Betatron Tune and Resonances," these Proc.

BEAM TRANSFER, INJECTION, AND EJECTION

Summary Report of Working Group*

L. C. Teng
Fermi National Accelerator Laboratory
A. van Steenbergen
Brookhaven National Laboratory

Before starting the discussion of the summary of the Beam Transfer Group effort, I have been asked to apologize for the absence of Lee Teng, the Chairman of the group, who would have given this presentation, but had to leave early this morning to report back to FNAL before going on vacation. His absence today is certainly not due to a lack of enthusiasm, since we worked late last night in order to complete the essence of this summary report.

The best way of discussing the group's effort is to outline the objectives for the group as they were formulated prior to the study and sequentially then to deal with each of these topics. A summary of the objectives is as follows:

Beam Manipulation in the AGS and ISA
Transfer Synchronization and Component Tolerances
Phase Space Clean-Up, Transfer Dilution, Distributions
Injection Kicker Stray Field Tolerance on the Stack
Injection Components, Impedances.

Ejection, Slower Versus Existing Fast Ejection
Analysis of Ejection System Losses and Tolerances
Particle Spectrum Downstream of Ejection Septum
Protective Beam Dump Trigger Logic
Redundant Internal Dump
Ejection Components, Impedances.

---

* L. Blumberg, H. Brown, A. Faltens, J. Peterson, J. Ranft, A. Stevens, L. C. Teng, A. van Steenbergen

Beam Scraping at Injection, During Acceleration, Ejection
Residual Phase Space Distributions
Effectiveness of Scraping at High Energy
Impedances of Beam Scraping Hardware
Beam Dump Absorber, Caloric Denisty Distribution
Cascade Data vs Primary Energy, Beam Size, etc.
Absorber Design Criteria, Stress vs Melting Point Criteria.

ISA Beam Losses, Definition of Sources and Characteristics
Shielding, etc.

Even though the design of the injection and ejection-beam dump systems were essentially complete, it was the group's desire to spend some time on reviewing the details of this in order to arrive at independent judgments and to see if one could come up with clever solutions, improvements, etc. It was decided to spend the first half of the first week on this subject and, if the right ideas evolved to follow through on these or, alternatively, if the concepts were found to be basically sound, to accept these and then to proceed with the outlined objectives. Since I may be slightly prejudiced on the subject, I will quote here the statement of the external chairman verbatim, as follows: "We spent some time in examining these designs and found them sound and workable and that there are no obvious ways to improve upon them". Consequently, after the first half week the group turned to examine in detail the above mentioned objectives. The overriding considerations which crucially dominate the design of the injection, ejection and beam scraper systems are (1) longitudinal impedance, (Z/n) and (2) beam loss in the ISA Rings.

1. Longitudinal Impedance

Since the injected beam has a relatively small momentum spread it is readily susceptible to longitudinal instability. This puts a limit on the maximum allowable impedance (Z/n) of the beam enclosure. Various estimates put this limit at approximately 5 Ω. This is a very low value when considering standard injection and ejection

components as one encounters these, typically, in the FNAL accelerator or the BNL accelerator. Abrupt changes in cross section, etc., within the vacuum chamber can easily contribute more than 5 Ω at high mode numbers, n (GHz range), if special features are not incorporated in the design. An example of such an irregular structure is the ISA injection kicker (Fig. 1). This is a vertical fast kick injection device to direct the injected beam onto the injection orbit. Typically, this unit was examined in detail with regards to structure in order to arrive at a small component impedance, Z/n, It can be stated, in general, that the group made a special effort to insure that none of the injection, ejection and beam scraper components would add significantly to the (undesirable) Z/n magnitude.

As a preliminary conclusion it can be stated that the impedance sum of all the components involved in the above systems is expected to be less than 1 Ω.

2. Beam Loss in the ISA Rings

The superconducting magnets in the ring will quench when struck by an excessive amount of stray beam. Theoretical and experimental results indicate an ultimate upper limit on the tolerable energy deposition in the superconductor-copper matrix of $\sim$ 30 mJ/cm^3. One order of magnitude less than this is considered safe. During normal beam injection and stacking there is a significant amount (up to 50%) of beam loss of the 30 GeV beam associated with the desire to "overstack" in order to obtain high phase-space density. Also, during normal protective ejection there is an approximately 0.1% loss of 200 GeV beam on the ejection septum. In the event of component failure, more disastrous beam loss may occur. In order to absorb safely these losses, high efficiency beam scraping and absorption systems must be incorporated which can effectively reduce the energy deposited by stray beams anywhere in the superconducting magnets to below 3 mJ/cm^3 at all times.

at $\beta_x = 40$ m ; $\beta_y = 8$ m ; $X_p = 1.7$ m

with $A_H = A_V = 0.4\ \pi\ 10^{-6}$ rad-m

Note : Prior to stack rebunching, the beam would be centered by field adjustment. Simultaneous with rebunching the beam would be scraped to the 0.7% high density stack only.

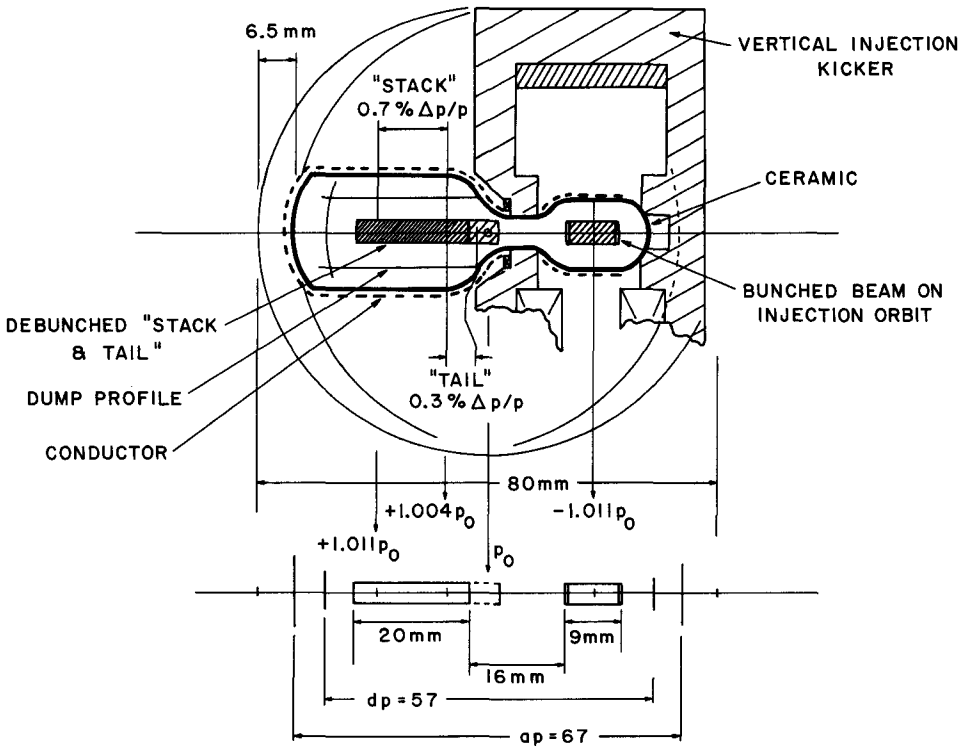

Fig. 1. ISA aperture subdivision during beam stacking at the injection kicker location.

A significant part of the group's effort was directed to the identification and characterization of the normal operational and potential accidental beam losses. Also, conceptual designs of scraper-absorber combinations have been worked out. Available computer programs were used to evaluate the development of the nuclear cascades in the absorbers and hence the energy deposition. Realistic ISA model geometries could not be used yet in the study of the effectiveness of the absorber units because of certain limiting features of the existing programs. Specific cascade programs are now underway from CERN, with which it will be possible to simulate the ISA geometries realistically. These should then be used to refine the proposed scraper-absorber designs and evaluate its final overall efficiency.

As a preliminary conclusion of the group's effort in the design of the scraper-absorber systems it can be stated that all normal operation particle losses can be absorbed safely in the scraper-absorber systems as conceptually designed, that a fast accidental beam dump on the internal absorber at 30 GeV will not damage the absorber or drive the superconducting structure normal, that the same holds true for a fast internal beam dump at 200 GeV, except that in the latter case the beam absorber would suffer local damage.

The present arrangement for the scraper-absorber system and cascade shield distribution in Insertion VIII is shown in Figs. 2 and 3.

Having discussed so far the main emphasis of the group's effort let me now turn back and mention some of the results and efforts related to the list of original objectives. Beam manipulation in the AGS and ISA was left to the rf group, although some aspects of this were considered in connection with the study of Transfer Synchronization and Component Tolerances. This latter topic was examined closely and it was concluded that the AGS-ISA transfer beam manipulation and synchronization did not demand excessive parameter tolerances. A quick check was made of the acceptable stray field

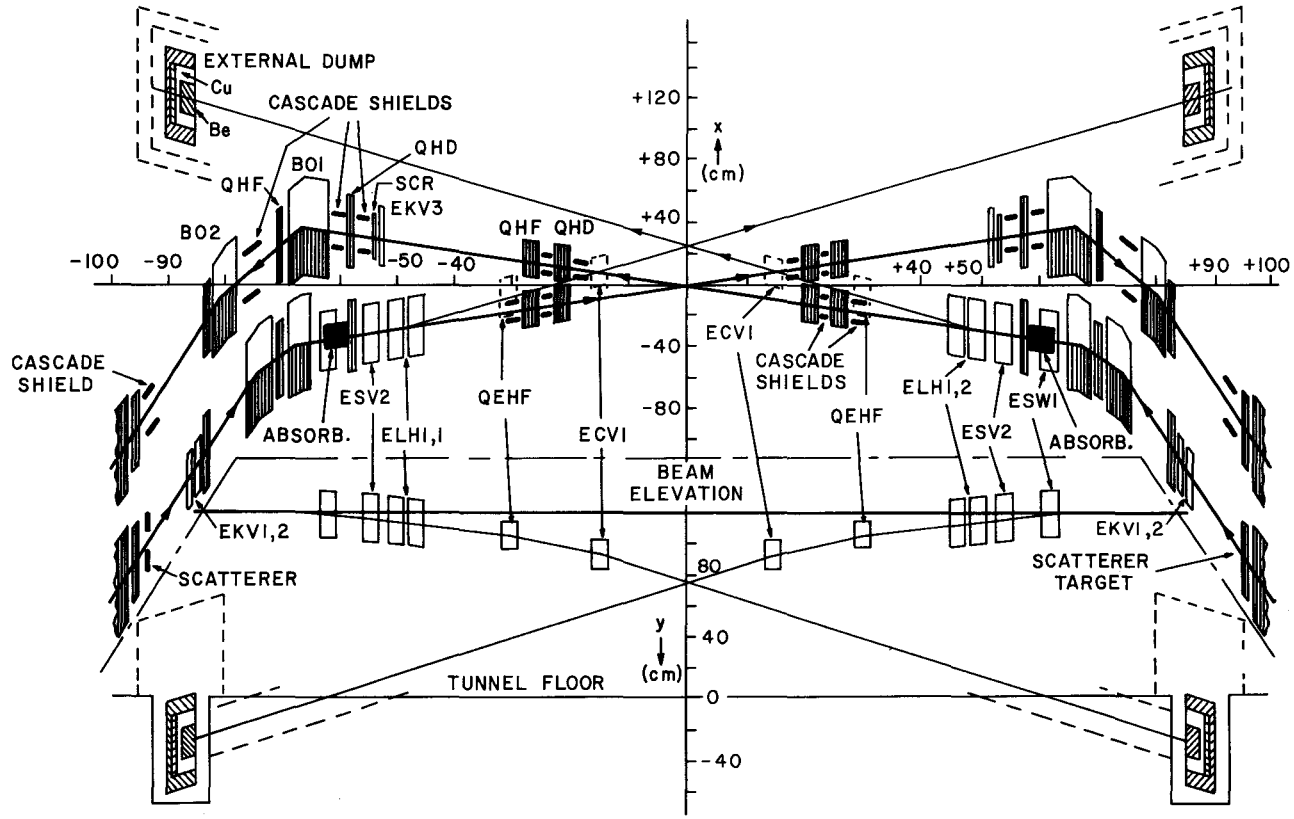

Fig. 2. Beam scraper-absorber combinations for beam clean-up in insertion VIII.

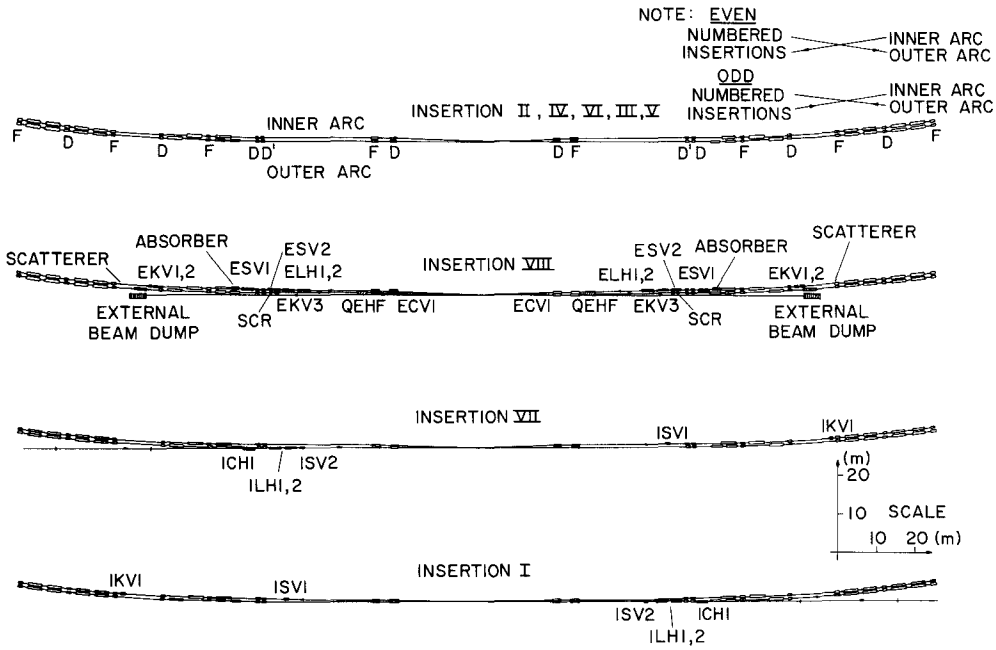

Fig. 3. ISA insertion, distribution auxiliary components.

of the injection kicker and its effect on the stack leading to a confirmation of the calculations carried out at BNL before. The injection components were studied, as indicated before, mainly with the objective of reducing impedance.

No further study was made of the possibility of a slower mode of ejection, mainly because of the difficulty associated with the protection against the cascade particles resulting from the ejection component losses and also because the cost savings would only be very modest. The protective beam dump logic was examined and it was concluded that the addition of the dump profile sensors to the usual trigger elements such as dI/dt, etc., would be advantageous. Also, the essentialness and basic design of the redundant internal dump absorber, a last "ditch stand" element in the ISA superconducting magnet protective system was confirmed. Use would be made of fast dumping on the internal absorber only, if the external beam dump sequence fails. Again, impedance aspects were studied associated with the ejection components.

Most aspects of the beam scraping-absorber systems have already been mentioned. There was no time to go into details and analytics of the beam residual phase-space distributions. The maximum caloric deposition criteria for the beam dump absorber were examined. In this respect it may be useful to define the magnitude of the caloric deposition problem as follows:

Deposition into Supercon Magents $\ll 30\ mJ/cm^3$

Reality; total beam stored energy 20 MJ

Example; dump 7×10^{14} p , 1 mm^2 beam,

into Aluminum $\rightarrow \hat{D}_{A\ell} \sim 40\ kJ/cm^3$

into Copper $\rightarrow \hat{D}_{Cu} \sim 1\ MJ/cm^3$

External Dump Absorber; 7×10^{14} p, 200 mm^2 beam,

into Beryllium $\rightarrow \hat{D}_{Be} \sim 0.8\ kJ/cm^3$

Some cascade calculations were carried out for the dump absorber, confirming the earlier empirical expressions for caloric deposition densities which were based on published isodensity

contours for various materials and 400 GeV protons. As a result the precise structure of the sequence of absorber elements in the dump absorber could be finalized.

Although anticipated beam losses were detailed, this was mainly done with the objective of designing the shields for the superconducting magnets. No effort was devoted in this group to the ISA biological shield design. This concludes this summary report.

STACKING AND ACCELERATION

Summary Report of Working Group*

W. Schnell

CERN

I. General Consideration

We assume that 11 bunches, containing a total of 5.2×10^{12} protons, are transferred from the AGS to ISABELLE at a total energy of E = 29.4 GeV. Each bunch is assumed to have an area in longitudinal phase space 1.02 eV s (or 0.0306 in units of $\Delta p/mc$ and rf radians). This implies that the density in these bunches is a factor of $\sqrt{2}$ larger than the density required in the finished 30 GeV stack, thus, allowing a small margin for dilution during stacking. Originally half the number of protons in 0.36 times the phase-plane area had been considered, but the longitudinal stability criterion given below made us choose an intensity close to the maximum that the AGS can deliver, at a density not much above the minimum consistent with the nominal ISABELLE performance.

The 11 bunches are directly trapped in an ISABELLE rf system, working at the AGS radiofrequency of 4.5 MHz and a maximum peak voltage of 12 kV, available from a single cavity per ring. A description of this cavity and its power source is given in Ref. 1. The bunches can be shaped in the AGS such that they immediately match the ISABELLE bucket trajectories. This requires an adiabatic rf voltage reduction in the AGS, and ejection from a flat top. It may be more convenient to eject directly during the full rate of acceleration, and perform the matching of the bunches — which tend to be too high in momentum and too short in phase — in ISABELLE by one of the customary methods. This could, however, lead

---

* J. Claus, A. Faltens, S. Giordano, A. Hofmann, E. Messerschmid, E. C. Raka, and W. Schnell.

1. S. Giordano, "Stacking RF System", these Proc.

to an intermediate situation which is even less favorable for longitudinal stability, than what is outlined below.

After capture, the beam is accelerated away from the injection orbit and the rf voltage is reduced adiabatically until the buckets fit tightly around the bunches. As there are only 11 bunches, 33 out of 44 buckets have to be suppressed to avoid unnecessary dilution of the stacked beam. Fortunately, this is required after the voltage is reduced, i.e., when the buckets approach the stack as it would be impossible at maximum voltage.

We propose, tentatively, to start suppressing the unwanted buckets at a level of 1.2 kV peak. This corresponds to a switching current of 7 A peak for a ferrite-loaded cavity with about 200 pF equivalent capacitance. Suppressing buckets at somewhat higher voltages is possible (e.g. by increasing the number of cavities) but expensive. At 1.2 kV peak rf voltage full buckets correspond to $\Gamma = \sin \varphi_s = 0.7$ (or a little less, if the beam-induced field in inductive walls is taken into account). Such values of Γ are reasonable from the point of view of stacking efficiency and of rf tolerances. We propose, therefore, to stop the adiabatic voltage reduction at this point and continue acceleration into the stack with these parameters.

The beam's space charge and the field due to the inductive walls tend to change the bucket area.[2] This can be compensated for by reducing the value of Γ. An estimate has been made of this contribution, assuming an inductive wall impedance approximately equal to the stability limit ($Z/n \approx 5\ \Omega$). The resulting value is $\Gamma = 0.63$. With these parameters the rate of acceleration into the stack equals about 17 times the equivalent "unbunched" momentum spread (viz. the bunch area divided by 2π) per second. The

---

2. S. Hansen, H. G. Hereward, A. Hofmann, K. Hübner, S. Myers, IEEE Trans. Nucl. Sci. NS-22, No. 3, 1381 (1975).

theoretical phase-space efficiency[3] of stacking 125 beam pulses with $\Gamma = 0.63$ is 86% (out of the total margin of $1/\sqrt{2}$).

II. Longitudinal Stability

The coupled longitudinal oscillations of the eleven bunches will probably be unstable. We have not studied this effect, but it is unlikely to present an insurmountable problem. If the growth time of the instability is too fast to be tolerated (in the ISR this instability does occur, but produces little or no blow up before the end of a stacking cycle), a feedback system, handling the dipole and quadrupole modes of each bunch, can be built.

A more serious problem seems to be presented by instability inside a bunch at high inside-bunch mode numbers, for which the growth time becomes comparable with, or shorter than, the phase oscillation period. It is believed,[4] that under these conditions the stability threshold is given by the well established criterion for unbunched beams, given below, into which the instantaneous values of beam current and momentum spread inside the bunch have to be inserted. The criterion is

$$\left|\frac{Z}{n}\right| < F \frac{E_o}{e} \frac{\eta}{I\gamma} \left(\frac{\Delta p}{m_o c} \right)^2 = F \frac{\gamma E_o}{e} \frac{\eta}{I} \left(\frac{\Delta p}{p} \right)^2 \qquad (1)$$

with

$$\eta = \frac{1}{\gamma_t^2} - \frac{1}{\gamma^2}$$

where $|Z/n|$ is the total longitudinal coupling impedance of ISABELLE divided by the mode number, $E_o/e = 0.938 \times 10^9$ V, γE_o is the total energy, γ_t is the transition energy in units of $m_o c^2$, I is the local beam current and Δp the full local momentum spread at half height.

---

3. M. J. de Jonge, E. Messerschmid, IEEE Trans. Nucl. Sci. NS-22, No. 3, 796 (1975).

4. D. Boussard, CERN Lab Report II/RF/Int./75-2.

The form factor F depends on the shape of the density distribution. We assume an approximately parabolic line density distribution – giving the same local instability threshold everywhere inside the bunch – with rounded edges, and take F = 0.7.

We first evaluate the situation at injection. With 12 kV rf, $\varphi_s = 0$, and the given bunch area and intensity, the bunching factor is about 6 and the peak current in the bunch is 2.8 A. The full momentum spread at the bottom is $\Delta p/p = 1.2 \times 10^{-3}$ and the value to be inserted in Eq. (1) is a factor 0.866 smaller. The criterion yields

$$\left|\frac{Z}{n}\right|_i = 9.1\ \Omega\ .$$

As the tolerable impedance is proportional to the square of the momentum spread over the current, the situation becomes even worse at reduced rf voltage. At 1.2 kV and $\Gamma = 0.7$, we find $Z/n = 4.0\ \Omega$.

It is believed that a stacked beam, surrounding the newly injected bunches in phase space, "shields" the bunches from the wall impedance, i.e. leads to a reduction of the rf currents seen by the walls, by a factor equal to the ratio of densities inside and outside the buckets. However, for as long as the empty buckets are not suppressed this factor can at most be 4/3 in threshold impedance. Applying this factor, we get

$$\left|\frac{Z}{n}\right|_{fo} = 5.3\ \Omega\ .$$

Finally, the effect on the bucket of inductive walls with $Z/n = 5\ \Omega$ and of space charge requires a change of Γ to 0.63 to maintain the given area. Then one finds

$$\left|\frac{Z}{n}\right|_f = 4.6\ \Omega$$

again assuming a factor 4/3 from shielding.

This is a rather low value. For the ISR a value of roughly 25 Ω has been measured. However, the ISR vacuum chamber was designed and built at a time when the problem at hand was unknown. We believe that a total coupling impedance Z/n of no more than a few ohms can

be achieved by careful design of the vacuum chamber and all components inside. The relevant parts are chamber cross section variations, bellows, clearing plates, pick-up electrodes, inflectors, dump kickers, cavity gap regions and — last but not least — the collision regions.

In order to increase the minimum value of $\Delta p^2/p^2 I$, one might consider increasing the voltage at which suppressed buckets can come on. But the gain in permissible impedance would be very small, at the price of a steep increase in cost of the rf system. Suppressed buckets could be abandoned altogether if one filled the ISABELLE circumference with four successive pulses from the AGS, prior to each stacking cycle. This would require a more expensive injection system (with a faster rising field in the injection kicker), make the effect of the coupled bunch instability more severe (the injected beam would be kept bunched for a longer time) and lead to the very undesirable complications of having to synchronize two rings. The gain in tolerable coupling impedance would still be small — perhaps to $Z/n = 5.6\ \Omega$, corresponding to full buckets at 7.5 kV and $\Gamma = 0.85$ (ignoring the "shielding" by the surrounding tail of the stack, also the reduction of bucket area by wall fields). Making the buckets fit tightly around the bunches at even higher voltgages would lead to values of Γ intolerably close to one, leading to bad stacking efficiency and overtight rf tolerances. In addition, the tight bunching resulting from such a choice — while being favorable for stability according to Eq. (1) — would make the influence of wall fields on bucket area intolerable, since this effect scales with the cube of the bunch-length.[2]

In any case, one should accelerate in the AGS at as high a current as is possible without further decreasing the longitudinal phase-plane density or increasing transverse emittance.

The reason for the problem with longitudinal stability is, of course, the small value of η, which is ten times smaller at injection in ISABELLE than in the ISR. The situation would be relieved

if one could lower the transition energy. To see the basic limitation to this course of action one may write Eq.(1) in the form of

$$\left|\frac{Z}{n}\right| < F \frac{E_o}{e} \left(\frac{\Delta p}{m_o c I} \right) \left(\eta \frac{\Delta p}{p} \right) \tag{1a}$$

The term $\Delta p/m_o cI$ (with the local values of Δp and I inside the bunch) is the inverse of the invariant phase-plane density and hence of a direct figure of merit of the storage ring and its injector. For energies far above the transition energy the last term tends towards $\Delta R/R$, where $2\pi\ \Delta R$ is the spread of path lengths in the injected beam, and R the average machine radius.

The most radical solution to the problem would be an intermediate storage ring in which one could stack ten or so AGS pulses prior to transfer to ISABELLE. This would relieve the main storage ring from a constraint that disappears once the stack has been made. Such an intermediate ring, housed in the AGS tunnel, could be relatively cheap and might, perhaps, be considered as part of a future improvement program.

III. The Accelerating RF System

It is proposed to rebunch the stacked beam and to accelerate it by a separate rf system operating at the second harmonic, i.e. at f = 202 kHz. A description of the hardware of the system is given in Ref. 5. Four ferrite-loaded cavities per ring will provide a maximum peak rf voltage of 40 kV. It is proposed to group the four cavities of one ring into one straight section. They occupy roughly two meter total length and 70 cm outer diameter. We propose to place the two groups into one of the modified bending cells. The power amplifier will be arranged to provide a maximum gap impedance – at the cavity resonance – of about 50 Ω per cavity. The effect of this impedance (and of other possible coupling impedances) on the trapping process has still to be studied. If necessary, the cavity impedance could be reduced by a beam-load compensation system consisting of a pick-up electrode and amplifier

5. S. Giordano, "Accelerating RF System", these Proc.

injecting into the cavity gap a current approximately equal and opposite to the beam current.

The choice of the harmonic number two is expected to avoid instability of coupled longitudinal bunch oscillations. In addition, the large spread of phase-oscillation frequencies (up to 40%) in a full bucket is expected to provide ample Landau damping. If all this fails, feedback systems for only two bunches per ring — and for dipole and quadrupole oscillations at least —would not be difficult to build.

In connection with the stacking rf system we discussed longitudinal stability inside a bunch, for high mode numbers, for which growth time is larger than the phase oscillation period. Since the tolerable coupling impedance for a given longitudinal phase-plane density increases with $\Delta p/p$, the stacked beam — once it has been made — should always be stable, even more so when it is bunched.

Acceleration by phase displacement, using a separate high frequency rf system, has also been studied. This is discussed in Ref. 6.

---

6. E. Messerschmid and M. Month, "Phase Displacement Acceleration for the ISABELLE Stack", these Proc.

PERFORMANCE LIMITATIONS

Summary Report of Working Group*

E. Keil

CERN

The Performance Limitation Working Group looked at the transverse stability of coasting beams. Let me briefly describe what that means. Consider the graph in Fig. 1 for that purpose. We draw a frequency scale at the bottom, and we draw an impedance scale perpendicular to it. We know that we get a threshold for Landau damping which will be a linear function of the frequency, where the offset is given by the chromaticity. The higher the chromaticity (that means the length of the working line essentially), the higher the offset. The slope of the curve is given by η (that's the parameter that Smith and Schnell used already), and the higher η, the steeper the curve becomes. Now, obviously, this impedance scale has to be compared to the actual impedances which are present in the machine, and the dotted line gives you some kind of vague idea what that impedance may look like, and some of the wiggles on it are of particular significance. There is a tiny little wiggle at the very low frequency end which in ISABELLE is the resistive component of the impedance, because of the aluminum chambers. The rather flat part of the impedance comes mainly from wall inductivity and capacity, and at frequencies well beyond the right edge of the graph, which are related to the transverse dimensions of the vacuum chamber, one gets into the resonant region which is vaguely indicated by a little peak on the right. Now, in order to make some kind of quantita-

---

* E. Courant, H. Hereward, K. Hübner, E. Keil, C. Pellegrini and A. Ruggiero

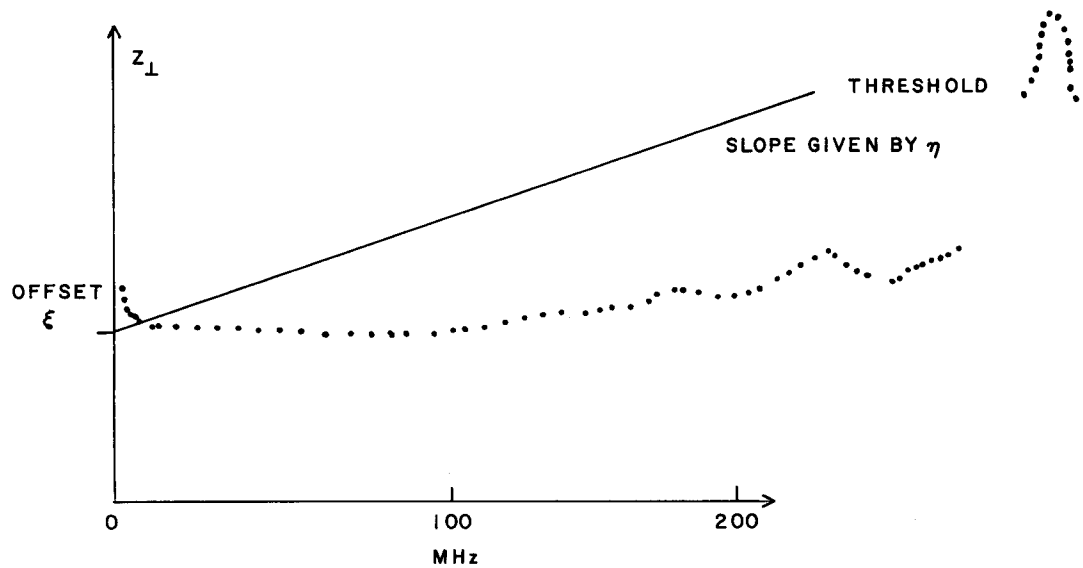

Fig. 1. Transverse stability of coasting beams.
Quantitative analysis done assuming that actual impedance is $(1 + \alpha)$ times the impedance of a smooth resistive chamber wall, at all frequencies.

At 30 GeV $\Delta\nu > 0.022 \quad (1 + \alpha)$

$f > \quad 200 \quad (1 + \alpha)$ MHz

At 200 GeV $\Delta\nu > 0.0012 \quad (1 + \alpha)$

$f > \quad 25 \quad (1 + \alpha)$ MHz.

tive analysis of those phenomena, we have taken the attitude that we know how to calculate the impedance of the smooth resistive vacuum chamber, and we assume that the impedance of the whole machine including all the other things like bellows, clearing electrodes, and other equipment, and all the flares in the vacuum chamber for the experiments, can be described by saying that actual impedance is a factor of $(1 + \alpha)$ bigger than the impedance we can calculate. Doing it this way, we can come up with two numbers. One is the ν-spread required if one wants to Landau damp the instability by chromaticity from the lowest frequency onward, and that gives the number of 0.022 times the factor $(1 + \alpha)$ at 33 GeV. The ν-spread required at 200 GeV is 1.2×10^{-3} $(1 + \alpha)$. I have written down another set of numbers which are the frequencies above which the spread and revolution frequency will be sufficient for damping purposes, and that is 200 $(1 + \alpha)$ MHz in the first case and 25 $(1 + \alpha)$ MHz in the second case. The numbers for 200 GeV really look very good as Lloyd Smith already showed on one of his transparencies. The spread and length of the working line is rather small so there shouldn't be much trouble with resonances, etc. And, if one wants to do it even better, one could probably design a feedback system which has a bandwidth of this order of magnitude. At 30GeV, the situation doesn't look that good, but one should remember that one only stays at 30 GeV for accumulating the beam and accelerating it to the operating energy almost immediately, in which case one probably could stand a lot of spread in the working line and just cross resonances and suffer a certain particle loss. Or, one could build a feedback system with a large bandwidth which then might be rather noisy, but that doesn't matter either because one only stays there for a short period of time. On the other hand, if one really wants to do colliding beam physics at this low energy one may have to reduce the current in the machine. One does reduce the luminosity this way, but one reduces the tune spread in

proportion to the current. So much for the transverse stability situation.

What one still has to do is to do a proper job of estimating the impedances of all the actual elements in the machine. Now, that can only be done as the design of the machine progresses. One should remember certain things which are, for instance, that we profit from the effect that the outer chamber is made of aluminum which has a very good conductivity and therefore resistive impedances are small. However, any resonant box made of aluminum is likely to have a much higher quality factor than the same box made of stainless steel. Therefore, it might be important to damp those resonances. As far as scaling from smaller machines like the ISR is concerned, one might mention that for the objects which repeat many many times in the machine, the situation doesn't seem to get worse when the radius of the machine goes up. For all the elements which are only once in the machine, like injection kickers and the like, the situation might be even slightly better.

A feedback system against transverse instability has to fulfill a certain number of requirements. First of all, the damping rate must exceed the growth rate of the instability, by a certain factor. The growth times are 24 msec or larger at 200 GeV and 3.5 msec at 33 GeV. The bandwidth of the feedback system must reach into the frequency range where one has enough Landau damping and that's related to the frequency I had on the previous transparency. And, finally, one must avoid blowing up the beam by the noise in the feedback system, and that gives the tolerance on the noise. So if I impose the condition that one may tolerate doubling of the square of the amplitude in ten hours at 200 GeV, and I assume that that safety factor is 10, then I get a noise figure on the pick-up electrodes, that the dipole moments (current times displacement) must be less than 20 μA-m. Those requirements, generally speaking, are less than what has been done in

the area already, which mainly has to with the larger risetimes of the instability.

The beam is bunched and this, of course, might develop the transverse instabilities on two occasions, during stacking and during the acceleration to 200 GeV or whatever the operating energy is. The harmonic numbers for the rf systems in both cases and the rf voltages applied are rather small. The synchrotron frequencies are small, and they tend to be small compared to the growth times of the instabilities. Hence, one can use the transverse coasting beam stability criteria which I have just been talking about, and one should get away with that. There is just one comment that, since the beam is bunched, the instantaneous current is higher, but it goes up in the same proportion as the momentum spread in the beam, and therefore even the same chromaticity should be enough. We have talked about the choice of the harmonic number in the accelerating rf system and we agree with the conclusions that harmonic number 2 is fine, but any other harmonic number would do just as well.

As you might remember from Ernest Courant's talk at the beginning of this study, another important performance limitation is the limit on the beam-beam interaction which usually is expressed as a limit on the beam-beam tuneshift. He has done a couple of computer simulations over the past year or two. The computer simulation consists of a succession of kicks and linear transformations which are repeated many many times, while one watches the amplitude of the particles. There are two forms of kicks which have been studied in some detail. One is a sharp kick where the force as a function of amplitude is going up linearly at the beginning and then going down like a hyperbola. The other is an exponential kick where this sharp edge is removed and replaced by a smooth curve. The kick amplitude is either constant in time or is modulated, which means that over 500 turns or so it goes up, then it's constant for another 500 turns and

then it comes down in 500 turns and then the whole process is repeated. Now, with the sharp kicks, one finds a steady growth of amplitudes which lasts for the whole duration of the simulation which is of the order of a million turns, and the growth starts at a tune shift of 0.002 which is lower than the conventional limit, and the growth becomes stronger, the higher this number is. It is rather insensitive to whether the kick is modulated in time or whether it is constant in time. For the exponential kick, the behavior is somewhat different. One sees a rapid growth of amplitude for only 15 000 turns and then nothing more happens up to the end of the experiment. And that kind of growth sets in at very much higher tune spreads, of the order of 0.04 for the modulated case, and 0.05 for the unmodulated case.

Now what shall we conclude from all that? Well, it has turned out, I think, in the design of ISABELLE and a couple of other machines that the beam-beam tune shift limit, which was considered a severe limitation at 0.005, is now avoided for other reasons and that one doesn't get the beam-beam tune shift up to that point anyway. The computer simulation then seems to show that the limit of 0.005 is indeed a pessimistic limit; and that for beams of reasonable smoothness on the edge, the actual limit is somewhat higher.

In addition to all this, we have looked at a couple of coupling effects due to the beam-beam interaction. This happens in particular while both beams are bunched and it isn't clear to me at this moment, whether this condition is inevitable during the operation of ISABELLE or whether it can be avoided by suitably scheduling the various beam manipulations. There is, of course, the coupling about which I have just been talking - beam-beam tune shift. In addition, there may be coupled oscillations of the bunched beams, and there one gets many more modes than in a single beam, and it might happen that the coupled modes are unstable even if the single beam modes are stable. One avoids

them by operating the two rings at different values of ν_x and ν_y, where the separation is related to the tune shifts, $\Delta\nu_x$ and $\Delta\nu_y$. If the two beams cross at an angle, there are new effects which arise. One of them is the coupling between synchrotron oscillations and transverse oscillations which results in a change in the synchrotron frequency; in fact, it is an increase for the case where one has particles of like charges in the two rings. In ISABELLE, that effect turns out to be rather small. It changes the synchrotron frequency by a couple of percent, and the coupling can be avoided by making the synchrotron frequencies in the two rings that much different.

A similar effect to that one occurs in the ep option of ISABELLE, and because the electrons have the opposite charge the effect becomes defocusing. If one assumes that the protons are unbunched, one has a funny effect where the bunched electron beam pushes the protons into a direction such that the protons try to avoid the electron bunches which would lead to a reduction in the luminosity. Theoretically, this is somewhat equivalent to putting empty buckets into the stack of protons with the empty buckets in the locations of the electron bunches. In this picture it becomes quite obvious how one has to judge this effect. One has to compare the height of the empty buckets to the height of the whole stack which is the momentum spread in the stack. If the momentum spread is large, compared to the stack, one makes tiny little holes and one gets a rather small effect on the luminosity. If the two things are comparable, one is bound to lose a large fraction of the luminosity. In ISABELLE this results in luminosity reduction of perhaps several percent, maybe 10%, 20% of the luminosity and that seems to hold at all energies because, although the buckets become smaller at higher energy, so does the momentum width of the proton beam.

MAGNET AND CRYOGENICS

Summary Report of Working Group*

D. B. Thomas

Rutherford High Energy Laboratory

1. Introduction

The Working Group was comprised of representatives from the majority of the superconducting magnet development groups in high energy physics laboratories in the USA and Europe and was therefore able to bring a broad experience to bear on the superconducting and cryogenics aspects of ISABELLE.

The Working Group set as its objectives:

1.1 To review critically the present status of the BNL superconducting magnet program and future plans with particular reference to ISABELLE.

1.2 To make recommendations where appropriate on:

a) possible technical improvements,

b) future development program,

c) areas where cost reduction should be sought.

In following these objectives the members of the Working Group first brought themselves up-to-date with the status of the BNL program by hearing oral presentations and by visits to examine prototype hardware. In addition, brief informal descriptions of the superconducting magnet development programs of all the other participating laboratories were given with emphasis placed on the latest unpublished results.

---

*F. Arendt, J.A. Bamberger, D.A. Baynham, G. Bronca, N. Cunliffe, P.F. Dahl, G.T. Danby, W.B. Fowler, H. Hahn, D.A. Kassner, P.O. Mazur, A.D. McInturff, G. Parzen, J. Perot, A.G. Prodell, R.H. Remsbottom, W.B. Sampson, P.A. Sanger, R.I. Schermer, D. Sutter, B.P. Strauss, D.B. Thomas, S.T. Wang.

2. Technical Improvements

The discussions following these presentations generated many ideas for technical improvement in engineering detail. The consensus view of the Working Group was that no major change was called for in the overall design philosophy of the ISA magnets. Whilst each participating laboratory tends to favor its own individual approach to magnet design, there was general approval of the validity of the BNL approach. For an accelerating storage ring, a design which embodies as cosθ current distribution in a single layer of superconducting solder-filled braid has, in the opinion of the Working Group, been demonstrated to be an excellent choice. The ISA-IV 1 m long prototype dipole magnet, for example, after reassembly reached a field level of 44 kG at 4.6 K on the first quench and exhibited no training whatsoever - a significant milestone in the world picture in the technology of superconducting accelerator magnets.

The dipoles required for ISABELLE are 4¼ m long: scaling from a 1 m long to a 4¼ m long magnet with 50% larger aperture should present no undue difficulty. Protecting the longer magnet against damage following an accidental quench is, however, that much more difficult since the energy stored in the magnetic field is about 10 times as large. This energy can all be dumped in a localized region of the windings at quench if thermal propagation of the resistive region is too slow to encompass the entire 4¼ m long magnet. The first 4¼ m ISA prototype dipole encountered this problem on test. Modifications to the design have been undertaken which should circumvent the difficulty.

The question of protection of a number of 4¼ m long dipoles operating together is dealt with in a separate paper in these

proceedings[1] as are some other important aspects of magnet design.[2-5]

3. Recommended Preproduction Magnet and Cryogenics Proving Program

The Working Group devoted time to defining what it considered should be demonstrated before procurement of 500 or so superconducting magnets for ISABELLE could be undertaken. The following recommendations emerged:

3.1 Four (identical) preproduction 4¼ m dipoles and two 1¼ m preproduction quadrupoles should be built and tested individually for:

a) absence of training,

b) behavior on quench,

c) field quality under dc and pulsed conditions without correction coils energized,

d) field quality under dc and pulsed conditions with correction coils energized; special attention to be paid to cancellation of rate-dependent terms from magnetization currents in superconducting braid,

e) repeated thermal cycling from 300 K to 4 K to 300 K.

3.2 The four dipoles and two quadrupoles should be assembled together in the configuration of one lattice cell and tested together for:

a) quench behavior with proposed protection system,

---

1. D. A. Baynham, "Magnet Protection", these Proc.

2. A.D. McInturff, B.P. Strauss and R.H. Remsbottom, "Conductor Considerations for ISABELLE Dipoles", these Proc.

3. G. Parzen, "ISABELLE Magnet Correction System", these Proc.

4. P. F. Dahl and G. Parzen, "50 kG ISABELLE Dipole", these Proc.

5. J. Perot, "Some Remarks on Mechanical and Thermal Behavior of the Coils", these Proc.

b) 10000 energizations to design magnetic field as a meaningful life-test,

c) performance under various induced refrigerator system malfunctions.

3.3 At least one dipole and one quadrupole should be operated in a particle beam line to measure tolerance levels to radiation-induced heating.

3.4 The cryostats used in the above tests should be identical with the design proposed for the production versions.

3.5 The magnet cooling system employed should simulate that proposed for ISABELLE, i.e., pool boiling.

3.6 The magnet alignment system to be used in ISABELLE should be checked out on the assembled cell.

3.7 The amount of industrial involvement in this preproduction program should be maximized so that a smooth transition to the production stage is possible.

4. Resulting Future Program - Consequences of Above Recommendations

The Working Group assumed that the time scale for approval and construction of ISABELLE would be as given in the latest project report (A Proposal for Construction of a Proton-Proton Storage Accelerator Facility - ISABELLE, BNL 20161, June 1975). On this assumption procurement of critical accelerator components including the superconducting magnets will start in April 1977.

With this time scale in mind, the opinion of the Working Group is that the present ISA magnet design with only minor modifications (some of which are already underway) could be used without violating the program schedule. These modifications are listed below:

4.1 Change in 'end' winding configuration to produce coil ends with perfect field integrals.

4.2 Greater external diameter iron yoke.

4.3 Inclusion of 3θ and 5θ correction windings.

4.4 Replace split iron yoke with a one piece iron yoke and incorporate additional cooling passages to allow magnet to be tested with forced convective cooling as well as with pool boiling cooling as specified for ISABELLE.

4.5 Reduce the number of blocks of windings approximating to the $\cos\theta$ distribution from 6 to 5 (or perhaps 4).

4.6 Consider metal spacers and poles between winding blocks to improve heat conduction on quench.

The resulting magnet will have a 'short sample' field close to 48 kG at 4.8 K. It is the opinion of the Working Group that this magnet design should be defined as a 40 kG operational magnet. It could then be adopted for use at this field level in ISABELLE with a reasonably operating safety margin. The magnetic field rise time for ISABELLE of approximately 150 sec can be comfortably handled by this design. Even at this rise time, sextupolar and other correction terms which are functions of rate of change of magnetic field will be needed to compensate for the effect of magnetization currents. This particular magnet design is not appropriate to rise times to full field of much less than 100 sec.

The Working Group expressed some concern that no prototype superconducting quadrupole of the type required for ISABELLE was yet in construction. Whilst development of the quadrupole is likely to be easier than the dipole, it is considered that a rapid design and construction program should be started immediately. A number of correction coils will be required in the quadrupole to handle both magnet imperfections and some aspects of orbit correction. A separate paper in these proceedings deals with this subject.[3]

Some concern is also felt that no prototype cryostats or transfer lines of the type required for ISABELLE are yet in construction.

Testing of these components will provide essential data on which to fix the size, and therefore the cost, of the refrigeration system. A detailed examination of the advantages of intermediate temperature radiation shields in cryostats and transfer lines in addition to superinsulation is recommended by the Working Group. (The magnet cryostats which have demonstrated the lowest losses to date all incorporate this feature.)

The Working Group considers that it is essential to complete the above development program before construction of ISABELLE is undertaken. It is well appreciated that adoption of this recommendation will entail a substantial increase in the resources in both manpower and money devoted to this work at BNL over that presently employed.

5. Underlying Research and Development Program

The Working Group wishes to recommend that an underlying R and D program should also be sustained and concentrated on the items listed below:

5.1 Design and construction of prototype 1 m long dipole using Nb-Ti superconductor to operate at 50 kG. This higher field design than the present ISA series of magnets should use a two layer coil construction with four blocks of conductor per layer. The specification should be based on a 'short sample' field of 60 kG at 4.8 K with a defined operating field of 50 kG at 4.8 K. The radial thickness of each of the coil layers will be less than that of the present one layer ISA design. A narrower superconducting braid, or indeed a flat cable, could then be used, so yielding smaller rate-dependent magnetization terms to be corrected.

5.2 Design and construction of a prototype 1 m long (or shorter) dipole using Nb_3Sn superconductor. The design should aim at an operating field of at least 50 kG, preferably 60 kG.

5.3 Evaluation of a single phase helium forced convective cooling system for use in ISABELLE as an alternative to pool boiling. If

this system proves to be feasible, considerable reduction in complexity of cryogenic control loops should result.

The following comments should be made. There are two competing design configurations for a superconducting dipole presently being worked on at BNL, a cosθ current distribution version and a 'window frame' version. A cursory examination of the two options by the Working Group failed to reveal any first order advantage of one over the other in either performance or estimated production cost. The Working Group recommends that design of each option should be pursued until it becomes clear whether one configuration has any second order advantage over the other. The design (and cost estimation) of both the alternatives should be carried out by one engineering group. The resulting uniformity of treatment will ensure as much commonality as possible between the two designs in engineering detail.

If sufficient R and D resources are available a 1 m long prototype version of each of the two designs should be constructed. If not, the choice should be made on the basis of estimated relative production costs.

The Working Group considered the time scales on which the suggested R and D items could be incorporated into ISABELLE if approval of construction were delayed. It agreed that the 50 kG magnet described in Section 5.1 could be introduced into the construction program if a delay of one year occurred. The niobium-tin prototype described in Section 5.2 involves a far greater development content, and consequently in the opinion of the Working Group would take about 5 years to bring to the stage where use in a working accelerator could be contemplated. In contrast, it was felt that the forced convection system mentioned in Section 5.3 could be incorporated into the ISABELLE construction program marginally on the present schedule but certainly if a delay in project approval of six months or more were encountered.

6. Areas of Potential Cost Reduction

The restricted time available to the Working Group to study this important aspect did not allow detailed recommendations to be formulated.

Three general areas were isolated as worthy of special study and it is suggested in particular that these should be scrutinized by the ISABELLE team. They are superconducting materials, cryostats plus associated equipment and helium refrigerators.

Recent quotations received from American Industry by FNAL indicate significant reductions in the price of composite superconducting wire over those earlier prices given in the ISABELLE proposal document. Since the type of composite is similar but not identical in the two cases, revised supply quotation for ISABELLE should now show 30 to 50% cost reductions.

The design of cryostats, transfer lines, etc., for ISABELLE has not yet proceeded to the point where accurate costing is possible. The Working Group was of the opinion that more detailed work would reveal where worthwhile (but not dramatic) cost reductions could be made.

The total capacity of the helium refrigerators specified for ISABELLE has been estimated on the basis of assumed figures for thermal losses in cryostats, current leads, etc. The absence of firm experimental data obtained with prototype hardware has inevitably led to conservative estimates being adopted. In the opinion of the Working Group some reduction in specified total refrigeration load should be possible once prototypes have been built and the necessary measurements taken.

A preliminary comparison was made of the cost of ISABELLE with 50 kG magnets rather than 40 kG magnets as specified. Storage rings of maximum energy 200 GeV were assumed for both cases. The comparison based on simple scaling of costs with quantity of superconductor involved, length of tunnel, length of cryogenic lines, etc.,

yielded the result that the two options did not differ in price by more than 5%. Whilst no great reliance should be placed on this rough comparison, it is already clear that no dramatic savings in the overall project cost can be made by using higher field magnets.

RADIATION EFFECTS

Summary Report of Working Group*

P.A. Sanger†

Fermi National Accelerator Laboratory

and

G.T. Danby

Brookhaven National Laboratory

The Radiation Effects Group considered three major topics:

1. Shielding,
2. Radiation Damage,
3. Radiation Heating.

The contributors to the Group were mostly also involved in other Summer Study topics. Its meetings interacted strongly with several groups, especially Beam Transfer and Superconducting Magnets.

1. The radiation shielding studies have been reviewed and were found to be adequate and consistent with present day dosage limits. Shielding considerations should be strongly borne in mind in the final design of insertion structures and penetrations. These may change the effectiveness and the cost of the shielding design.

2. Long term radiation damage due to displacements in the conductor lattice was discussed by the Radiation Effects Group. During preliminary design of ISABELLE and other superconducting accelerators, this question was considered secondary since the damage is expected to be small. At this time the Radiation Effects Group feels that damage to the conductor or insulator (not considered in the study) could be encountered in some extreme cases, and therefore feedback into the magnet and ring design and storage ring operating procedures

*The following participants while also working in other sections, contributed to the Radiation Section: G. Bronca, Y. Cho, G.T. Danby, D.A. Edwards, S. Lindenbaum, D. Lowenstein, J. Perot, J. Peterson, A.G. Prodell, P. Sanger, A. Stevens, B.P. Strauss, D. Sutter, L.C. Teng, A.M. Thorndike, A. van Steenbergen, C.L. Wang, S.T. Wang.

†Work supported by Universities Research Associates and the University of Wisconsin.

would be beneficial. It was the consensus of the Radiation Efforts Group that conductor damage even if it occurred in some areas can be satisfactorily reduced by occasional room temperature anneals and is not expected to limit the performance of the superconducting magnets.

3. The world experience on significant radiation heating exposure of superconducting magnets is very limited and for the most part qualitative. This is summarized as part of this study.[1] Both analysis and experiment indicate heating to be a very important question.

Strong interaction with the Beam Transfer Group was beneficial in better defining and minimizing the radiation heating to which the superconducting magnets will be exposed. Under various realistic fault conditions both the density and time structure of radiation heating to be expected around the ISABELLE lattice will need to be developed in greater detail. Experiments to study the effect of such heating on actual magnets are recommended.

Interaction with the Magnet Group was also strong during the study. The capacity to absorb heat as a function of time structure must be considered another design criteria at the present advanced state of superconducting magnet development.

The Radiation Group recommends that, in the immediate future, considerable effort be put into experimental study and understanding of radiation heating effects on superconducting magnets with various coil constructions. This program must simulate the heating effects to be expected under loss conditions of varying probability. It should include actual radiation exposure experiments on ISA magnets.

This heat absorption problem can no doubt be coped with, but it is essential that it be completely understood, so that it can feed back into the final detailed design of ISABELLE and strongly minimize the risk of quenches during operation.

---

1. G. Danby, "Radiation Heating: Experience and Projections", these Proc.

VACUUM SYSTEM

Summary Report of Working Group*

J. P. Hobson
National Research Council of Canada

I. Introduction

The Yellow Book, "A Proposal for Construction of a Proton-Proton Storage Facility", June 1975, proposes a vacuum system for ISABELLE. In our report we present an analysis of this proposal as it stands without recommendations for major changes, our primary objective being to answer the question "Are the design parameters acceptable and practical?" from the vacuum viewpoint. Detailed discussions are included in these proceedings. Suggestions for major changes have arisen during our discussions and where we have considered them worthy of record we have also added them as brief papers. It must be recognized that the latter represent ideas in embryonic form which may prove to be impractical later.

The proposed ISABELLE vacuum design is a conventional ultra-high vacuum system at room temperature based firmly on the ISR experience at CERN. Even the possibility of pumping on parts of the wall near 4.2 K, presented by the use of superconducting magnets, has been rejected on the grounds of practical engineering considerations and uncertainties about pressure bumps. We considered cold bore briefly. However, we have not discussed this question in sufficient depth to give any opinion on warm bore vs cold bore.

Thus it would appear important to examine the major differences and similarities pertaining to vacuum between ISABELLE and ISR. In Section II we tabulate these and in Section III we comment.

*D. Blechschmidt, O. Gröbner, H. J. Halama, J. C. Herrera, J. P. Hobson, R. C. Wolgast, and M. Y. Yu.

II. Vacuum Comparison of ISABELLE and ISR

Subject	ISABELLE	ISR	Remarks
1. Beam Chamber	8 cm Ø Warm Bore 5 m between pumps	Mainly elliptical 16 cm x 5 cm 3-5 m between pumps	
2. Material of Walls	Bore Al (Al Alloy 6061). Pumping Chambers S.S.	S.S. (316L+N)	
3. Specific Outgassing Rate	10^{-14} Torr liters $sec^{-1}cm^{-2}$ mainly H_2 from Al	2×10^{-13} Torr liter $sec^{-1}cm^{-2}$ mainly H_2 from S.S.	Ref. 1 Ref. 2
4. Background Pressure	a) $\leq 10^{-11}$ Torr H_2 in experimental areas b) 3×10^{-11} Torr H_2 in the lattice	a) 10^{-11} Torr H_2 in experimental areas b) $< 3 \times 10^{-11}$ Torr H_2 in the lattice	We found these pressures most difficult to establish for ISABELLE
5. Treatment of Materials	Chemical polish for Al. Argon glow discharge at 150°C O_2 glow discharge at 150°C	900 C for several hours at $P < 10^{-4}$ Torr. Argon +10% O_2 glow discharge, 10^{18} ions cm^{-2} at 300°C	
6. Mechanical Junctions	Welding in situ for tube. Flanges for gauges and pumps	Conflat flanges with Ag-covered Au gaskets	
7. Ne/Np in Beam	$\sim 1.5 \times 10^{-4}$	$< 5 \times 10^{-4}$ and below e-P instability threshold	ISABELLE projected value ISR estimated value Ref. 3 Ref. 4

1. H. J. Halama and J. C. Herrera, "Thermal Desorption of Gases from Aluminum Alloy Al 6061, Their Rates and Activation Energies", these Proc.
2. J. P. Hobson, "Alternative Interpretation of the Measurements of Specific Outgassing Rates of Materials", these Proc.
3. J. C. Herrera, "Beam Clearing and Space-Charge Tune Depression", these Proc.
4. O. Gröbner, "Clearing Requirements in ISABELLE Based on the e-p Instability", these Proc.

8. Clearing Electrodes	1 pair of electrodes per magnet 20 cm x 4 cm. Spaced 8 cm. Extraction voltage 5 kV. Extra electrodes at all points of change in cross section of bore. Average clearing rate $R_c \simeq 100\ sec^{-1}$	2 pairs of electrodes per magnet 25 cm x 10 cm. Spaced 5 cm. Extraction voltage +6 kV. Extra electrodes at all point of change in chamber diameter.	ISABELLE specifications subject to change. Especially critical at experimental intersections.
9. Allowable Local η (net desorption coefficient)	~3(10 A in beam)	~3(30 A in beam)	In most places ISR has achieved $\eta \sim 0$ Ref. 5 Ref. 6
10. Pressure Measurement	Proposed gauges: Extractor gauge, perhaps with modulator. Lower limit of reliable measurement $\sim 5 \times 10^{-13}$ Torr (N_2-equiv) Quadrupole mass spectrometers lowest partial pressure $\sim 3 \times 10^{-13}$ Torr.	Gauges: Modulated Bayard-Alpert gauges and some extractor gauges. Lower limit of reliable measurement in low 10^{-12} Torr (equiv N_2) range	Most gauges in both machines located near pumps and do not directly measure tube pressure. In ISR better average measurement made from electron clearing current. Ref. 7
11. Pumps	Turbomolecular, Titanium Sublimation, Ion pumps (sputter or orb-ion)	Turbomolecular, Titanium Sublimation Sputter ion, He cryo pumps	
12. Sectors and valves	Av 80 m between valves	Av 62 m between valves	

5. D. Blechschmidt, "η Measurements in Glow Discharged Chambers at ISR", these Proc.

6. H.J. Halama and J.C. Herrera, IEEE Trans. NS-22, 1492 (1975).

7. D. Blechschmidt, "Pressure Measurement at ISABELLE", these Proc.

13. Leak Detection	Prebake: He + commercial leak detector. Post bake: Ar + gauges or mass spectrometers	Prebake: He + commercial leak detector Post bake: Ar + gauges or mass spectrometers	
14. Bakeout	200°C by heating of the tube by heaters on either side of the magnets. Magnets remain cold during bakeout.	300°C by heating with heater jackets around the tube	
15. Experimental Areas	Particular to experiment	Particular to experiment	Ref. 8 Ref. 9

III. Comments on Design Figures

1. Beam Chamber

It is calculated that with a H_2 pumping speed of 1800 ℓ/s at the input to the ring a maximum pressure of $P_{max} = 3 \times 10^{-11}$ Torr H_2 at the center of the magnets will be achieved if q (specific outgassing rate) = 6×10^{-13} Torr liters $cm^{-2}sec^{-1}$ of H_2. This calculation is based upon the assumption that no pumping takes place in the tube. (On this point there was not unanimous agreement. Some of us, in particular Hobson, believe that the outgassing measurements do not prove that this pumping is negligible, and he adds Ref. 2 describing this reservation. It is not clear whether this effect is beneficial or not to ISABELLE.)

2. Materials of Walls

It is not clear at the present time whether Al or stainless steel is preferable from the viewpoint of:

---

8. H. J. Halama, "Experimental Insertions", these Proc.
9. J. P. Hobson, "Demountable Ultrahigh Vacuum Sections for ISABELLE", these Proc.

a) base pressure,

b) ion-molecule desorption,

c) leaks.

It is recommended that comparative measurements between Al and SS on the same test system be carried out on these points. Some measurements are in progress and others are planned. Al bellows for ultrahigh vacuum are not well developed.

3. Specific Outgassing Rate

The ISABELLE values refer to net outgassing rate[1]. Reference 2 suggests another interpretation of the measurements.

4. Background Pressures

a) Experimental Areas

For 10^{-11} Torr H_2 in the intersection regions there is a total background of 2×10^5 particles sec^{-1} (Yellow Book) with 10 A beam. This is acceptable to experimenters.

Also in the ISR 10^{-11} Torr H_2 is the upper bound for an acceptable pressure in these areas.

b) Lattice

Here the Yellow Book value of 1×10^{-11} Torr referred to equivalent N_2 pressures. This corresponds to 3×10^{-11} Torr H_2. This pressure is satisfactory in terms of residual neutralization, neutralization ν shift[3] and e-p instability.[4]

5. Treatment of Materials

BNL laboratory measurements on the outgassing of Al indicate that no severe thermal pretreatment (vacuum firing) will be required, if glow discharge is used.

Glow discharges are required in the ISR for reducing the ion desorption coefficient[5] η. This is likely to be the ISABELLE experience. Further laboratory tests[6] are being carried out at BNL.

Glow discharges are found at BNL to reduce residual pressures in an Al tube. In general, this is not found for SS at CERN.

In situ glow discharges offer the possibility of not requiring a bake thereafter, and the possibility of using sputtered pumping layers in the tube. All aspects of glow discharge cleaning should be studied extensively, including rf discharges.

6. Mechanical Junctions

Aluminum welding would not appear to present any problems in principle. Welding can be done as quickly as coupling flanges. Large flanges have been the major source of leaks in the ISR. A program to investigate Al welding and cutting should be initiated. SS ultrahigh vacuum flanges will be necessary to adapt to gauges and pumps since Conflat style Al flanges are not satisfactory for $200^{\circ}C$ bakeout. Al-SS transitions produced by explosive bonding have been found reliable at SLAC and BNL.

7. Beam Neutralization Ne/Np

The requirements for the tolerable residual neutralization are outlined in Refs. 3 and 4. The average neutralization in ISABELLE, $1\text{-}2 \times 10^{-4}$, is determined mainly by ν shift considerations[3] and by the e-p instability threshold.[4] The calculations show that the quoted figure can be achieved with short electrostatic clearing electrodes placed between magnets as proposed in the Yellow Book. Localized electron traps where clearing is provided by the slow beam heating effect only must be carefully avoided by installing special electrodes. This will be particularly true for the insertions. ISR experience would suggest that electrons may also be trapped in the D-quadrupoles but this effect on average neutralization is estimated to be negligible at the ISA design pressure($Ne/Np < 10^{-5}$ from this source).

Further considerations could be devoted to other clearing schemes, e.g., clearing by rf as it is being studied at CERN with the aim of reducing the number of electrodes and hence reducing their impedance effect on the beam.

8. Clearing Electrodes

The physical structure and clearing voltage will be controlled primarily by impedance rather than vacuum considerations. They will be used for pressure measurement using the electron current in the presence of a beam.

9. η - Net Desorption Coefficient

A design value of $\eta < 3$ is conservative as no pressure bumps were observed in glow discharged chambers.[5] BNL has measured ion desorption cross sections for carbon containing molecules on Al and SS samples.[10]

BNL experience is that exposure to air after glow discharge returns η to the predischarge value, even after bakeout. This is not in agreement with ISR experience where η remains near zero after prolonged atmospheric exposure followed by bakeout.

10. Pressure Measurement

Quantitative pressure measurement below 10^{-11} Torr remain difficult requiring attention to a variety of residual effects.

Low pressure gauges of the extractor type (possibly equipped with modulators) are recommended[7] for ISABELLE. In the straight sections, special gauges, probably equipped with secondary electron multipliers might be useful. Reservations were expressed whether modulated Bayard-Alpert gauges are appropriate for pressures less than 5×10^{-12} Torr N_2 equivalent.

Stray magnetic fields may affect the gauge readings.

A few gauges, properly screened from the beam potential, are recommended to be mounted at strategic positions directly on the beam pipe to provide pressure information in the pipe.

Some quadrupole mass spectrometers have to be mounted, in particular, near experimental areas.

---

10. Ming Yu, "Ion Desorption Cross Section of Carbon Containing Molecules on Aluminum and Stainless Steel", these Proc.

11. Pumps

Conventional bakeable pumps (ion and titanium getter) and turbomolecular pumps, similar to those used in the ISR, would appear to be satisfactory for ISABELLE.

Sorption pumps could be more economical and cleaner than turbomolecular pumps although a dust problem exists.

Orb-Ion or Electro Ion type pumps might be tested as replacements for sputter-ion pumps since pumping speed is maintained to lower pressures, and argon from the glow discharge cleaning might become an important residual gas as well as methane from the titanium.

Cryopumps similar to those developed at the ISR will probably be necessary for special purposes in the experimental areas.

12. Sectors and Valves

In the ISR sector valves terminate the sectors. These close, leak tight, in 1 sec. At sensitive intersections fast closing (20 msec) but nonleak-tight flap valves protect the ring against accidental implosions. ISABELLE will require similar valves. Physical separation of the sector valves from pumping stations is recommended based on practical experience at the ISR where this condition is not met.

13. Leak Detection

In general there is no reason for ISABELLE to deviate from ISR practice.

14. Bakeout

Within the magnets no heating equipment is required in ISABELLE because Al can be heated by thermal conduction from clamp-on heaters at the ends of the magnets and insulation is provided by superinsulation between the pipe and magnet. No experience is provided by the ISR on this point.

15. Experimental Areas

These will be specific to each experiment, but will, in general, follow the pattern of the ISR in the first generation of experiments.[9]

IV. Conclusion

We have found no fundamental reasons why the ISABELLE vacuum design as presented in the Yellow Book is unacceptable or impractical.

COMPUTER CONTROL AND MONITORING

Summary Report of Working Group*

K. B. Mallory

Stanford Linear Accelerator Laboratory

The controls working group consisted of the chairman and co-chairman plus several people of Brookhaven. The fixed points we had to start from were Dimmler's CRISP report[1] on the proposed structure of the computer control system and the fact that the system must control ISABELLE. It appeared that many of the group did not understand the report and others wanted to learn what were the operational requirements for the control system. An educational program was required. The group turned into a seminar with discussions based on interviews and presentations by members of the group and guests, mostly from ISR.

We talked primarily about the operational requirements, but were always sniffing around the edges of what the computer system must be. There is no point in discussing here the laundry list of functions required. Every one can write his own, they will all be equally good; they will all be wrong. The requirements cannot be known until equipment design has begun. The following comments represent the gist of what was learned.

There are two distinguishable aspects to the analysis of a control system. On one side, the one covered by courses in control theory, are all the regulators and servo loops that adjust equipment in accordance with set parameters. On the other are the man-machine interface and the major computational operations needed to analyze performance and decide what parameter changes are required.

In an accelerator environment, the concept of "control" has come to mean the analysis of performance and the act of changing

---

*D.G. Dimmler, K.K. Li, D. Lowenstein, K.B. Mallory, R.J. Nawrocky.

1. D.G. Dimmler, BNL Informal Rept. CRISP 75-5 (1975) and "Computer Control and Monitoring", these Proc.

parameters to make improvements. This is a consequence of the organization of accelerator design projects, which tends to leave most of the closed-loop controls to the individual subsystems designers, and the data-transmission system, the console and the analysis equipment to a bunch of people who eventually come to be known as a "Controls Group", whether they like it or not.

Accelerators have been built and operated with computer controls. The point of the computer is three-fold: 1) to simplify programming large sets of switches, servo gain knobs or digital thumb-wheels, 2) to take over for the operator routine responses to minor variations in parameters, and 3) to record and analyze data for evaluating and predicting improvements of performance. A computer system or network can add one more feature: a unified data-transmission system that allows distributed execution of the first three tasks and may possibly save some money over an installation with separate networks for each subsystem.

As digital control and the use of computers have become more popular, there has been a tendency to dump much of the closed-loop control logic into the central computer systems. This is wrong. Even if the closed-loop controls should be performed in a computer, it should be a computer that is local to the equipment - possibly dedicated to that job only - and connected to the central computer system only as tightly as required to allow monitoring and modification of parameters. In this way, responsibility for the design of the servo loop remains with the equipment designer where it belongs.

At the start of construction, a single style (or "compatible line") of computer would be selected for use whenever programs need to be dynamically loaded and modified. In this way only one kind of operating system, one set of link hardware and protocols, file management system need be designed, and the same style of programming can be used when writing code for any computer. This will eliminate large amounts of duplicated effort.

It would also be advisable to select a single kind of "computer on a chip" and to specify a standard set of hardware and software for linking it to higher levels of computers.

If the interface of all of the local "intelligent controllers" to the data-transmission system is standardized in this way, it appears that the interface between the equipment designed and the "controls group" may shift in a novel way. Instead of being defined at some hardware location, it can be made in the software within a computer. The consequences of such a relocation of the logical interface should be studied further.

The computer control system then should be a large number of rather specialized computers, of one or at most two types. They should all use the same structure for programming, data management and linking. And so we come full circle back to the very system described in Dimmler's CRISP report, where we started.

OPTIONS

Summary Report of Working Group*

M. Tigner

Cornell University

The work of the option group was concentrated on examining the $\bar{p}p$ and e-p options. We looked for weak points in the options as proposed and tried to think of ways to improve the presently conceived designs.

Insofar as we have been able to investigate them, we find the methods proposed for providing colliding $\bar{p}p$ and ep beams are basically sound and can be expected to perform at the levels given in the proposal.

Additionally, we tried to think of ways to produce the $\bar{p}p$ and ep colliding beams which might offer improved performance and/or lower cost. While we cannot report any revolutionary breakthroughs we have seen some promising directions for further investigation.

In particular, it is clear that some method of reducing the phase space of the beams, such as stochastic cooling, would pay big dividends in both $\bar{p}p$ and pp work and is worth considerable effort. In the case of the ep option longitudinal polarization of the electrons is attractive, but needs further work to become practical.

Finally, we have identified some areas where work needs to be done to clarify possible problems. In particular the background caused by Compton scattering of the synchrotron radiation that we would encounter in the e-p option needs study.

$\bar{p}p$ Option

$\bar{p}p$ physics possibilities and advantages have been reviewed by Halzen, Paschos, Trueman and Wang.[1] Briefly they find that $\bar{p}p$

* D. Berley, H. Bruck, A. Carroll, R. Chasman, Y. Cho, V. Fitch, K. Hübner, J. Maidment, A. Mann, K. Steffen, M. Tigner.

1. F. Halzen, E. Paschos, T. L. Trueman, L.L. Wang, "$\bar{p}p$ Option", these Proc.

physics at low $p_\perp$, e.g. total cross sections and Coulomb interference experiments can be done with $\bar{p}p$ at lower luminosity than with pp. In addition, at sufficiently high energy and Q^2, the fundamental process involving fermion-antifermion annihilation is of particular significance in its ability to make new massive particles.

A scheme for producing a beam of $\bar{p}$'s is presented in the Gray Book (BNL 18891). In this scheme the 200 GeV proton beam is brought on to a target and the emerging $\bar{p}$'s are introduced into the second ISA ring. By using a special high harmonic rf system in that ring the injection process can be repeated 10 or more times resulting in circulating $\bar{p}$ currents of about one mA. This scheme has been reviewed by various people. Fitch[2] has looked into the question of energy loss in the superconductor as a result of the decay of π's and K's injected along with the $\bar{p}$'s and the loss of $\bar{p}$'s due to inefficiencies in the capture process. He calculates that a negligibly small temperature rise will be experienced by the superconductor so that this phenomena is not of immediate concern. Hübner[3] has checked the production rate of these unwanted particles and made suggestions on amelioration of the problem should it become necessary. He also suggests chopping the 30 GeV $\bar{p}$ beam after the target to improve capture efficiency. This method could perhaps raise the luminosity somewhat and should be investigated further.

It is concluded that a luminosity of 10^{29} $cm^{-2}sec^{-1}$ or slightly more should be achieved. To bring the luminosity to this value, extra dipole magnets in which the p's and $\bar{p}$'s experience opposite fields will be required to reduce the crossing angle. This interaction region geometry is shown in Fig. 1.

If one could produce $\bar{p}$'s in sufficient quantity, $\bar{p}p$ collisions could be carried out in a single ring. This is an inspiring thought

---

2. V. Fitch, "Heating Effects of an Unseparated $\bar{p}$ Beam Injected into the ISA Ring", these Proc.

3. K. Hübner, "On the Contamination During Antiproton Injection Into ISABELLE", these Proc.

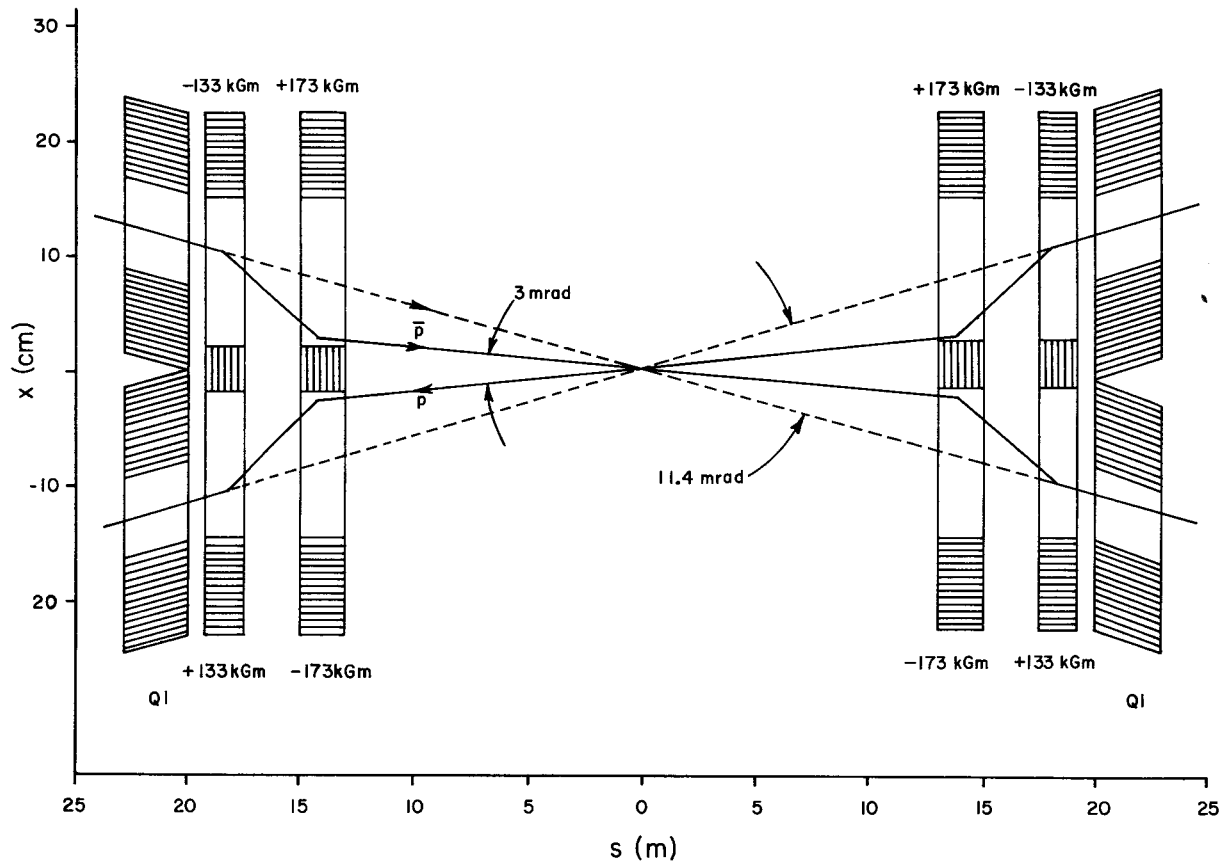

Fig. 1. Variable angle horizontal crossing geometry for $\bar{p}$-p collisions. Maximum crossing angle 11.4 mrad, minimum crossing angle 3 mrad.

since it allows one to dispense with one of the ISA rings and thus effect a substantial cost saving. Berley, Carroll and Mann[4] have pursued this concept vigorously and with great ingenuity.

Several possibilities including that of an intermediate accelerator ring were examined. The most promising possibility is one in which $\bar{p}$'s are made by 30 GeV protons from the AGS, injected into the ISA at 10 GeV and are held there in rather tight bunches. Successive injection bursts from the AGS are stacked in transverse phase space until the required number of $\bar{p}$'s have been accumulated. The $\bar{p}$'s are then accelerated to 30 GeV and counter-circulating protons are injected. Following this, the total beam is accelerated to the operating energy. If the AGS pulses once per second, enough $\bar{p}$'s for a luminosity of 10^{30} $cm^{-2}sec^{-1}$ can be made in 10 hours. The technical problem that needs to be solved is how to inject all of these $\bar{p}$'s into the phase space volume accepted by the ISA. To do this some form of damping is necessary. One method that has been examined is the use of the stochastic cooling invented and under development at CERN. At the present state-of-the-art, the cooling times that can be achieved are too long to be practical.

It is clear that a practical cooling method would be of great benefit not only for $\bar{p}$'s but for p's too.

Areas that need detailed consideration are the targeting of the 200 GeV protons in the proposed $\bar{p}p$ option and the conduction of the emergent p's to the beam dump.

e-p Option

As previously conceived, this option would provide for collisions between electrons and protons in each of the 2 lepton halls.[5] Sulak has looked briefly at the dimensions of these halls as compared with the dimensions of apparatus suggested in preliminary

4. D. Berley, A. Carroll, A. Mann, "Single Ring $\bar{p}$-p Colliding Beams as an Interim ISABELLE", these Proc.

5. R. Chasman, "Status of ISABELLE at Time of Summer Study 1975", these Proc.

studies at the Fermilab 1973 Summer Study and the EPIC ep Study. The dimensions seem compatible, but further development of experiments will be necessary before final conclusions can be drawn.

The principal efforts of those working on the e-p option were to check the proposed scheme, suggest practical crossing geometries and the necessary matching optics, assess the practicality of using one of the p-rings for electrons, begin looking into various electromagnetic background problems and into the possibility of doing experiments with longitudinally polarized electrons.

Steffen, Maidment, and Cho[6,7] worked at suggestions by Steffen and Garren about crossing geometries. Several practical geometries were found. In layouts where a separate e-ring is disposed above or below the p-rings, it was pointed out by Garren that by alternating from top to bottom, the vertical dispersion problem can be solved very neatly, thus recommending this geometry strongly. The e-ring would then be on top in ½ of the machine and on the bottom in the other half. This could be alternated at each octant, if desired. For electron energies of 15 GeV, a luminosity of about $\frac{1}{2} \times 10^{32}$ or slightly more seems possible. At lower electron energies it may be possible to get somewhat higher luminosities.

Two practical methods for handling operational interferences between e-p and pp operations are seen. One possibility is to introduce the electron beam into one of the proton pipes at each crossing region. By doing this little or no geometrical interference arises but it will not be possible to use the e-ring while both p-rings are in use. A second possibility is to put bulges into the e-ring at the interaction regions allowing the electron ring to go around the apparatus in these places. This method prevents independent operation of the e-ring, but is expensive. A blend of the two may be the best compromise.

---

6. K. Steffen, J. Maidment and Y. Cho, "Review of e-p Collision Geometries", these Proc.

7. J. Maidment, "Comments on Injection into ISABELLE Electron Ring", these Proc.

The possibility of using one of the ISA rings for electrons was examined.[8] The conclusion was that there is no fundamental reason why it can't be done, but that at 15 GeV the extra shielding required to protect the cold region of the magnet from the 5.3 MW of synchrotron radiation would be prohibitively expensive. At 7.5 GeV the problem is quite manageable. In order to use one of the p-rings for e's,certain provisions, none of which appear to be terribly expensive, would need to be made in the original design:

First, a 2 mm wall Al tube, concentric with the present bore tube, would have to be added both to form a water jacket for the inner tube and to provide extra shielding; secondly, the pick-up electrodes and clearing electrodes and their enclosures will need to be designed for low interaction impedance at microwave frequencies; third, a careful study of field errors at very low excitation will need to be made and provision made for their correction. It should be noted that although the electron ring rf system will be rather modest at 7.5 GeV, its shunt impedance will be large enough that it will probably have to be removed from the ring each time a changeover from e to p ring is made, thus causing a delay in achieving a running vacuum for the p's.

It is beginning to be widely appreciated that in electron machines the synchrotron radiation that shines on the interaction region from the last magnet can cause important background effects, either by the penetration of the synchrotron x-rays directly through the wall of the vacuum enclosure and into the detection apparatus, or the scattering of these photons off the oncoming beam. It is even possible that π photoproduction events will occur if the last bend adjacent to the straight section is made as strong as the bend in the ring arcs since there would be a few photons in the MeV region shining on to the countermoving p-beam. It was recently

---

8. M. Tigner, "Storing and Accelerating Electrons in One of the p-Rings of ISABELLE", these Proc.

pointed out at SLAC by Patterson that one should use a soft bend adjacent to the straight sections to reduce the energy of the x-rays shining on to the interaction region. It is quite feasible to do this in the e-p option where one needs to bring the critical energy from 43 keV down to 8 keV or so (15 GeV electrons). Keeping the critical energy low will also prevent photoproduction for all practical purposes. The Compton scattering is another matter and requires further study. Not only is there radiation from the last bending magnet, but from the quadrupoles which focus the beam on to the interaction point. The total Compton scattering rates seem to be of the order of 0.1 to 1 per second with most of the photons going along the proton beam line. Computations of this and other electromagnetic scattering effects are being made by Bruck.[9]

We also looked briefly at polarization and its manipulation. At 15 GeV the polarization time is about 10 minutes and the polarization is 92% antiparallel to the guide field ($\bar{e}$'s). Considerable attention has been given to the subject of this polarization at the 1974 PEP Summer Study.[10] In addition, there have been studies at Rutherford Lab. which are referred in the PEP Summer Study report, and in the CERN LSR Storage Ring Study of an e-p option to be published shortly. The conclusion is that with methods invented so far the control of transverse polarization can be handled well while no really satisfactory method for obtaining longitudinal polarization in a useful experimental arrangement has yet been conceived.

In conclusion, the e-p option is attractive and feasible, but more study needs to be given to the control of the longitudinal polarization and to the effects of the synchrotron radiation.

---

9. H. Bruck, "e-p Coulomb Interactions", these Proc.
10. Proceedings of the 1974 PEP Summer Study, PEP-137, (1974)

NOVEL MECHANISMS FOR PARTICLE ACCELERATION

Summary Report of Working Group*

W. J. Willis

CERN

I. Introduction

Consider a time, which we hope is soon, when ISABELLE and perhaps even larger storage rings have shown they can do all we now hope for, and probably more. It may then be unlikely that one could muster arguments strong enough to bring about the construction of a very large synchrotron. Then we must be left with a nagging feeling that we have missed a crucial discovery for the lack of stationary target experiments with mesons, neutrinos, etc. This fear is relieved somewhat by the possibilities of $\bar{p}$-p, e-p, and virtual photon collisions in storage rings, but the basic problem remains.

One of the beautiful features of a storage ring is its 100% duty cycle. A possible alternative to the synchrotron is some kind of zero duty cycle accelerator. We can see that any alternative must probably have zero duty cycle. Almost by definition, the alternative does not have a ring magnet, and must then be a linear accelerator. In order to produce interesting energies on a reasonable site, the acceleration must be 1 GeV/m or more. We would like 10^{10} particles or more per pulse. Then the power going into the beam must be at least 0.5×10^9 watts. Allowing for efficiency, the power going into the accelerator must be a couple of orders of magnitude higher. We know of only three sources of that kind of power: intense relativistic electron beams (IREB); lasers; and explosions. The last sounds a bit too violent, and we reject it (reluctantly, for simple considerations seem to show the highest gradients and efficiencies with this method).

* C. L. Olson, R. B. Palmer, R. H. Pantell, W. J. Willis

There have been many suggestions for the use of IREB and lasers for particle acceleration. There are recent reviews of the former by Olsen[1] and of the latter by Lawson.[2] Very few of them show any promise. In our sessions we have tried to find out which of the existing suggestions remain interesting, in one case how one might scale to a multi-Tev accelerator, and to discuss some new ideas.

II. IREB Collective Effect Accelerators

None of the older methods of collective ion acceleration seem of interest at this time, at least for high energy accelerators. Two methods are currently being pursued with IREB: the IREB/cyclotron wave[3] and the IREB space-charge effect.[2] The former has yet to be resolved. The space charge effect has been observed at a number of laboratories, as shown in Fig. 1, which gives the typical parameters. Olsen's theory of the acceleration process is illustrated in Fig. 2. Electrons pass down the neutralized portion of the beam which can accelerate positive ions. This theory seems to explain essentially all of the rather copious data. The current record for proton energy is 16 MeV. The currents are up to hundreds of amperes of ions, with accelerations of MeV per cm. It is known that the electron beams can be propagated over 10 meters or more, so that this mechanism could lead to multi-GeV accelerators. What is needed is a means of controlling the velocity of the beam front, or charge neutralization, and suggestions have been made for accomplishing that, by a uv laser control for example.

One interesting feature of this device is that the acceleration has been shown to be proportional to the charge of the ion. This

---

1. C. Olsen, "Collective Acceleration with Intense Electron Beams", Sandia Laboratories, 1974.
2. J. L. Lawson, "Laser Accelerators?", RL-75-043, Rutherford Laboratory.
3. M. Sloan and W. Drummond, Phys. Rev. Lett. 31, 1234 (1973).

IREB/gas ($\sim$ 0.1 Torr, H_2)

IREB:	$\sim$ 1 MeV, $\sim$ 50 kA, $\sim$ 50 nsec, $r_b \sim 1$ cm	
IONS:	$\mathcal{E}_i > \mathcal{E}_e$, $N \sim 10^{13}$, $T \sim 3$ nsec	
PARAMETERS:	$\mathcal{E}_e$, l_o, t_r, t_v, t_b, r_b, R, L, M, Z_i, p, t	
EXPERIMENTS:	IPC	Graybill, Uglum, et al. (1968-1972)
	PI	Rander, Ecker, Yonas, Drickey, Putnam, et al. (1970-1974)
	SANDIA	Kuswa, Bradley, Yonas, Swain, et al. (1973-1974)
	LLL	VandeVender (1969)
	AFWL	Miller, Straw (1974, 1975)
	LEBEDEV	Kolomensky, et al. (1974)
	KHARKOV	Tkach, et al. (1974).

Fig. 1 - Summary of parameters concerned with IREV space-charge effect.

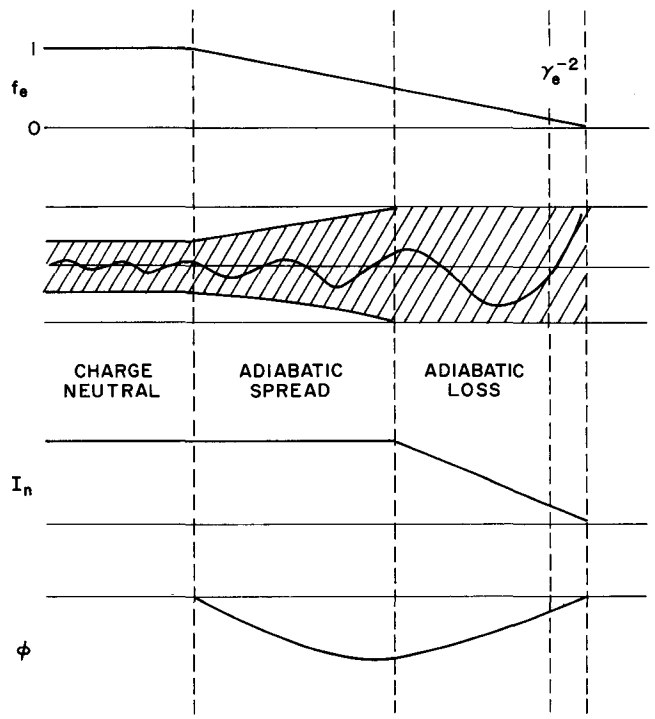

Fig. 2 - Schematic illustration of space charge effect acceleration process.

might give us a cheap source of uranium ions of the correct velocity for injection into the AGS.

With this mechanism, the ions must remain slower than the electrons, so that it cannot be used for very high energies. One of our suggestions was to use this means of generating relativistic ions, and then switching to a mode wherein the ion bunch is accelerated by the trailing edge of an electron beam modulated by a powerful laser.[4] Olsen believed that the laser beam interaction was difficult to calculate, and would have to be determined by experiment.

III. Laser Accelerators

Lawson's review[2] gives an example of a system which would work in principle. It was based on phase matching by the use of a glass rod, and the gradient was limited to about 200 MeV/m by the breakdown strength of the glass.

Pantell has recently published his results on the acceleration of electrons by a laser, with phase matching in gaseous helium at one atmosphere.[5] (See Fig. 3.) The electrons from the Stanford Mark III accelerator were used, and an energy gain of about 40 keV obtained with a 2 MW laser beam 1 mm in diameter. From the discussions it seems to emerge that gasses are better than glass because there are fewer breakdown mechanisms, and one can reach the gradients which are consistent with efficient use of the laser power without breakdown. Helium is particularly suitable because of its wide atomic level spacing. Also,by using gas, with the light entering at the Cerenkov angle, one does not need to fabricate a structure, and with helium the multiple scattering is acceptable if the particle simply passes through the gas.

4. W. Willis, CERN 75-9. (1975).
5. M. A. Piestrup, G. B. Rothbart, R. N. Fleming, and R. H. Pantell, J. Appl. Phys. 46, 132 (1975).

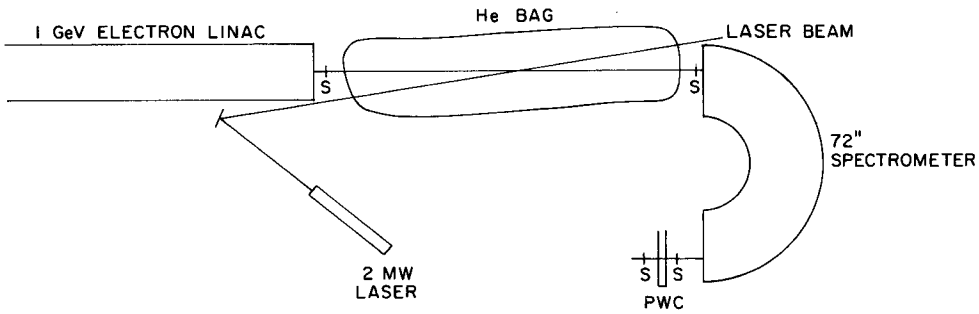

Fig. 3 - Arrangement of Pantell experiment on laser acceleration of electrons.

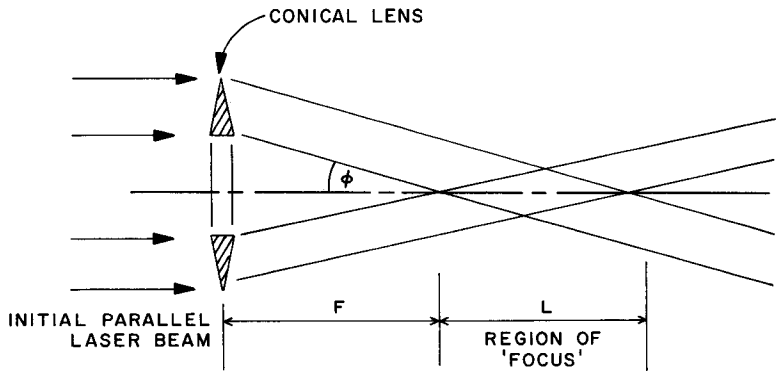

Fig. 4 - Focusing by axicon optics for laser acceleration.

We note that if axicon optics is used to replace the simple lens of Pantell's setup, as shown in Fig. 4, the energy gain is somewhat improved,[6] and can be written

$$\Delta E = 3 \times 10^{-5} \sqrt{PLD}$$

where

P = laser power in watts

L = length of the acceleration medium in cm

D = density of the helium in atm

ΔE = energy gain in MeV.

We now consider two cases. First, what would be obtained if we took <u>one</u> of the powerful lasers which now exist, and focus it over a reasonable length, say 5 m? Some care is necessary in choosing the helium pressure. The breakdown power is proportional to the length of the pulse, for pulses shorter than 1 nsec.[7] The breakdown is due to electron avalanches. The breakdown is also inversely proportional to the laser wavelength. The large Nd glass lasers at Livermore have sufficient bandwidth to produce pulses of 50 psec or a little less. Then one is permitted a D of about 10 atm. For a power of 2×10^{12} watts, one obtains a ΔE of 3 GeV. This would seem to be useful mainly as a demonstration, and we would not recommend doing it until such lasers become cheaper than they are now.

Second, we consider the case where we wish to obtain several TeV, and allow a 5 km acceleration length. We suppose there are 100 lasers side by side covering the acceleration length, each generating 5×10^{12} watts. To obtain radial focusing, we provide four such laser beams in each cross section, as shown in Fig. 5. Note the polarization directions. It is possible to obtain laser operation in the TM_{on} modes, which have the desired character,[8] but this

---

6. R. Palmer, J. Appl. Phys. <u>43</u>, 3014 (1972).

7. C. C. Wang and L. I. Davis, Jr., Phys. Rev. Lett. <u>26</u>, 822 (1971), and D. Smith, J. Appl. Phys. <u>41</u>, 4501 (1970).

8. D. Pohl, Appl. Phys. Lett. <u>20</u>, 266 (1972).

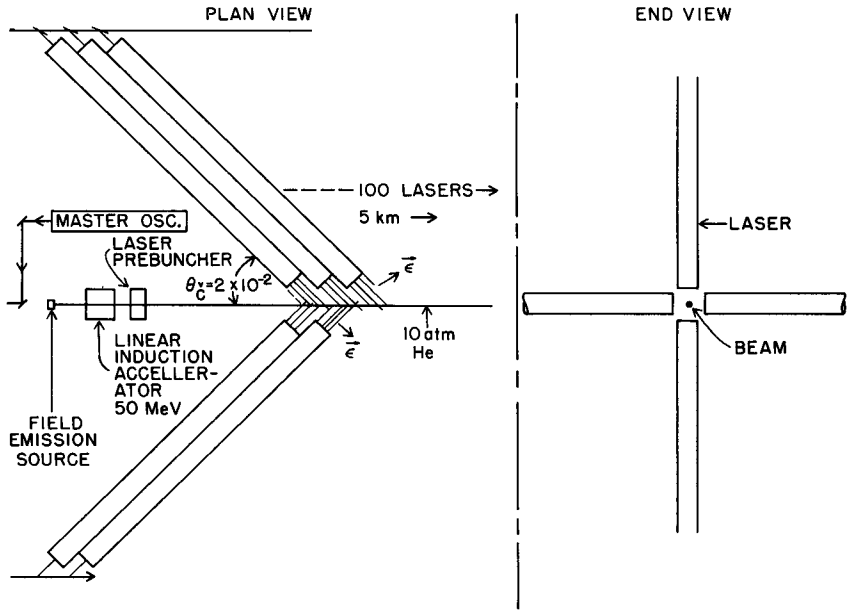

Fig. 5 - Schematic arrangement for a 3 TeV accelerator using a multiple laser assembly.

seems to have no advantage over the use of conventional lasers with the polarizations as shown. With the pressure again at 10 atm, the energy produced is 3 TeV.

The particles to be accelerated we assume to be electrons, because they cannot be accelerated to these energies by other devices, the injection sources have the necessary brightness, and the injection energy for phase matching is not too high.

We compute the possible current by starting with a field emission electron source of 3×10^8 A/m^2/str (Ref. 2) and noting that for 1 micron light, and a Cerenkov angle of 2×10^{-2}, the radius of the beam is about 25 microns. The radial focusing is very strong, admitting angles up to 0.2 radians for 50 MeV injection.

Having chosen to have radial focusing, we have longitudinal defocusing. Pantell, in his work on the optical klystron, has shown us that the injected beam can be very highly bunched, so that the beam can survive the trip through the accelerator without longitudinal stability, due to the extreme Lorentz contraction. However, the need for the injected particles to satisfy a paraxial condition to keep the energy gain constant reduces the acceptance for 50 MeV to 1 mrad. We assume we can accelerate the electrons from the field emission source to 50 MeV in a linear induction accelerator without loss of brightness (?) and obtain an accepted current of

$$I = 3 \times 10^8 \, (25 \times 10^{-6})^2 \, 10^{-6} \, (50/0.1)^2$$
$$= 0.4 \text{ A}$$

or with a 50 psec beam, 10^8 particles per pulse. Only 0.1% of the light energy has gone into the particles. If the first section of the device works at 1 atm permitting higher power, the number of particles is up by 10^2 but the injector has become somewhat formidable.

There is no problem with the coherence length of the light since the Cerenkov angle is small: 30 cm will do. The maintenance of the mechanical tolerances is more dubious. If that problem can

be solved, the attractiveness of this project depends largely on the cost of the lasers. That involves especially the laser efficiency. We are asking for a total of 10^5 joules in the laser output. This will be reasonable if the efficiency is a percent or more. Such lasers are promised, but not now available.

IV. Laser Driven Collective Accelerators

This seems to be a new category.[4] We can imagine it in at least two forms, of which we first consider a simple one. Suppose a light beam is incident on a single free electron. This problem seems to have first been solved by McMillen.[9] For weak fields, the electron simply quivers, oscillating in the direction of the propagation of the wave. In no case does the electron accumulate any acceleration, for reasonable shaped wave packets, as shown by Reiss and Eberly.[10] The electron does get a displacement in the direction of the wave, however, which can be written,[4]

$$W/z = 11.5\ k^2\ \text{J/cm}$$

where

W is the energy in the laser pulse
z is the displacement of the electron
$k^2 = A/\lambda^2$ where A is the area of the light beam, and
λ is the wave length.

For a reasonable optical system, k = 30, and the energy required for a 1 mm displacement is about 1000 J. This is reasonable for one laser.

If there are electrons distributed along the focus, this effect leads to an accumulation of excess charge in the region of the wave packet, as shown in Fig. 6.

---

9. E. McMillen, Phys. Rev. 79, 498 (1950).
10. H. Reiss and J. Eberly, Phys. Rev. 151, 1058 (1966).

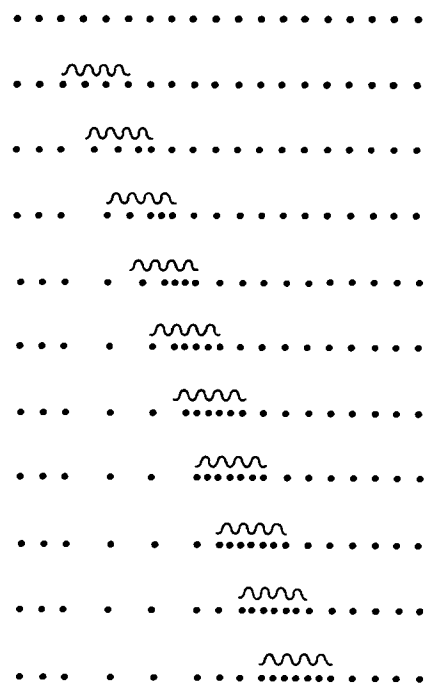

Fig. 6 - Schematic of electron accumulation by laser wave packet.

For example, if the electrons are in a plasma, the positive ions will not respond to the light wave, while the electrons will be displaced, and an electric field will result. This will continue until the electrical field balances the force due to the laser. Consider the somewhat unnatural case of a pulse short compared to its width, so that we can make a one-dimensional calculation. Then the resulting longitudinal field is

$$E_a \cong \frac{1}{50}\frac{e\lambda}{mc^2} E_o^2$$

where e is the electron charge and m its mass, and E_o is the field strength in the light beam. This expression shows that this process only becomes efficient when $\lambda E_o/mc^2$ is of the order of one, so that the electron quiver becomes relativistic.

The resulting electric field E_a can be used to accelerate positive ions. Moreover, since there is attractive charge on the axis and in front of the accelerated particles, there is both longitudinal and transverse stability. The accelerating field can be about 10 GeV/m, and any heavy positive ion can be accelerated (probably not positrons).

Since the summer study, evidence (the first as far as I know) for this effect has appeared.[11] A number of questions can be raised about the practicality of this effect as an accelerator. One is the question of radial disassembly of the electron bunch in the case of a long laser pulse. (Note however that remarkable magnetic fields are being generated which hinder radial motion.) Another is the laser power needed. The required power density can certainly be created at a sharp focus, but we want to accelerate the particles over many meters, and the total power required corresponds to 10^5 J or more.

One possibility of getting the laser power requirement down is to use the laser beam to chop a hole in an IREB, as mentioned before.

---

11. M. Marhic, Phys. of Fluids 18, 837 (1975).

A number of other interaction mechanisms then come into play, as discussed in Ref. 4, and the required power may fall by several orders of magnitude, while the same kind of longitudinal field is available for accelerating ions.

Similar effects have been considered by the NRL group from the point of view of the generation of bunches of electrons surrounded by enormous magnetic fields.[12] The generation of such currents by lasers is a way of getting around the Budker current limit. One might raise the possibility of whether this new method allows the creation of bunches which satisfy the criterion for Veksler's Impact Acceleration.

V. Conclusion

We see nothing that one wants to go out and build but we are not in the epoch described in the Introduction either. Meanwhile it will be interesting to follow out the new ideas and see where they lead.

We wish to thank Dr. C. Olsen and R. Pantell for visiting us, and Dr. A. J. Glass for valuable discussions.

---

12. J. Stamper, "Laser Matter Interaction Studies at NRL", Third Workshop on "Laser Interactions and Related Plasma Phenomena" H. Hora, ed. (1973).